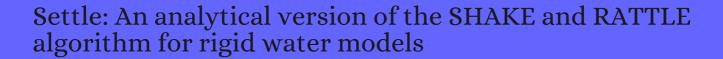
CITATION REPORT List of articles citing



DOI: 10.1002/jcc.540130805 Journal of Computational Chemistry, 1992, 13, 952-962.

Source: https://exaly.com/paper-pdf/23700703/citation-report.pdf

Version: 2024-04-10

This report has been generated based on the citations recorded by exaly.com for the above article. For the latest version of this publication list, visit the link given above.

The third column is the impact factor (IF) of the journal, and the fourth column is the number of citations of the article.

#	Paper	IF	Citations
2268	References. 557-586		
2267	Taming Rugged Free Energy Landscapes Using an Average Force.		
2266	Mechanism of Protein Supercharging by Sulfolane and mNitrobenzyl Alcohol: Molecular Dynamics Simulations of the Electrospray Process.		
2265	•		
2264	Dynamic Conformational States Dictate Selectivity toward the Native Substrate in a Substrate-Permissive Acyltransferase.		
2263	Fucose-Functionalized Precision Glycomacromolecules Targeting Human Norovirus Capsid Protein.		
2262	New Insight into the Aggregation of Graphene Oxide Using Molecular Dynamics Simulations and Extended DerjaguinLandauVerweyOverbeek Theory.		
2261	Silicate Binding and Precipitation on Iron Oxyhydroxides.		
2260	DNA Structural Distortions Induced by a Monofunctional Trinuclear Platinum Complex with Various Cross-Links Using Molecular Dynamics Simulation.		
2259	MCPB.py: A Python Based Metal Center Parameter Builder.		
2258	pmx Webserver: A User Friendly Interface for Alchemistry.		
2257	Averaged Solvent Embedding Potential Parameters for Multiscale Modeling of Molecular Properties.		
2256	Rigidity Theory-Based Approximation of Vibrational Entropy Changes upon Binding to Biomolecules.		
2255	All-Atom Simulations Reveal Protein Charge Decoration in the Folded and Unfolded Ensemble Is Key in Thermophilic Adaptation.		
2254	Capturing Phase Behavior of Ternary Lipid Mixtures with a Refined Martini Coarse-Grained Force Field.		
2253	Thermodynamics of Adsorption on Graphenic Surfaces from Aqueous Solution.		
2252	Addressing Polarization Phenomena in Molecular Machines Containing Transition Metal Ions with an Additive Force Field.		

- 2251 Fragment Binding Pose Predictions Using Unbiased Simulations and Markov-State Models. On Obtaining Boltzmann-Distributed Configurational Ensembles from Expanded Ensemble Simulations with Fast State Mixing. Drude Polarizable Force Field Parametrization of Carboxylate and NAcetyl Amine Carbohydrate 2249 Derivatives. 2248 Implicit Micelle Model for Membrane Proteins Using Superellipsoid Approximation. 2247 Improving Temperature Generator in Parallel Tempering Simulation in the NPT Condition. Discovery of Potent, Selective, and Orally Bioavailable Inhibitors against Phosphodiesterase-9, a Novel Target for the Treatment of Vascular Dementia. Validation of Phosphodiesterase-10 as a Novel Target for Pulmonary Arterial Hypertension via 2245 Highly Selective and Subnanomolar Inhibitors. Atropoisomerism in Biflavones: The Absolute Configuration of ()-Agathisflavone via Chiroptical Spectroscopy. Pterosin Sesquiterpenoids from Pteris cretica as Hypolipidemic Agents via Activating Liver X Receptors. Force Field for Mg2+, Mn2+ Zn2+, and Cd2+ Ions That Have Balanced Interactions with Nucleic 2241 Effects of Polymer Conjugation on Hybridization Thermodynamics of Oligonucleic Acids. 2240 Simulating the Favorable Aggregation of Monolacunary Keggin Anions. 2239 Slow-Down in Diffusion in Crowded Protein Solutions Correlates with Transient Cluster Formation. 2238 Stretch-Induced Interdigitation of a Phospholipid/Cholesterol Bilayer. 2237 Identification of Single Nucleotides by a Tiny Charged Solid-State Nanopore.
- Droplets.

 Two-Step Adsorption of PtCl62 Complexes at a Charged Langmuir Monolayer: Role of Hydration and Ion Correlations.

Correlation between Surface Tension and the Bulk Dynamics in Salty Atmospheric Aquatic

2236 Headgroup Structure and Cation Binding in Phosphatidylserine Lipid Bilayers.

2233	Curvature of Buckybowl Corannulene Enhances Its Binding to Proteins.
2232	pH-Controlled Fluorescence Probes for Rotaxane Isomerization.
2231	Pair Distribution Function from Electron Diffraction in Cryogenic Electron Microscopy: Revealing Glassy Water Structure.
2230	The Unfolding Journey of Superoxide Dismutase 1 Barrels under Crowding: Atomistic Simulations Shed Light on Intermediate States and Their Interactions with Crowders.
2229	Simulating the Activation of Voltage Sensing Domain for a Voltage-Gated Sodium Channel Using Polarizable Force Field.
2228	Preserved Transmembrane Segment Topology, Structure and Dynamics in Disparate Micellar Environments.
2227	Bobbing of Oxysterols: Molecular Mechanism for Translocation of Tail-Oxidized Sterols through Biological Membranes.
2226	Calcium Sensing by Recoverin: Effect of Protein Conformation on Ion Affinity.
2225	Merging In-Solution X-ray and Neutron Scattering Data Allows Fine Structural Analysis of MembraneProtein Detergent Complexes.
2224	Breakdown of Linear Dielectric Theory for the Interaction between Hydrated Ions and Graphene.
2223	Impact of Mutations on the Binding Pocket of Soybean Lipoxygenase: Implications for Proton-Coupled Electron Transfer.
2222	Higher Accuracy Achieved in the Simulations of Protein Structure Refinement, Protein Folding, and Intrinsically Disordered Proteins Using Polarizable Force Fields.
2221	Enhanced Cavitation and Hydration Crossover of Stretched Water in the Presence of C60.
2220	Atomistic Model for Nearly Quantitative Simulations of Langmuir Monolayers.
2219	Molecular Dynamics Simulation of DNA Capture and Transport in Heated Nanopores.
2218	Pro-Nifuroxazide Self-Assembly Leads to Triggerable Nanomedicine for Anti-cancer Therapy.
2217	Unpicking the Cause of Stereoselectivity in Actinorhodin Ketoreductase Variants with Atomistic Simulations.
2216	PeptideMembrane Interaction between Targeting and Lysis.

- Hexahydropyrrolo[2,3b]indole Compounds as Potential Therapeutics for Alzheimers Disease.
- Stabilization Mechanism for a Nonfibrillar Amyloid Oligomer Based on Formation of a Hydrophobic Core Determined by Dissipative Particle Dynamics.
- 2213 Conformational Dynamics of AcrA Govern Multidrug Efflux Pump Assembly.
- Interference-Free Detection of Genetic Biomarkers Using Synthetic Dipole-Facilitated Nanopore Dielectrophoresis.
- 2211 Small Molecules Targeting the Inactive Form of the Mnk1/2 Kinases.
- 2210 Initial Studies Directed toward the Rational Design of Aqueous Graphene Dispersants.
- 2209 Hydration Dynamics of a Peripheral Membrane Protein.
- 2208 Structural Model of the Tubular Assembly of the Rous Sarcoma Virus Capsid Protein.
- 2207 Base-Independent DNA Base-Excision Repair of 80xoguanine.
- Water Sculpts the Distinctive Shapes and Dynamics of the Tumor-Associated Carbohydrate Tn Antigens: Implications for Their Molecular Recognition.
- 2205 Multivalent Cation-Induced Actuation of DNA-Mediated Colloidal Superlattices.
- 2204 Rosette Nanotube Porins as Ion Selective Transporters and Single-Molecule Sensors.
- 2203 Universal and Nonuniversal Aspects of Electrostatics in Aqueous Nanoconfinement.
- Toward Atomistic Resolution Structure of Phosphatidylcholine Headgroup and Glycerol Backbone at Different Ambient Conditions.
- Free-Energy Analysis of Peptide Binding in Lipid Membrane Using All-Atom Molecular Dynamics Simulation Combined with Theory of Solutions.
- Accurate Binding of Sodium and Calcium to a POPC Bilayer by Effective Inclusion of Electronic Polarization.
- Aggregation of Heteropolyanions in Aqueous Solutions Exhibiting Short-Range Attractions and Long-Range Repulsions.
- 2198 Water-Controlled Switching in Rotaxanes.

2197 Free-Energy Landscape of Stepwise, Directional Motion in Multiple Molecular Switches. Photoactive Yellow Protein Chromophore Photoisomerizes around a Single Bond if the Double 2196 Bond Is Locked. Refined Parameterization of Nonbonded Interactions Improves Conformational Sampling and 2195 Kinetics of Protein Folding Simulations. Effective Polarization in Pairwise Potentials at the GrapheneElectrolyte Interface. Sequential Proton-Coupled Electron Transfer Mediates Excited-State Deactivation of a Eumelanin 2193 Building Block. 2192 Carbon Nanotubes Facilitate Oxidation of Cysteine Residues of Proteins. Perturbation of the F19-L34 Contact in Amyloid (1-40) Fibrils Induces Only Local Structural Changes 2191 but Abolishes Cytotoxicity. Conformational Behavior of dLyxose in Gas and Solution Phases by Rotational and NMR 2190 Spectroscopies. 2189 Distinct and Nonadditive Effects of Urea and Guanidinium Chloride on Peptide Solvation. Mosaic Cooperativity in Slow Polypeptide Topological Isomerization Revealed by Residue-Specific 2188 NMR Thermodynamic Analysis. Substrate-to-Product Conversion Facilitates Active Site Loop Opening in Yeast Enolase: A Molecular 2187 Dynamics Study. Effect of Chemically Distinct Substrates on the Mechanism and Reactivity of a Highly Promiscuous 2186 Metallohydrolase. Identification of Inhibitors of CD36-Amyloid Beta Binding as Potential Agents for Alzheimers 2185 Disease. Molecular Simulations Reveal Terminal Group Mediated Stabilization of Helical Conformers in Both Amyloid-42 and Synuclein. Discovery of Novel Neuraminidase Inhibitors by Structure-Based Virtual Screening, Structural 2183 Optimization, and Bioassay. Molecular Docking Studies of Royleanone Diterpenoids from Plectranthus spp. as PGlycoprotein 2182 Inhibitors. Membrane Fluidity Sensing on the Single Virus Particle Level with Plasmonic Nanoparticle 2181 Transducers. Mechanochemical Energy Transduction during the Main Rotary Step in the Synthesis Cycle of 2180 F1-ATPase.

2179	Water Dynamics from the Surface to the Interior of a Supramolecular Nanostructure.		
2178	Stress Propagation through Biological Lipid Bilayers in Silico.		
2177	Protein Hydration Waters Are Susceptible to Unfavorable Perturbations.		
2176	Nonadditive Ion Effects Drive Both Collapse and Swelling of Thermoresponsive Polymers in Water.		
2175	Exploring Gatekeeper Mutations in EGFR through Computer Simulations.		
2174	PACO: PArticle COunting Method To Enforce Concentrations in Dynamic Simulations.		
2173	pKa Values of Titrable Amino Acids at the Water/Membrane Interface.		
2172	A Multidimensional BSpline Correction for Accurate Modeling Sugar Puckering in QM/MM Simulations.		
2171	Polarizable QM/MM Approach with Fluctuating Charges and Fluctuating Dipoles: The QM/FQF Model.		
2170	Molecular Determinants Conferring the Stoichiometric-Dependent Activity of Conotoxins at the Human 910 Nicotinic Acetylcholine Receptor Subtype.		
2169			
2168	YASP: A molecular simulation package. 1993 , 78, 77-94		163
2167	LIN: A new algorithm to simulate the dynamics of biomolecules by combining implicit-integration and normal mode techniques. <i>Journal of Computational Chemistry</i> , 1993 , 14, 1212-1233	3.5	58
2166	Bond-distance and bond-angle constraints in reaction-path dynamics calculations. 1993 , 99, 2723-2738		39
2165	Modelling of peptide and protein structures. 1994 , 7, 175-202		4
2164	Long-time overdamped Langevin dynamics of molecular chains. <i>Journal of Computational Chemistry</i> , 1994 , 15, 997-1012	3.5	31
2163	The Langevin/implicit-Euler/normal-mode scheme for molecular dynamics at large time steps. 1994 , 101, 4995-5012		46
2162	AMBER, a package of computer programs for applying molecular mechanics, normal mode analysis, molecular dynamics and free energy calculations to simulate the structural and energetic properties of molecules. 1995, 91, 1-41		2509

2161	Gradient SHAKE: An improved method for constrained energy minimization in macromolecular simulations. <i>Journal of Computational Chemistry</i> , 1995 , 16, 1351-1356	11
2160	Configurational space of biological macromolecules as seen by semi-empirical force fields: inherent problems for molecular design and strategies to solve them by means of hierarchical force fields. 1995 , 336, 245-259	3
2159	Molecular Dynamics Simulations on Shared-Memory Multiple Processor Computers. 1995 , 15, 273-280	5
2158	Implicit discretization schemes for Langevin dynamics. 1995 , 84, 1077-1098	23
2157	Protein structure prediction: recognition of primary, secondary, and tertiary structural features from amino acid sequence. 1995 , 30, 1-94	113
2156	Hydration effects on the duplex stability of phosphoramidate DNA-RNA oligomers. 1997 , 25, 830-5	22
2155	Biomolecular dynamics at long timesteps: bridging the timescale gap between simulation and experimentation. 1997 , 26, 181-222	105
2154	Molecular Modeling of Proteins and Mathematical Prediction of Protein Structure. 1997 , 39, 407-460	120
2153	Molecular dynamics simulation study of DNA dodecamer d(CGCGAATTCGCG) in solution: conformation and hydration. 1997 , 272, 553-72	98
2152	Conformational analysis using distance geometry methods. 1997 , 15, 18-36	56
2151	Quasi-Hamiltonian equations of motion for internal coordinate molecular dynamics of polymers. 1997 , 18, 1354-1364	34
2150	LINCS: A linear constraint solver for molecular simulations. <i>Journal of Computational Chemistry</i> , 1997 , 18, 1463-1472	10241
2149	Can one predict protein stability? An attempt to do so for residue 133 of T4 lysozyme using a combination of free energy derivatives, PROFEC, and free energy perturbation methods. 1998 , 32, 438-458	20
2148	Binding domain of human parathyroid hormone receptor: from conformation to function. 1998 , 37, 12737-43	67
2147	Pathways to a protein folding intermediate observed in a 1-microsecond simulation in aqueous solution. 1998 , 282, 740-4	1076
2146	A systematic study of water models for molecular simulation: Derivation of water models optimized for use with a reaction field. 1998 , 108, 10220-10230	514
2145	The early stage of folding of villin headpiece subdomain observed in a 200-nanosecond fully solvated molecular dynamics simulation. 1998 , 95, 9897-902	139
2144	Ionic charging free energies: Spherical versus periodic boundary conditions. 1998 , 109, 10921-10935	114

2143	Addressing the tertiary structure of human parathyroid hormone-(1-34). 1998, 273, 10420-7	90
2142	New Free Energy Calculation Methods for Structure-Based Drug Design and Prediction of Protein Stability. 1999 , 37-52	1
2141	A molecular dynamics study of the 41-56 beta-hairpin from B1 domain of protein G. 1999 , 8, 2130-43	104
2140	Improving efficiency of large time-scale molecular dynamics simulations of hydrogen-rich systems. <i>Journal of Computational Chemistry</i> , 1999 , 20, 786-798	618
2139	Molecular dynamics simulations of biomolecules: long-range electrostatic effects. 1999 , 28, 155-79	473
2138	A New Leapfrog Integrator of Rotational Motion. The Revised Angular-Momentum Approach. 1999 , 22, 213-236	13
2137	A new soft-core potential function for molecular dynamics applied to the prediction of protein loop conformations. <i>Journal of Computational Chemistry</i> , 2000 , 21, 388-397	21
2136	Development of molecular dynamics programs for proteins with a parallelized Barnes-Hut tree code. 2000 ,	3
2135	Molecular Dynamics Simulations of Dodecylphosphocholine Micelles at Three Different Aggregate Sizes: Micellar Structure and Chain Relaxation. 2000 , 104, 6380-6388	250
2134	Molecular Dynamics Simulation of the Kinetics of Spontaneous Micelle Formation. 2000 , 104, 12165-12173	248
2133	A New 2,2,2-Trifluoroethanol Model for Molecular Dynamics Simulations. 2000 , 104, 12347-12354	99
2132	Molecular Dynamics Simulations of Water with Novel Shell-Model Potentials. 2001 , 105, 2618-2626	151
2131	Model of 1,1,1,3,3,3-Hexafluoro-propan-2-ol for Molecular Dynamics Simulations. 2001 , 105, 10967-10975	66
2130	Investigation of the mechanism of domain closure in citrate synthase by molecular dynamics simulation. 2001 , 310, 1039-53	44
2129	Effect of Undulations on Surface Tension in Simulated Bilayers. 2001 , 105, 6122-6127	237
2128	Molecular dynamics simulations of wild-type and mutant forms of the Mycobacterium tuberculosis MscL channel. 2001 , 81, 1345-59	83
2127	Molecular dynamics study of peptide-bilayer adsorption. 2001 , 80, 579-96	46
2126	A refined structure of human aquaporin-1. 2001 , 504, 206-11	110

2125	Molecular dynamics simulations of stratum corneum lipid models: fatty acids and cholesterol. 2001 , 1511, 156-67		185
2124	Potential of Mean Force Computations of Ions Approaching a Surface. 2001 , 17, 7929-7934		24
2123	GROMACS 3.0: a package for molecular simulation and trajectory analysis. 2001 , 7, 306-317		5502
2122	Free energy barrier estimation of unfolding the alpha-helical surfactant-associated polypeptide C. 2001 , 43, 395-402		9
2121	Influence of rotational energy barriers to the conformational search of protein loops in molecular dynamics and ranking the conformations. 2001 , 44, 167-79		18
2120	A fast SHAKE algorithm to solve distance constraint equations for small molecules in molecular dynamics simulations. <i>Journal of Computational Chemistry</i> , 2001 , 22, 501-508	3.5	647
2119	Theoretical equations of state for temperature and electromagnetic field dependence of fluid systems, based on the quasi-Gaussian entropy theory. 2002 , 116, 4437-4449		16
2118	Structure-activity relationships of linear and cyclic peptides containing the NGR tumor-homing motif. 2002 , 277, 47891-7		144
2117	Mechanism by which 2,2,2-trifluoroethanol/water mixtures stabilize secondary-structure formation in peptides: a molecular dynamics study. 2002 , 99, 12179-84		406
2116	Solvation phenomena of a tetrapeptide in water/trifluoroethanol and water/ethanol mixtures: a diffusion NMR, intermolecular NOE, and molecular dynamics study. 2002 , 124, 7737-44		159
2115	Molecular dynamics simulations of mixed micelles modeling human bile. 2002 , 41, 5375-82		81
2114	Determining the shear viscosity of model liquids from molecular dynamics simulations. 2002 , 116, 209		509
2113	Flexible constraints: An adiabatic treatment of quantum degrees of freedom, with application to the flexible and polarizable mobile charge densities in harmonic oscillators model for water. 2002 , 116, 9602-9610		27
2112	Probing the structural determinants of type II' beta-turn formation in peptides and proteins. 2002 , 124, 1203-13		88
2111	Structures of neat and hydrated 1-octanol from computer simulations. 2002 , 124, 15085-93		101
2110	Molecular Modeling and Simulation. 2002,		318
2109	Response of SCP-2L domain of human MFE-2 to ligand removal: binding site closure and burial of peroxisomal targeting signal. 2002 , 323, 99-113		13
2108	Molecular dynamics study of the folding of hydrophobin SC3 at a hydrophilic/hydrophobic interface. 2002 , 83, 112-24		44

2107	Water permeation through gramicidin A: desformylation and the double helix: a molecular dynamics study. 2002 , 82, 2934-42	80
2106	Evidence of complete hydrophobic coating of bombesin by trifluoroethanol in aqueous solution: an NMR spectroscopic and molecular dynamics study. 2002 , 8, 1663-9	81
2105	Calculation of the free energy of solvation for neutral analogs of amino acid side chains. <i>Journal of Computational Chemistry</i> , 2002 , 23, 548-53	157
2104	Folding and stability of the three-stranded beta-sheet peptide Betanova: insights from molecular dynamics simulations. 2002 , 46, 380-92	45
2103	Signal transduction in the photoactive yellow protein. II. Proton transfer initiates conformational changes. 2002 , 48, 212-9	36
2102	Signal transduction in the photoactive yellow protein. I. Photon absorption and the isomerization of the chromophore. 2002 , 48, 202-11	61
2101	Energetic and entropic contributions to the interactions between like-charged groups in cationic peptides: A molecular dynamics simulation study. 2002 , 11, 2001-9	10
2100	Methodological Issues in Lipid Bilayer Simulations. 2003 , 107, 9424-9433	314
2099	Calculation of the water-cyclohexane transfer free energies of neutral amino acid side-chain analogs using the OPLS all-atom force field. <i>Journal of Computational Chemistry</i> , 2003 , 24, 1930-5	98
2098	Relative stability of protein structures determined by X-ray crystallography or NMR spectroscopy: a molecular dynamics simulation study. 2003 , 53, 111-20	44
2097	Correlated ab initio study of nucleic acid bases and their tautomers in the gas phase, in a microhydrated environment and in aqueous solution. guanine: surprising stabilization of rare tautomers in aqueous solution. 2003 , 125, 7678-88	192
2096	Mixing Distributions within the Quasi-Gaussian Entropy Theory: Multistate Thermal Equations of State Valid for Large Temperature Ranges. 2003 , 107, 1410-1422	5
2095	Conformational studies of a bombolitin III-derived peptide mimicking the four-helix bundle structural motif of proteins. 2003 , 125, 15314-23	5
2094	The Influence of Trifluoromethyl Groups on the Miscibility of Fluorinated Alcohols with Water: A Molecular Dynamics Simulation Study of 1,1,1-Trifluoropropan-2-ol in Aqueous Solution. 2003 , 107, 4855-486	1 ¹¹
2093	Brute-Force Molecular Dynamics Simulations of Villin Headpiece: Comparison with NMR Parameters. 2003 , 107, 11178-11187	58
2092	Advances in biomolecular simulations: methodology and recent applications. 2003 , 36, 257-306	116
2091	Understanding binding affinity: a combined isothermal titration calorimetry/molecular dynamics study of the binding of a series of hydrophobically modified benzamidinium chloride inhibitors to trypsin. 2003 , 125, 10570-9	90
2090	The mechanism of proton exclusion in the aquaporin-1 water channel. 2003 , 333, 279-93	233

2089	Conformational dynamics of the F1-ATPase beta-subunit: a molecular dynamics study. 2003, 85, 1482-91	38
2088	Investigating lipid composition effects on the mechanosensitive channel of large conductance (MscL) using molecular dynamics simulations. 2003 , 85, 1512-24	86
2087	Effect of sodium chloride on a lipid bilayer. 2003 , 85, 1647-55	452
2086	Structure of sphingomyelin bilayers: a simulation study. 2003 , 85, 3624-35	127
2085	Selective excitation of native fluctuations during thermal unfolding simulations: horse heart cytochrome c as a case study. 2003 , 84, 1876-83	42
2084	Molecular dynamics simulations of phospholipid bilayers with cholesterol. 2003 , 84, 2192-206	411
2083	Molecular dynamics simulations of lignin peroxidase in solution. 2003 , 84, 3883-93	36
2082	Dynamic properties of water/alcohol mixtures studied by computer simulation. 2003, 119, 7308-7317	238
2081	Verlet-I/R-RESPA/Impulse is Limited by Nonlinear Instabilities. 2003, 24, 1951-1973	67
2080	Different models for the calculation of solvent effects on 17O nuclear magnetic shielding. 2003 , 118, 8863-8872	65
2079	Bilayer ice and alternate liquid phases of confined water. 2003 , 119, 1694-1700	114
2078	A fast multipole method combined with a reaction field for long-range electrostatics in molecular dynamics simulations: The effects of truncation on the properties of water. 2003 , 118, 10847-10860	77
2077	Optimal reduced dimensional representation of classical molecular dynamics. 2003, 119, 5379-5387	9
2076	Simulation of the folding equilibrium of alpha-helical peptides: a comparison of the generalized Born approximation with explicit solvent. 2003 , 100, 13934-9	235
2075	On the use of the quasi-Gaussian entropy theory in the study of simulated dilute solutions. 2004 , 120, 5226-34	9
2074	Heat capacity effects associated with the hydrophobic hydration and interaction of simple solutes: a detailed structural and energetical analysis based on molecular dynamics simulations. 2004 , 120, 10605-17	69
2073	Correlations among hydrogen bonds in liquid water. 2004 , 93, 087801	58
2072	Temperature dependence of the hydrophobic hydration and interaction of simple solutes: an examination of five popular water models. 2004 , 120, 6674-90	241

2071	Electrofreezing of confined water. 2004 , 120, 7123-30	99
2070	Conformational transitions induced by the binding of MgATP to the vitamin B12 ATP-binding cassette (ABC) transporter BtuCD. 2004 , 279, 45013-9	76
2069	Differential peptide dynamics is linked to major histocompatibility complex polymorphism. 2004 , 279, 28197-201	74
2068	NMR and molecular dynamics studies of an autoimmune myelin basic protein peptide and its antagonist: structural implications for the MHC II (I-Au)-peptide complex from docking calculations. 2004 , 271, 3399-413	18
2067	Molecular-dynamics simulation of amphiphilic bilayer membranes and wormlike micelles: a multi-scale modelling approach to the design of viscoelastic surfactant solutions. 2004 , 362, 1625-38	25
2066	Characterization of the conformational space of a triple-stranded beta-sheet forming peptide with molecular dynamics simulations. 2004 , 57, 734-46	6
2065	A molecular dynamics study of the structural stability of HIV-1 protease under physiological conditions: the role of Na+ ions in stabilizing the active site. 2005 , 58, 450-8	19
2064	Study of the Villin headpiece folding dynamics by combining coarse-grained Monte Carlo evolution and all-atom molecular dynamics. 2005 , 58, 459-71	52
2063	Theoretical investigations of prostatic acid phosphatase. 2005 , 58, 295-308	14
2062	Computer simulations of voltage-gated potassium channel KvAP. 2004 , 100, 1071-1078	14
2061	Calculation of affinities of peptides for proteins. <i>Journal of Computational Chemistry</i> , 2004 , 25, 393-411 3.5	20
2060	Modeling the alpha-helix to beta-hairpin transition mechanism and the formation of oligomeric aggregates of the fibrillogenic peptide Abeta(12-28): insights from all-atom molecular dynamics simulations. 2004 , 23, 263-73	25
2059	Molecular dynamics simulation of a decasaccharide fragment of heparin in aqueous solution. 2004 , 339, 281-90	61
2058	Toward the understanding of the structure and dynamics of protein-carbohydrate interactions: molecular dynamics studies of the complexes between hevein and oligosaccharidic ligands. 2004 , 339, 985-94	23
2057	Angular resolution and range of dipole-dipole correlations in water. 2004 , 120, 4393-403	34
2056	Water network dynamics at the critical moment of a peptide's beta-turn formation: a molecular dynamics study. 2004 , 121, 4925-35	15
2055	Molecular simulations suggest protein salt bridges are uniquely suited to life at high temperatures. 2004 , 126, 2208-14	73
2054	Structural and Dynamic Properties of the CAGQW Peptide in Water: A Molecular Dynamics Simulation Study Using Different Force Fields. 2004 , 108, 18734-18742	16

2053	Molecular dynamics simulation of the LOV2 domain from Adiantum capillus-veneris. 2004, 44, 1788-93	14
2052	How C-terminal carboxyamidation alters the biological activity of peptides from the venom of the eumenine solitary wasp. 2004 , 43, 5608-17	80
2051	Molecular Dynamics Simulation of a GM3 Ganglioside Bilayer. 2004 , 108, 20322-20330	23
2050	Structural stability of wild type and mutated alpha-keratin fragments: molecular dynamics and free energy calculations. 2004 , 5, 2165-75	34
2049	Structure and aggregation number of a lyotropic liquid crystal: a fluorescence quenching and molecular dynamics study. 2004 , 20, 5703-8	10
2048	Molecular interaction model for the C1B domain of protein kinase C-gamma in the complex with its activator phorbol-12-myristate-13-acetate in water solution and lipid bilayer. 2004 , 47, 6547-55	19
2047	Size dependent ion hydration, its asymmetry, and convergence to macroscopic behavior. 2004 , 120, 4457-66	133
2046	The range and shielding of dipole-dipole interactions in phospholipid bilayers. 2004 , 87, 2433-45	79
2045	Direct simulation of transmembrane helix association: role of asparagines. 2004 , 87, 1650-6	36
2044	Predicting the three-dimensional structure of the human facilitative glucose transporter glut1 by a novel evolutionary homology strategy: insights on the molecular mechanism of substrate migration, and binding sites for glucose and inhibitory molecules. 2004 , 87, 2990-9	158
2043	Reversible temperature and pressure denaturation of a protein fragment: a replica exchange molecular dynamics simulation study. 2004 , 93, 238105	132
2042	A conserved arginine plays a role in the catalytic cycle of the protein disulphide isomerases. 2004 , 335, 283-95	109
2041	Molecular dynamics simulation study of the interaction of trehalose with lipid membranes. 2004 , 20, 7844-51	102
2040	Computer simulation of the KvAP voltage-gated potassium channel: steered molecular dynamics of the voltage sensor. 2004 , 564, 325-32	47
2039	Cationic DMPC/DMTAP lipid bilayers: molecular dynamics study. 2004 , 86, 3461-72	147
2038	Structure and dynamics of sphingomyelin bilayer: insight gained through systematic comparison to phosphatidylcholine. 2004 , 87, 2976-89	126
2037	Toluene Model for Molecular Dynamics Simulations in the Ranges 298 2004, 108, 11774-11781	21
2036	The Binary Mixing Behavior of Phospholipids in a Bilayer: A Molecular Dynamics Study. 2004 , 108, 2454-2463	104

2035	Distribution of pentachlorophenol in phospholipid bilayers: a molecular dynamics study. 2004 , 86, 337-45	52
2034	Molecular dynamics simulation of a palmitoyl-oleoyl phosphatidylserine bilayer with Na+counterions and NaCl. 2004 , 86, 1601-9	159
2033	Insights into the induced fit mechanism in antithrombin-heparin interaction using molecular dynamics simulations. 2005 , 24, 203-12	37
2032	WIGGLE: A new constrained molecular dynamics algorithm in Cartesian coordinates. 2005 , 210, 171-182	9
2031	Conformational and dynamical properties of the niruriside in aqueous solution: a molecular dynamics approach. 2005 , 714, 189-197	2
2030	A dynamic perspective on the molecular recognition of chitooligosaccharide ligands by hevein domains. 2005 , 340, 1039-49	11
2029	Effect of hexafluoroisopropanol alcohol on the structure of melittin: a molecular dynamics simulation study. 2005 , 14, 2582-9	65
2028	Advanced approaches for the characterization of a de novo designed antiparallel coiled coil peptide. 2005 , 3, 1189-94	22
2027	Solvation free energies of amino acid side chain analogs for common molecular mechanics water models. 2005 , 122, 134508	329
2026	Molecular dynamics simulations of the adipocyte lipid binding protein reveal a novel entry site for the ligand. 2005 , 44, 4275-83	32
2025	A molecular dynamics study of human serum albumin binding sites. 2005 , 60, 485-95	47
2024	A decoy set for the thermostable subdomain from chicken villin headpiece, comparison of different free energy estimators. 2005 , 6, 301	14
2023	Incorporating the effect of ionic strength in free energy calculations using explicit ions. <i>Journal of Computational Chemistry</i> , 2005 , 26, 115-22	35
2022	Development of a multipoint model for sulfur in proteins: a new parametrization scheme to reproduce high-level ab initio interaction energies. <i>Journal of Computational Chemistry</i> , 2005 , 26, 283-93 ³⁻⁵	14
2021	GROMACS: fast, flexible, and free. <i>Journal of Computational Chemistry</i> , 2005 , 26, 1701-18	10273
2020	Structural and dynamic properties of cytochrome P450 BM-3 in pure water and in a dimethylsulfoxide/water mixture. 2005 , 78, 259-67	23
2019	Lateral pressure profiles in cholesterol-DPPC bilayers. 2005 , 35, 79-88	76
2018	Elastic properties, Young's modulus determination and structural stability of the tropocollagen molecule: a computational study by steered molecular dynamics. 2005 , 38, 1527-33	118

2017 Molecular dynamics simulation of PAMAM dendrimer in aqueous solution. 2005 , 46, 3481-3488	83
2016 Protein surface dynamics: interaction with water and small solutes. 2005 , 31, 433-52	7
2015 Non-iterative and exact method for constraining particles in a linear geometry. 2005 , 43, 911-916	5
Determinants of protein stability and folding: comparative analysis of beta-lactoglobulins and liver basic fatty acid binding protein. 2005 , 61, 366-76	20
2013 Generalized correlation for biomolecular dynamics. 2006 , 62, 1053-61	278
The determinants of stability in the human prion protein: insights into folding and misfolding from the analysis of the change in the stabilization energy distribution in different conditions. 2006 , 62, 69	98-707 ³¹
Evidence of a double-lid movement in Pseudomonas aeruginosa lipase: insights from molecular dynamics simulations. 2005 , 1, e28	45
An approximate but fast method to impose flexible distance constraints in molecular dynamics simulations. 2005 , 122, 144106	14
2009 Simulation studies of pore and domain formation in a phospholipid monolayer. 2005 , 122, 024704	48
2008 Fast evaluation of polarizable forces. 2005 , 123, 164107	54
2007 Surface solvation for an ion in a water cluster. 2005 , 122, 024513	74
Identification of a hydrophobic residue as a key determinant of fructose transport by the facilitative hexose transporter SLC2A7 (GLUT7). 2005 , 280, 42978-83	43
2005 Simulations of the pressure and temperature unfolding of an alpha-helical peptide. 2005 , 102, 6765-	70 103
2004 A methodology for efficiently sampling the conformation space of molecular structures. 2005 , 2, S10)8-15 11
Alternative splicing of SNAP-25 regulates secretion through nonconservative substitutions in the SNARE domain. 2005 , 16, 5675-85	56
2002 Fluidity of hydration layers nanoconfined between mica surfaces. 2005 , 94, 026101	156
A strand-loop-strand structure is a possible intermediate in fibril elongation: long time simulations of amyloid-beta peptide (10-35). 2005 , 127, 15408-16	74
Electric-field-induced redox potential shifts of tetraheme cytochromes c3 immobilized on 2000 self-assembled monolayers: surface-enhanced resonance Raman spectroscopy and simulation studies. 2005 , 88, 4188-99	56

(2005-2005)

1999	Comparison of two approaches to potential of mean force calculations of hydrophobic association: particle insertion and weighted histogram analysis methods. 2005 , 103, 3153-3167	18
1998	Experimental and theoretical study of the interaction of single-stranded DNA homopolymers and a monomethine cyanine dye: nature of specific binding. 2005 , 4, 798-802	19
1997	On the salt-induced stabilization of pair and many-body hydrophobic interactions. 2005 , 109, 642-51	113
1996	Molecular dynamics simulations of helix-forming, amine-functionalized m-poly(phenyleneethynylene)s. 2005 , 109, 7548-56	19
1995	Molecular Dynamics Simulation of a GM3 Ganglioside Bilayer. 2005 , 109, 6036-6036	
1994	Supercooled water in PVA matrixes. II. A molecular dynamics simulation study and comparison with QENS results. 2005 , 109, 8091-6	25
1993	Solvophobic and steric effects of side groups on polymer folding: molecular modeling studies of amine-functionalized m-poly(phenyleneethynylene) foldamers in aqueous solution. 2005 , 109, 19952-9	17
1992	Solubility of methane in water: the significance of the methane-water interaction potential. 2005 , 109, 23596-604	26
1991	Orientation and dynamics of benzyl alcohol and benzyl alkyl ethers dissolved in nematic lyotropic liquid crystals. 2H NMR and molecular dynamics simulations. 2005 , 109, 6644-51	8
1990	Bench meets bedside: a 10-year-old girl and amino acid residue glycine 75 of the facilitative glucose transporter GLUT1. 2005 , 44, 12621-6	5
1989	Structural basis for the enantioselectivity of an epoxide ring opening reaction catalyzed by halo alcohol dehalogenase HheC. 2005 , 127, 13338-43	62
1988	Thermostat Algorithms for Molecular Dynamics Simulations. 2005 , 105-149	321
1987	Molecular origin of anticooperativity in hydrophobic association. 2005 , 109, 8108-19	26
1986	Sequence dependence of amyloid fibril formation: insights from molecular dynamics simulations. 2005 , 349, 583-96	83
1985	Reproducible polypeptide folding and structure prediction using molecular dynamics simulations. 2005 , 354, 173-83	150
1984	Protonation state of Asp30 exerts crucial influence over surface loop rearrangements responsible for NO release in nitrophorin 4. 2005 , 579, 5392-8	22
1983	Correlation of temperature induced conformation change with optimum catalytic activity in the recombinant G/11 xylanase A from Bacillus subtilis strain 168 (1A1). 2005 , 579, 6505-10	40
1982	Probing the pH-dependent structural features of alpha-KTx12.1, a potassium channel blocker from the scorpion Tityus serrulatus. 2005 , 14, 1025-38	12

1981	Ligand-binding regulation of LXR/RXR and LXR/PPAR heterodimerizations: SPR technology-based kinetic analysis correlated with molecular dynamics simulation. 2005 , 14, 812-22	42
1980	Penetratin-membrane association: W48/R52/W56 shield the peptide from the aqueous phase. 2005 , 88, 939-52	61
1979	Predicting the signaling state of photoactive yellow protein. 2005 , 88, 3525-35	23
1978	A molecular dynamics study of the formation, stability, and oligomerization state of two designed coiled coils: possibilities and limitations. 2005 , 89, 3701-13	23
1977	Osmolyte trimethylamine-N-oxide does not affect the strength of hydrophobic interactions: origin of osmolyte compatibility. 2005 , 89, 858-66	130
1976	Molecular dynamics of a protein surface: ion-residues interactions. 2005 , 89, 768-81	62
1975	Probing conformational disorder in neurotensin by two-dimensional solid-state NMR and comparison to molecular dynamics simulations. 2005 , 89, 2113-20	46
1974	Spontaneous formation of detergent micelles around the outer membrane protein OmpX. 2005 , 88, 3191-204	48
1973	Interaction of the antimicrobial peptide cyclo(RRWWRF) with membranes by molecular dynamics simulations. 2005 , 89, 2296-306	36
1972	Water dependent properties of cutinase in nonaqueous solvents: a computational study of enantioselectivity. 2005 , 89, 999-1008	36
1971	Reorganization and conformational changes in the reduction of tetraheme cytochromes. 2005 , 89, 3919-30	21
1970	A salt-bridge motif involved in ligand binding and large-scale domain motions of the maltose-binding protein. 2005 , 89, 3362-71	61
1969	Effect of monovalent salt on cationic lipid membranes as revealed by molecular dynamics simulations. 2005 , 109, 21126-34	64
1968	Asymmetry of lipid bilayers induced by monovalent salt: atomistic molecular-dynamics study. 2005 , 122, 244902	99
1967	On the Ewald artifacts in computer simulations. The test-case of the octaalanine peptide with charged termini. 2005 , 23, 135-42	23
1966	Mechanism of helix nucleation and propagation: microscopic view from microsecond time scale MD simulations. 2005 , 109, 20064-7	33
1965	Low-temperature and high-pressure induced swelling of a hydrophobic polymer-chain in aqueous solution. 2005 , 7, 2780-6	38
1964	The influence of different treatments of electrostatic interactions on the thermodynamics of folding of peptides. 2005 , 109, 21322-8	29

1963	Lipids out of equilibrium: energetics of desorption and pore mediated flip-flop. 2006 , 128, 12462-7	187
1962	Molecular dynamics simulations of water droplets on polymer surfaces. 2006 , 125, 144712	102
1961	Dynamics in atomistic simulations of phospholipid membranes: Nuclear magnetic resonance relaxation rates and lateral diffusion. 2006 , 125, 204703	100
1960	Collective Langevin dynamics of conformational motions in proteins. 2006 , 124, 214903	89
1959	Computer simulation of the distribution of hexane in a lipid bilayer: spatially resolved free energy, entropy, and enthalpy profiles. 2006 , 128, 125-30	121
1958	Membrane protein simulations with a united-atom lipid and all-atom protein model: lipid-protein interactions, side chain transfer free energies and model proteins. 2006 , 18, S1221-34	138
1957	Effect of quantum partial charges on the structure and dynamics of water in single-walled carbon nanotubes. 2006 , 125, 114701	102
1956	Vstx1, a modifier of Kv channel gating, localizes to the interfacial region of lipid bilayers. 2006 , 45, 11844-55	33
1955	Hydrophobic aided replica exchange: an efficient algorithm for protein folding in explicit solvent. 2006 , 110, 19018-22	71
1954	Comparative molecular dynamics study of lipid membranes containing cholesterol and ergosterol. 2006 , 90, 2368-82	133
1953	Modulation of amphotericin B membrane interaction by cholesterol and ergosterola molecular dynamics study. 2006 , 110, 16743-53	42
1952	The influence of amino acid protonation states on molecular dynamics simulations of the bacterial porin OmpF. 2006 , 90, 112-23	55
1951	Influence of chain length and unsaturation on sphingomyelin bilayers. 2006 , 90, 851-63	100
1950	Fatty acid binding proteins: same structure but different binding mechanisms? Molecular dynamics simulations of intestinal fatty acid binding protein. 2006 , 90, 1535-45	35
1949	Kinetics and thermodynamics of type VIII beta-turn formation: a CD, NMR, and microsecond explicit molecular dynamics study of the GDNP tetrapeptide. 2006 , 90, 2745-59	38
1948	Conformational transitions in RNA single uridine and adenosine bulge structures: a molecular dynamics free energy simulation study. 2006 , 90, 2450-62	36
1947	Molecular simulation study of structural and dynamic properties of mixed DPPC/DPPE bilayers. 2006 , 90, 3951-65	134
1946	A molecular dynamics study of the effect of Ca2+ removal on calmodulin structure. 2006 , 90, 3842-50	35

1945	Does CO2 permeate through aquaporin-1?. 2006 , 91, 842-8	118
1944	Minor groove deformability of DNA: a molecular dynamics free energy simulation study. 2006 , 91, 882-91	38
1943	A molecular dynamics study and free energy analysis of complexes between the Mlc1p protein and two IQ motif peptides. 2006 , 91, 2436-50	30
1942	B-DNA under stress: over- and untwisting of DNA during molecular dynamics simulations. 2006 , 91, 2956-65	44
1941	Amino-acid solvation structure in transmembrane helices from molecular dynamics simulations. 2006 , 91, 4450-63	66
1940	The Origin of Layer Structure Artifacts in Simulations of Liquid Water. 2006 , 2, 1-11	164
1939	Lifting a wet glass from a table: a microscopic picture. 2006 , 22, 5666-72	13
1938	Small-molecule targeting of heat shock protein 90 chaperone function: rational identification of a new anticancer lead. 2006 , 49, 7721-30	79
1937	Free energy of a trans-membrane pore calculated from atomistic molecular dynamics simulations. 2006 , 124, 154905	123
1936	Aggregation and dispersion of small hydrophobic particles in aqueous electrolyte solutions. 2006 , 110, 22736-41	84
1935	Molecular dynamics study of the properties of capsaicin in an 1-octanol/water system. 2006, 110, 2351-7	15
1934	Proton antenna effect of the gamma-cyclodextrin outer surface, measured by excited state proton transfer. 2006 , 110, 26354-64	30
1933	Structural changes in the cytoplasmic domain of phospholamban by phosphorylation at Ser16: a molecular dynamics study. 2006 , 45, 11752-61	27
1932	Equilibrium distributions of dipalmitoyl phosphatidylcholine and dilauroyl phosphatidylcholine in a mixed lipid bilayer: atomistic semigrand canonical ensemble simulations. 2006 , 110, 25875-82	26
1931	Molecular dynamics simulation of electro-osmotic flows in rough wall nanochannels. 2006, 73, 051203	93
1930	Electrostatic, steric, and hydration interactions favor Na(+) condensation around DNA compared with K(+). 2006 , 128, 14506-18	123
1929	What NMR Relaxation Can Tell Us about the Internal Motion of an RNA Hairpin: A Molecular Dynamics Simulation Study. 2006 , 2, 1228-36	34
1928	Synthetic polymers and biomembranes. How do they interact? Atomistic molecular dynamics simulation study of PEO in contact with a DMPC lipid bilayer. 2006 , 110, 26170-9	24

(2006-2006)

1927	Inverse temperature transition of a biomimetic elastin model: reactive flux analysis of folding/unfolding and its coupling to solvent dielectric relaxation. 2006 , 110, 3576-87	26
1926	Phase behavior of a phospholipid/fatty acid/water mixture studied in atomic detail. 2006 , 128, 2030-4	43
1925	Can principal components yield a dimension reduced description of protein dynamics on long time scales?. 2006 , 110, 22842-52	78
1924	A Novel Hamiltonian Replica Exchange MD Protocol to Enhance Protein Conformational Space Sampling. 2006 , 2, 217-28	112
1923	Conformational polymorphism of the PrP106-126 peptide in different environments: a molecular dynamics study. 2006 , 110, 1423-8	34
1922	Molecular dynamics simulation of a phosphatidylglycerol membrane. 2006 , 580, 144-8	66
1921	Structural features of the reprolysin atrolysin C and tissue inhibitors of metalloproteinases (TIMPs) interaction. 2006 , 347, 641-8	4
1920	The acidic domain of hnRNPQ (NSAP1) has structural similarity to Barstar and binds to Apobec1. 2006 , 350, 288-97	11
1919	Kinetic computational alanine scanning: application to p53 oligomerization. 2006 , 357, 1039-49	16
1918	High-resolution structures of Escherichia coli cDsbD in different redox states: A combined crystallographic, biochemical and computational study. 2006 , 358, 829-45	34
1917	Computational sampling of a cryptic drug binding site in a protein receptor: explicit solvent molecular dynamics and inhibitor docking to p38 MAP kinase. 2006 , 359, 202-14	83
1916	Folding landscapes of the Alzheimer amyloid-beta(12-28) peptide. 2006 , 362, 567-79	74
1915	Role of each residue in catalysis in the active site of pyrimidine nucleoside phosphorylase from Bacillus subtilis: a hybrid QM/MM study. 2006 , 154, 20-6	13
1914	Molecular dynamics analysis of the engrailed homeodomain-DNA recognition. 2006, 155, 426-37	16
1913	A molecular dynamics analysis of the GCC-box binding domain in ethylene-responsive element binding factors. 2006 , 156, 537-45	3
1912	Lys296 and Arg299 residues in the C-terminus of MD-ACO1 are essential for a 1-aminocyclopropane-1-carboxylate oxidase enzyme activity. 2006 , 156, 407-20	27
1911	Similar folds with different stabilization mechanisms: the cases of Prion and Doppel proteins. 2006 , 6, 17	17
1910	Molecular-dynamic studies of carbon-water-carbon composite nanotubes. 2006 , 2, 1348-55	33

1909	Molecular dynamics simulations of the hydrophobin SC3 at a hydrophobic/hydrophilic interface. 2006 , 64, 863-73	27
1908	Molecular dynamics study of a calmodulin-like protein with an IQ peptide: spontaneous refolding of the protein around the peptide. 2006 , 64, 133-46	3
1907	Cofactor assisted gating mechanism in the active site of NADH oxidase from Thermus thermophilus. 2006 , 64, 465-76	11
1906	The planar conformation of a strained proline ring: a QM/MM study. 2006 , 64, 700-10	13
1905	Structural refinement of protein segments containing secondary structure elements: Local sampling, knowledge-based potentials, and clustering. 2006 , 65, 463-79	33
1904	Aggregating the amyloid Abeta(11-25) peptide into a four-stranded beta-sheet structure. 2006 , 65, 877-88	21
1903	Molecular dynamics studies of hexamers of amyloid-beta peptide (16-35) and its mutants: influence of charge states on amyloid formation. 2007 , 66, 575-87	20
1902	Enhanced sampling of peptide and protein conformations using replica exchange simulations with a peptide backbone biasing-potential. 2007 , 66, 697-706	90
1901	A comparison between two prokaryotic potassium channels (KirBac1.1 and KcsA) in a molecular dynamics (MD) simulation study. 2006 , 120, 1-9	27
1900	Interaction of local anesthetics with a peptide encompassing the IV/S4-S5 linker of the Na+channel. 2006 , 123, 29-39	11
1899	Molecular dynamics simulations of spontaneous bile salt aggregation. 2006 , 280, 182-193	86
1898	Serotype-selective, small-molecule inhibitors of the zinc endopeptidase of botulinum neurotoxin serotype A. 2006 , 14, 395-408	67
1897	Pressure denaturation of apomyoglobin: a molecular dynamics simulation study. 2006 , 1764, 506-15	12
1896	Binding mode analysis of the NADH cofactor in nitric oxide reductase: a theoretical study. 2006 , 25, 363-72	4
1895	Molecular dynamics simulation of GM1 gangliosides embedded in a phospholipid membrane. 2006 , 129, 86-91	10
1894	A hydrophobic gate in an ion channel: the closed state of the nicotinic acetylcholine receptor. 2006 , 3, 147-59	152
1893	Hydration thermodynamic properties of amino acid analogues: a systematic comparison of biomolecular force fields and water models. 2006 , 110, 17616-26	271
1892	Characterization of the interaction of hypericin with protein kinase C in U-87 MG human glioma cells. 2006 , 82, 720-8	19

1891	Structure of the 21-30 fragment of amyloid beta-protein. 2006 , 15, 1239-47	130
1890	Molecular dynamics simulations applied to the study of subtypes of HIV-1 protease common to Brazil, Africa, and Asia. 2006 , 44, 395-404	30
1889	Structural investigation of syringomycin-E using molecular dynamics simulation and NMR. 2006 , 35, 459-67	4
1888	The Thermodynamics of Folding of a Hairpin Peptide Probed Through Replica Exchange Molecular Dynamics Simulations. 2006 , 116, 262-273	13
1887	Solvent Effects on the UV (n -子) and NMR (170) Spectra of Acetone in Aqueous Solution: Development and Validation of a Modified AMBER Force Field for an Integrated MD/DFT/PCM Approach. 2006 , 116, 456-461	18
1886	Effect of pressure on the conformation of proteins. A molecular dynamics simulation of lysozyme. 2006 , 24, 254-61	17
1885	A methyl group at C7 of 11-cis-retinal allows chromophore formation but affects rhodopsin activation. 2006 , 46, 4472-81	4
1884	Computational design of proteins stereochemically optimized in size, stability, and folding speed. 2006 , 83, 122-34	7
1883	Toward understanding the inactivation mechanism of monooxygenase P450 BM-3 by organic cosolvents: a molecular dynamics simulation study. 2006 , 83, 467-76	26
1882	Biomolecular modeling: Goals, problems, perspectives. 2006 , 45, 4064-92	441
1882	Biomolecular modeling: Goals, problems, perspectives. 2006, 45, 4064-92 The effect of box shape on the dynamic properties of proteins simulated under periodic boundary conditions. <i>Journal of Computational Chemistry</i> , 2006, 27, 316-25 3-5	28
	The effect of box shape on the dynamic properties of proteins simulated under periodic boundary	
1881	The effect of box shape on the dynamic properties of proteins simulated under periodic boundary conditions. <i>Journal of Computational Chemistry</i> , 2006 , 27, 316-25 Flooding in GROMACS: accelerated barrier crossings in molecular dynamics. <i>Journal of</i>	28
1881 1880	The effect of box shape on the dynamic properties of proteins simulated under periodic boundary conditions. <i>Journal of Computational Chemistry</i> , 2006 , 27, 316-25 Flooding in GROMACS: accelerated barrier crossings in molecular dynamics. <i>Journal of Computational Chemistry</i> , 2006 , 27, 1693-702 3-5	28
1881 1880 1879	The effect of box shape on the dynamic properties of proteins simulated under periodic boundary conditions. <i>Journal of Computational Chemistry</i> , 2006 , 27, 316-25 Flooding in GROMACS: accelerated barrier crossings in molecular dynamics. <i>Journal of Computational Chemistry</i> , 2006 , 27, 1693-702 Biomolekulare Modellierung: Ziele, Probleme, Perspektiven. 2006 , 118, 4168-4198 Assessing the influence of electrostatic schemes on molecular dynamics simulations of secondary	28 53 29
1881 1880 1879 1878	The effect of box shape on the dynamic properties of proteins simulated under periodic boundary conditions. Journal of Computational Chemistry, 2006, 27, 316-25 Flooding in GROMACS: accelerated barrier crossings in molecular dynamics. Journal of Computational Chemistry, 2006, 27, 1693-702 Biomolekulare Modellierung: Ziele, Probleme, Perspektiven. 2006, 118, 4168-4198 Assessing the influence of electrostatic schemes on molecular dynamics simulations of secondary structure forming peptides. 2006, 18, S329-S345	28 53 29 18
1881 1880 1879 1878	The effect of box shape on the dynamic properties of proteins simulated under periodic boundary conditions. Journal of Computational Chemistry, 2006, 27, 316-25 Flooding in GROMACS: accelerated barrier crossings in molecular dynamics. Journal of Computational Chemistry, 2006, 27, 1693-702 Biomolekulare Modellierung: Ziele, Probleme, Perspektiven. 2006, 118, 4168-4198 Assessing the influence of electrostatic schemes on molecular dynamics simulations of secondary structure forming peptides. 2006, 18, S329-S345 Shear dynamics of hydration layers. 2006, 125, 104701	28 53 29 18 35

1873	Quaternary ammonium compounds as water channel blockers. Specificity, potency, and site of action. 2006 , 281, 14207-14	106
1872	The dynamics of the MgATP-driven closure of MalK, the energy-transducing subunit of the maltose ABC transporter. 2006 , 281, 28397-407	53
1871	Adding salt to an aqueous solution of t-butanol: is hydrophobic association enhanced or reduced?. 2006 , 124, 154508	14
1870	Solubility of simple, nonpolar compounds in TIP4P-Ew. 2006 , 124, 16102	20
1869	Equilibration of experimentally determined protein structures for molecular dynamics simulation. 2006 , 74, 061901	27
1868	Molecular dynamics simulation of micellar aggregates in aqueous solution of hexadecyl trimethylammonium chloride with different additives. 2006 , 104, 3645-3651	20
1867	Direct observation of Bin/amphiphysin/Rvs (BAR) domain-induced membrane curvature by means of molecular dynamics simulations. 2006 , 103, 15068-72	196
1866	Ion separation using a Y-junction carbon nanotube. 2006 , 17, 895-900	91
1865	Theoretical prediction of spectral and optical properties of bacteriochlorophylls in thermally disordered LH2 antenna complexes. 2006 , 125, 014903	41
1864	Sampling the multiple folding mechanisms of Trp-cage in explicit solvent. 2006 , 103, 15859-64	212
1863	Critical role of electrostatic interactions of amino acids at the cytoplasmic region of helices 3 and 6 in rhodopsin conformational properties and activation. 2007 , 282, 14272-82	17
1862	Hydrophobic association of alpha-helices, steric dewetting, and enthalpic barriers to protein folding. 2007 , 104, 6206-10	74
1861	Effects of lengthscales and attractions on the collapse of hydrophobic polymers in water. 2007 , 104, 733-8	105
1860	Inhomogeneity effects on the structure and dynamics of water at the surface of a membrane: a computer simulation study. 2007 , 126, 125103	10
1859	Molecular Dynamics with General Holonomic Constraints and Application to Internal Coordinate Constraints. 2007 , 75-136	6
1858	Interfacial surface charge and free accessibility to the PLA2-active site-like region are essential requirements for the activity of Lys49 PLA2 homologues. 2007 , 49, 378-87	55
1857	H bonding at the helix-bundle crossing controls gating in Kir potassium channels. 2007 , 55, 602-14	59
1856	Structural properties of ionic detergent aggregates: a large-scale molecular dynamics study of sodium dodecyl sulfate. 2007 , 111, 11722-33	153

(2007-2007)

1855	cysteine-rich domain. 2007 , 457, 41-6	31
1854	Location and dynamics of acyl chain NBD-labeled phosphatidylcholine (NBD-PC) in DPPC bilayers. A molecular dynamics and time-resolved fluorescence anisotropy study. 2007 , 1768, 467-78	74
1853	Interfacial interactions of glutamate, water and ions with carbon nanopore evaluated by molecular dynamics simulations. 2007 , 1768, 2319-41	5
1852	Interactions of amphotericin B derivatives with lipid membranesa molecular dynamics study. 2007 , 1768, 2616-26	12
1851	1-Alkanols and membranes: a story of attraction. 2007 , 1768, 2899-913	55
1850	Contribution of a putative salt bridge and backbone dynamics in the structural instability of human prion protein upon R208H mutation. 2007 , 364, 719-24	18
1849	Electric field effects on membranes: gramicidin A as a test ground. 2007 , 157, 545-56	34
1848	Replica exchange simulation of reversible folding/unfolding of the Trp-cage miniprotein in explicit solvent: on the structure and possible role of internal water. 2007 , 157, 524-33	105
1847	Role of sterol type on lateral pressure profiles of lipid membranes affecting membrane protein functionality: Comparison between cholesterol, desmosterol, 7-dehydrocholesterol and ketosterol. 2007 , 159, 311-23	107
1846	The structure of the Alzheimer amyloid beta 10-35 peptide probed through replica-exchange molecular dynamics simulations in explicit solvent. 2007 , 366, 275-85	125
1845	The Alzheimer's peptides Abeta40 and 42 adopt distinct conformations in water: a combined MD / NMR study. 2007 , 368, 1448-57	367
1844	Backbone dynamics in an intramolecular prolylpeptide-SH3 complex from the diphtheria toxin repressor, DtxR. 2007 , 374, 977-92	10
1843	Heterogeneity even at the speed limit of folding: large-scale molecular dynamics study of a fast-folding variant of the villin headpiece. 2007 , 374, 806-16	154
1842	Molecular dynamics simulations of palmitate entry into the hydrophobic pocket of the fatty acid binding protein. 2007 , 581, 1243-7	34
1841	The protonation state of the catalytic aspartates in plasmepsin II. 2007, 581, 4120-4	26
1840	The structure of LNA:DNA hybrids from molecular dynamics simulations: the effect of locked nucleotides. 2007 , 111, 9307-19	30
1839	Polyunsaturation in lipid membranes: dynamic properties and lateral pressure profiles. 2007 , 111, 3139-50	163
1838	Molecular dynamics simulations of mixed cationic/anionic wormlike micelles. 2007, 23, 6588-97	39

1837	Nanosecond field alignment of head group and water dipoles in electroporating phospholipid bilayers. 2007 , 111, 12993-6	69
1836	Domain coupling in the ABC transporter system BtuCD/BtuF: molecular dynamics simulation, normal mode analysis and protein-protein docking. 2007 ,	1
1835	Simulated interactions between angiotensin-converting enzyme and substrate gonadotropin-releasing hormone: novel insights into domain selectivity. 2007 , 46, 8753-65	22
1834	Effect of double bond position on lipid bilayer properties: insight through atomistic simulations. 2007 , 111, 11162-8	54
1833	Parameters of monovalent ions in the AMBER-99 forcefield: assessment of inaccuracies and proposed improvements. 2007 , 111, 11884-7	120
1832	A common, avoidable source of error in molecular dynamics integrators. 2007 , 126, 046101	82
1831	Pressure dependence of the compressibility of a micelle and a protein: insights from cavity formation analysis. 2007 , 105, 189-199	8
1830	Molecular aggregates in aqueous solutions of bile acid salts. Molecular dynamics simulation study. 2007 , 111, 9886-96	118
1829	Molecular dynamics simulations of ion distribution in nanochannels. 2007 , 33, 959-963	12
1828	Molecular dynamic simulations of eicosanoic acid and 18-methyleicosanoic acid langmuir monolayers. 2007 , 111, 10849-52	13
1827	Conformational dynamics of a lipid-interacting protein: MD simulations of saposin B. 2007, 46, 13573-80	8
1826	Evaporation from water clusters containing singly charged ions. 2007 , 9, 5105-11	55
1825	Interplay of electrostatic and hydrophobic effects with binding of cationic gemini surfactants and a conjugated polyanion: experimental and molecular modeling studies. 2007 , 111, 4401-10	65
1824	How sensitive are nanosecond molecular dynamics simulations of proteins to changes in the force field?. 2007 , 111, 6015-25	16
1823	Study of the interaction of human defensins with cell membrane models: relationships between structure and biological activity. 2007 , 111, 11318-29	32
1822	Ultrafast deactivation of an excited cytosine-guanine base pair in DNA. 2007 , 129, 6812-9	154
1821	Protein structures under electrospray conditions. 2007 , 46, 933-45	109
1820	Rapid, Accurate, and Precise Calculation of Relative Binding Affinities for the SH2 Domain Using a Computational Grid. 2007 , 3, 1193-202	15

1819	Influence of perfluorinated compounds on the properties of model lipid membranes. 2007, 111, 9908-18	39
1818	Enhanced hydrophobicity of rough polymer surfaces. 2007 , 111, 3336-41	32
1817	Hydrophobic Solvation: Aqueous Methane Solutions. 2007 , 84, 864	5
1816	Microscopic structure of phospholipid bilayers: comparison between molecular dynamics simulations and wide-angle X-ray spectra. 2007 , 111, 2484-9	11
1815	Implementation of the SCC-DFTB method for hybrid QM/MM simulations within the amber molecular dynamics package. 2007 , 111, 5655-64	183
1814	Accurate and efficient corrections for missing dispersion interactions in molecular simulations. 2007 , 111, 13052-63	141
1813	Energetics of peptide recognition by the second PDZ domain of human protein tyrosine phosphatase 1E. 2007 , 46, 1064-78	18
1812	Molecular dynamics simulations of rhodopsin in different one-component lipid bilayers. 2007 , 111, 7052-63	43
1811	On the orientation of a designed transmembrane peptide: toward the right tilt angle?. 2007 , 129, 15174-81	92
1810	L-alanine in a droplet of water: a density-functional molecular dynamics study. 2007 , 111, 4227-34	73
1809	Multiscale coarse-graining of monosaccharides. 2007 , 111, 11566-75	78
1808	Myosin V movement: lessons from molecular dynamics studies of IQ peptides in the lever arm. 2007 , 46, 14524-36	2
1807	Wetting of nanogrooved polymer surfaces. 2007 , 23, 7724-9	52
1806	Protonation of the chromophore in the photoactive yellow protein. 2007 , 111, 3765-73	16
1805	Morphology of bile salt micelles as studied by computer simulation methods. 2007 , 23, 12322-8	68
1804	Counterion and surface density dependence of the adsorption layer of ionic surfactants at the vapor-aqueous solution interface: a computer simulation study. 2007 , 111, 1769-74	41
1803	Atomic-scale structure and electrostatics of anionic palmitoyloleoylphosphatidylglycerol lipid bilayers with Na+ counterions. 2007 , 92, 1114-24	159
1802	The cPLA2 C2alpha domain in solution: structure and dynamics of its Ca2+-activated and cation-free states. 2007 , 92, 966-76	7

1801	Ion leakage through transient water pores in protein-free lipid membranes driven by transmembrane ionic charge imbalance. 2007 , 92, 1878-90	104
1800	What happens if cholesterol is made smoother: importance of methyl substituents in cholesterol ring structure on phosphatidylcholine-sterol interaction. 2007 , 92, 3346-57	88
1799	On the decrease in lateral mobility of phospholipids by sugars. 2007 , 92, 1598-605	59
1798	Simulation of the coupling between nucleotide binding and transmembrane domains in the ATP binding cassette transporter BtuCD. 2007 , 92, 2727-34	48
1797	Invariance of single-file water mobility in gramicidin-like peptidic pores as function of pore length. 2007 , 92, 3930-7	29
1796	Molecular dynamics simulations of lipid vesicle fusion in atomic detail. 2007 , 92, 4254-61	125
1795	Short-range order and collective dynamics of DMPC bilayers: a comparison between molecular dynamics simulations, X-ray, and neutron scattering experiments. 2007 , 93, 3156-68	72
1794	Folding of a DNA hairpin loop structure in explicit solvent using replica-exchange molecular dynamics simulations. 2007 , 93, 3218-28	47
1793	Atomic resolution modeling of the ferredoxin:[FeFe] hydrogenase complex from Chlamydomonas reinhardtii. 2007 , 93, 3034-45	37
1792	Molecular dynamics simulations of two tandem octarepeats from the mammalian prion protein: fully Cu2+-bound and metal-free forms. 2007 , 93, 3762-74	17
1791	Quantitative characterization of intrinsic disorder in polyglutamine: insights from analysis based on polymer theories. 2007 , 93, 1923-37	125
1790	New insights into the mechanism of Alzheimer amyloid-beta fibrillogenesis inhibition by N-methylated peptides. 2007 , 93, 3015-25	68
1789	Effect of ions on the hydrophobic interaction between two plates. 2007 , 129, 4678-86	208
1788	Multistructure 3D-QSAR studies on a series of conformationally constrained butyrophenones docked into a new homology model of the 5-HT2A receptor. 2007 , 50, 3242-55	19
1787	Stability of Hydrophobically Modified Poly(p-phenylenesulfonate) Bundles As Observed by Molecular Dynamics Simulation. 2007 , 40, 1703-1707	9
1786	Simulated surface tensions of common water models. 2007 , 126, 221101	153
1785	On the characterization of host-guest complexes: surface tension, calorimetry, and molecular dynamics of cyclodextrins with a non-ionic surfactant. 2007 , 111, 4383-92	89
1784	Clustering of Lennard-Jones particles in water: temperature and pressure effects. 2007 , 127, 104502	4

(2007-2007)

1783	Conformational changes upon calcium binding and phosphorylation in a synthetic fragment of calmodulin. 2007 , 88, 373-85	21
1782	Structural flexibility of the nucleosome core particle at atomic resolution studied by molecular dynamics simulation. 2007 , 85, 407-21	67
1781	Pressure and salt effects in simulated water: two sides of the same coin?. 2007, 46, 8907-11	76
1780	Druck- und Salzeffekte in simuliertem Wasser: zwei Seiten einer Medaille?. 2007 , 119, 9065-9069	10
1779	Modifying the OPLS-AA force field to improve hydration free energies for several amino acid side chains using new atomic charges and an off-plane charge model for aromatic residues. <i>Journal of Computational Chemistry</i> , 2007 , 28, 689-97	42
1778	Effect of different treatments of long-range interactions and sampling conditions in molecular dynamic simulations of rhodopsin embedded in a dipalmitoyl phosphatidylcholine bilayer. <i>Journal</i> 3.5 of Computational Chemistry, 2007 , 28, 1017-30	27
1777	Molecular dynamics simulations of conserved Hox protein hexapeptides II. Folded structures in water solution. 2007 , 805, 61-70	1
1776	Molecular dynamics simulations of conserved Hox protein hexapeptides. I. Folding behavior in water solution. 2007 , 810, 113-120	2
1775	Long-range interactions and parallel scalability in molecular simulations. 2007 , 176, 14-22	34
1774	Lipoate-based imprinted self-assembled molecular thin films for biosensor applications. 2007 , 22, 912-9	51
1773	Self-assembly and structural characterization of Echinococcus granulosus antigen B recombinant subunit oligomers. 2007 , 1774, 278-85	21
1772	The structure of the zwitterionic headgroups in a DMPC bilayer as seen from Monte Carlo simulation: Comparisons with ionic solutions. 2007 , 131-132, 225-234	4
1771	Synthesis of poly(N-isopropylacrylamide) copolymer containing anhydride and imide comonomers [] A theoretical study on reversal of LCST. 2007 , 48, 6707-6718	24
1770	Structural and functional behavior of biologically active monomeric melittin. 2007 , 25, 767-72	37
1769	Molecular dynamics analysis of HIV-1 matrix protein: clarifying differences between crystallographic and solution structures. 2007 , 26, 62-8	24
1768	Counterion and composition effects on discotic nematic lyotropic liquid crystals II. Ion exchange and molecular dynamics. 2007 , 316, 120-5	
1767	P-SHAKE: A quadratically convergent SHAKE in. 2007 , 220, 740-750	55
1766	Understanding the regulation mechanisms of PAF receptor by agonists and antagonists: molecular modeling and molecular dynamics simulation studies. 2007 , 67, 41-52	17

1765	Essential dynamics sampling study of adenylate kinase: comparison to citrate synthase and implication for the hinge and shear mechanisms of domain motions. 2007 , 67, 325-37	40
1764	Hydration of a hydrophobic cavity and its functional role: a simulation study of human interleukin-1beta. 2007 , 67, 868-85	17
1763	Molecular dynamics simulations from putative transition states of alpha-spectrin SH3 domain. 2007 , 69, 536-50	13
1762	The conformation of the extracellular binding domain of Death Receptor 5 in the presence and absence of the activating ligand TRAIL: a molecular dynamics study. 2008 , 70, 333-43	14
1761	Full correlation analysis of conformational protein dynamics. 2008, 70, 1294-312	108
1760	Position-resolved free energy of solvation for amino acids in lipid membranes from molecular dynamics simulations. 2008 , 70, 1332-44	56
1759	Energetics of protein homodimerization: effects of water sequestering on the formation of beta-lactoglobulin dimer. 2008 , 70, 1475-87	46
1758	Exploring the protein G helix free-energy surface by solute tempering metadynamics. 2008, 71, 1647-54	56
1757	C-Raf antagonizes apoptosis induced by IFN-alpha in human lung cancer cells by phosphorylation and increase of the intracellular content of elongation factor 1A. 2007 , 14, 952-62	42
1756	Probing the chemistry of thioredoxin catalysis with force. 2007 , 450, 124-7	224
1756 1755	Probing the chemistry of thioredoxin catalysis with force. 2007 , 450, 124-7 Modeling hydration mechanisms of enzymes in nonpolar and polar organic solvents. 2007 , 274, 2424-36	224 67
,,		
1755	Modeling hydration mechanisms of enzymes in nonpolar and polar organic solvents. 2007 , 274, 2424-36 A molecular dynamics simulation of micellar aggregates in aqueous solutions of hexadecyltrimethylammonium chloride with admixtures of low-molecular-weight substances. 2007 ,	67
1755 1754	Modeling hydration mechanisms of enzymes in nonpolar and polar organic solvents. 2007, 274, 2424-36 A molecular dynamics simulation of micellar aggregates in aqueous solutions of hexadecyltrimethylammonium chloride with admixtures of low-molecular-weight substances. 2007, 81, 1256-1262 Quantitative characterization of ion pairing and cluster formation in strong 1:1 electrolytes. 2007,	6 ₇
1755 1754 1753	Modeling hydration mechanisms of enzymes in nonpolar and polar organic solvents. 2007, 274, 2424-36 A molecular dynamics simulation of micellar aggregates in aqueous solutions of hexadecyltrimethylammonium chloride with admixtures of low-molecular-weight substances. 2007, 81, 1256-1262 Quantitative characterization of ion pairing and cluster formation in strong 1:1 electrolytes. 2007, 111, 6469-78 Docking and homology modeling explain inhibition of the human vesicular glutamate transporters.	67 7 106
1755 1754 1753 1752	Modeling hydration mechanisms of enzymes in nonpolar and polar organic solvents. 2007, 274, 2424-36 A molecular dynamics simulation of micellar aggregates in aqueous solutions of hexadecyltrimethylammonium chloride with admixtures of low-molecular-weight substances. 2007, 81, 1256-1262 Quantitative characterization of ion pairing and cluster formation in strong 1:1 electrolytes. 2007, 111, 6469-78 Docking and homology modeling explain inhibition of the human vesicular glutamate transporters. 2007, 16, 1819-29 Interaction of omeprazole with a methylated derivative of beta-cyclodextrin: phase solubility, NMR	67 7 106 42
1755 1754 1753 1752 1751	Modeling hydration mechanisms of enzymes in nonpolar and polar organic solvents. 2007, 274, 2424-36 A molecular dynamics simulation of micellar aggregates in aqueous solutions of hexadecyltrimethylammonium chloride with admixtures of low-molecular-weight substances. 2007, 81, 1256-1262 Quantitative characterization of ion pairing and cluster formation in strong 1:1 electrolytes. 2007, 111, 6469-78 Docking and homology modeling explain inhibition of the human vesicular glutamate transporters. 2007, 16, 1819-29 Interaction of omeprazole with a methylated derivative of beta-cyclodextrin: phase solubility, NMR spectroscopy and molecular simulation. 2007, 24, 377-89 Studying the unfolding kinetics of proteins under pressure using long molecular dynamic	67 7 106 42 60

(2008-2007)

1747	Dynamics Simulations. 2007 , 225, 1-5	23
1746	The molecular dynamics of assembly of the ubiquitous aortic medial amyloidal medin fragment. 2007 , 25, 903-11	5
1745	A theoretical study of repeating sequence in HRP II: a combination of molecular dynamics simulations and (17)O quadrupole coupling tensors. 2008 , 137, 76-80	1
1744	Molecular dynamics simulations of lung surfactant lipid monolayers. 2008, 138, 67-77	45
1743	Efficient constraint dynamics using MILC SHAKE. 2008 , 227, 8949-8959	14
1742	Comparison of multiple crystal structures with NMR data for engrailed homeodomain. 2008, 40, 189-202	16
1741	New insight into the discrimination between omeprazole enantiomers by cyclodextrins in aqueous solution. 2008 , 62, 345-351	2
1740	Structure and dynamics of the antifungal molecules Syringotoxin-B and Syringopeptin-25A from molecular dynamics simulation. 2008 , 37, 495-502	7
1739	Selectivity in the mechanism of action of antimicrobial mastoparan peptide Polybia-MP1. 2008, 37, 879-91	46
1738	Molecular dynamics simulations of the hydration of poly(vinyl methyl ether): Hydrogen bonds and quasi-hydrogen bonds. 2008 , 51, 736-742	5
1737	Cloning, expression and physicochemical characterization of a di-heme cytochrome c (4) from the psychrophilic bacterium Pseudoalteromonas haloplanktis TAC 125. 2008 , 13, 789-99	7
1736	Molecular modeling and dynamics studies of cytidylate kinase from Mycobacterium tuberculosis H37Rv. 2008 , 14, 427-34	15
1735	Is TEA an inhibitor for human Aquaporin-1?. 2008 , 456, 663-9	29
1734	Theoretical Modeling of PrkCc, SerineII hreonine Protein Kinase Intracellular Domain, Complexed with ATP Derivatives. 2008 , 27, 437-444	4
1733	Searching the global minimum of a peptide/bilayer potential energy surface by fast heating and cooling cycles of simulated annealing. 2008 , 108, 2403-2407	2
1732	Water penetration in the low and high pressure native states of ubiquitin. 2008, 70, 1175-84	57
1731	Electrostatic contribution to the thermodynamic and kinetic stability of the homotrimeric coiled coil Lpp-56: A computational study. 2008 , 70, 810-22	13
1730	Computational studies of the structure, dynamics and native content of amyloid-like fibrils of ribonuclease A. 2008 , 70, 863-72	18

1729	Detailed conformational dynamics of juxtamembrane region and activation loop in c-Kit kinase activation process. 2008 , 72, 323-32		24
1728	Protein thermal stabilization by charged compatible solutes: Computational studies in rubredoxin from Desulfovibrio gigas. 2008 , 72, 580-8		
1727	Refining homology models by combining replica-exchange molecular dynamics and statistical potentials. 2008 , 72, 1171-88		65
1726	Predicting functional residues in Plasmodium falciparum plasmepsins by combining sequence and structural analysis with molecular dynamics simulations. 2008 , 73, 440-57		18
1725	Effect of lipid composition on buforin II structure and membrane entry. 2008, 73, 480-91		23
1724	Anti-apoptotic Bcl-XL protein in complex with BH3 peptides of pro-apoptotic Bak, Bad, and Bim proteins: comparative molecular dynamics simulations. 2008 , 73, 492-514		40
1723	Study of the mechanism of action of anoplin, a helical antimicrobial decapeptide with ion channel-like activity, and the role of the amidated C-terminus. 2008 , 14, 661-9		52
1722	T-20 and T-1249 HIV fusion inhibitors' structure and conformation in solution: a molecular dynamics study. 2008 , 14, 442-7		16
1721	Potential proton-release channels in bacteriorhodopsin. 2008 , 9, 2751-8		16
1720	Thermodynamic and structural characterization of the transformation from a metastable low-density to a very high-density form of supercooled TIP4P-Ew model water. 2008 , 9, 2737-41		51
1719	The solvent-dependent shift of the amide I band of a fully solvated peptide as a local probe for the solvent composition in the peptide/solvent interface. 2008 , 9, 2742-50		11
1718	Temperature and concentration effects on the solvophobic solvation of methane in aqueous salt solutions. 2008 , 9, 2722-30		12
1717	Salt effects on the structure of water probed by attenuated total reflection infrared spectroscopy and molecular dynamics simulations. 2008 , 9, 2731-6		23
1716	Modeling the hERG potassium channel in a phospholipid bilayer: Molecular dynamics and drug docking studies. <i>Journal of Computational Chemistry</i> , 2008 , 29, 795-808	3.5	42
1715	A new method for determining the interfacial molecules and characterizing the surface roughness in computer simulations. Application to the liquid-vapor interface of water. <i>Journal of Computational Chemistry</i> , 2008 , 29, 945-56	3.5	155
1714	Parameterization of Ca+2-protein interactions for molecular dynamics simulations. <i>Journal of Computational Chemistry</i> , 2008 , 29, 1163-9	3.5	37
1713	A versatile AMBER-Gaussian QM/MM interface through PUPIL. <i>Journal of Computational Chemistry</i> , 2008 , 29, 1564-73	3.5	36
1712	Molecular simulation of multistate peptide dynamics: a comparison between microsecond timescale sampling and multiple shorter trajectories. <i>Journal of Computational Chemistry</i> , 2008 , 29, 1740	0 ² 5 ⁵ 2	47

1711 Electrophoretic mobility does not always reflect the charge on an oil droplet. 2008 , 318, 477-86	45
1710 Analysis of ligand binding to proteins using molecular dynamics simulations. 2008 , 254, 294-300	31
Computational alanine scanning and free energy decomposition for E. coli type I signal peptidase with lipopeptide inhibitor complex. 2008 , 26, 813-23	27
Molecular modeling study of CodX reveals importance of N-terminal and C-terminal domain in the CodWX complex structure of Bacillus subtilis. 2008 , 27, 1-12	1
Molecular dynamics simulations of a lipovitellin-derived amphiphilic beta-sheet homologous to apoB-100 beta-sheets at a hydrophobic decane-water interface. 2008 , 1784, 1668-75	5
Behavior of molecular oxygen at the liquid I quid interface: A molecular dynamics simulation study. 2008 , 457, 78-81	1
1705 Equilibrium exchange enhances the convergence rate of umbrella sampling. 2008 , 460, 375-381	19
1704 Modelling the behavior of 5-aminolevulinic acid and its alkyl esters in a lipid bilayer. 2008 , 463, 178-182	14
1703 Molecular modeling and dynamics simulations of PNP from Streptococcus agalactiae. 2008 , 16, 4984-93	32
1702 Molecular modeling and dynamics studies of Shikimate Kinase from Bacillus anthracis. 2008 , 16, 8098-10	8 19
Determining the solution conformational entropy of O-linked oligosaccharides at quasi-physiological conditions: size-exclusion chromatography and molecular dynamics. 2008 , 343, 132-8	15
1700 Nanodroplet impact and sliding on structured polymer surfaces. 2008 , 602, 1810-1818	31
1699 Molecular dynamics simulations of protein folding. 2008 , 413, 315-30	7
GROMACS 4: Algorithms for Highly Efficient, Load-Balanced, and Scalable Molecular Simulation. 2008 , 4, 435-47	11706
Early events in protein folding: Is there something more than hydrophobic burst?. 2008 , 17, 1424-33	14
Effect of ions on a dipalmitoyl phosphatidylcholine bilayer. a molecular dynamics simulation study. 2008 , 112, 1397-408	112
Vulnerability in Popular Molecular Dynamics Packages Concerning Langevin and Andersen Dynamics. 2008 , 4, 1669-1680	68
1694 Investigation of the interaction between the atypical agonist c[YpwFG] and MOR. 2008 , 275, 2315-37	24

1693	Structures of the chromophore binding sites in BLUF domains as studied by molecular dynamics and quantum chemical calculations. 2008 , 84, 1003-10	34
1692	Intrinsic aqueduct orifices facilitate K+ channel gating. 2008 , 582, 3320-4	6
1691	Characterization of the papillomavirus alpha(1)E2 peptide unfolded to folded transition upon DNA binding. 2008 , 582, 3619-24	3
1690	Computational methods in nanostructure design: replica exchange simulations of self-assembling peptides. 2008 , 474, 133-51	3
1689	Structure and dynamics of surfactant and hydrocarbon aggregates on graphite: a molecular dynamics simulation study. 2008 , 112, 2915-21	41
1688	Surfactant and hydrocarbon aggregates on defective graphite surface: structure and dynamics. 2008 , 112, 12954-61	28
1687	Role of water in mediating the assembly of Alzheimer amyloid-beta Abeta16-22 protofilaments. 2008 , 130, 11066-72	180
1686	Molecular dynamics study on the biophysical interactions of seven green tea catechins with lipid bilayers of cell membranes. 2008 , 56, 7750-8	123
1685	Solid-state NMR and MD simulations of the antiviral drug amantadine solubilized in DMPC bilayers. 2008 , 94, 1295-302	44
1684	Distribution of amino acids in a lipid bilayer from computer simulations. 2008 , 94, 3393-404	434
168 ₄	Distribution of amino acids in a lipid bilayer from computer simulations. 2008 , 94, 3393-404 A method to determine dielectric constants in nonhomogeneous systems: application to biological membranes. 2008 , 94, 1185-93	434 78
1683	A method to determine dielectric constants in nonhomogeneous systems: application to biological	
1683	A method to determine dielectric constants in nonhomogeneous systems: application to biological membranes. 2008 , 94, 1185-93	78
1683 1682	A method to determine dielectric constants in nonhomogeneous systems: application to biological membranes. 2008, 94, 1185-93 Predicting thymine dimerization yields from molecular dynamics simulations. 2008, 94, 3590-600 Investigating the mechanism of peptide aggregation: insights from mixed monte carlo-molecular	78 76
1683 1682 1681	A method to determine dielectric constants in nonhomogeneous systems: application to biological membranes. 2008, 94, 1185-93 Predicting thymine dimerization yields from molecular dynamics simulations. 2008, 94, 3590-600 Investigating the mechanism of peptide aggregation: insights from mixed monte carlo-molecular dynamics simulations. 2008, 94, 4414-26 Factors influencing local membrane curvature induction by N-BAR domains as revealed by	78 76 44
1683 1682 1681	A method to determine dielectric constants in nonhomogeneous systems: application to biological membranes. 2008, 94, 1185-93 Predicting thymine dimerization yields from molecular dynamics simulations. 2008, 94, 3590-600 Investigating the mechanism of peptide aggregation: insights from mixed monte carlo-molecular dynamics simulations. 2008, 94, 4414-26 Factors influencing local membrane curvature induction by N-BAR domains as revealed by molecular dynamics simulations. 2008, 95, 1866-76	78 76 44 84
1683 1682 1681 1680	A method to determine dielectric constants in nonhomogeneous systems: application to biological membranes. 2008, 94, 1185-93 Predicting thymine dimerization yields from molecular dynamics simulations. 2008, 94, 3590-600 Investigating the mechanism of peptide aggregation: insights from mixed monte carlo-molecular dynamics simulations. 2008, 94, 4414-26 Factors influencing local membrane curvature induction by N-BAR domains as revealed by molecular dynamics simulations. 2008, 95, 1866-76 Confirming the revised C-terminal domain of the MscL crystal structure. 2008, 94, 4662-7 Kinetics, statistics, and energetics of lipid membrane electroporation studied by molecular	78 76 44 84 7

1675	The selectivity of K+ ion channels: testing the hypotheses. 2008 , 95, 5062-72	59
1674	Small- and large-scale conformational changes of adenylate kinase: a molecular dynamics study of the subdomain motion and mechanics. 2008 , 95, 5901-12	70
1673	Interplay of unsaturated phospholipids and cholesterol in membranes: effect of the double-bond position. 2008 , 95, 3295-305	111
1672	The influence of 1-alkanols and external pressure on the lateral pressure profiles of lipid bilayers. 2008 , 95, 5766-78	47
1671	Water at polar and nonpolar solid walls. 2008 , 3, FC23-39	86
1670	Electrostatic contributions drive the interaction between Staphylococcus aureus protein Efb-C and its complement target C3d. 2008 , 17, 1894-906	29
1669	Molecular dynamics simulation of the interaction between the complex iron-sulfur flavoprotein glutamate synthase and its substrates. 2004 , 13, 2979-91	7
1668	Molecular dynamics simulation of interactions between a sodium dodecyl sulfate micelle and a poly(ethylene oxide) polymer. 2008 , 112, 2888-900	94
1667	Combined Electrostatically Embedded Multiconfiguration Molecular Mechanics and Molecular Mechanical Method: Application to Molecular Dynamics Simulation of a Chemical Reaction in Aqueous Solution with Hybrid Density Functional Theory. 2008 , 4, 1032-9	28
1666	A Two-step Aggregation Scheme of Bile Acid Salts, as Seen From Computer Simulations. 2008 , 181-187	2
1665	Interface water dynamics and porating electric fields for phospholipid bilayers. 2008 , 112, 13588-96	102
1664	Dynamics of cellulose-water interfaces: NMR spin-lattice relaxation times calculated from atomistic computer simulations. 2008 , 112, 2590-5	71
1663	Modeling and molecular dynamics simulation of the human gonadotropin-releasing hormone receptor in a lipid bilayer. 2008 , 112, 10704-13	31
1662	Ensuring Mixing Efficiency of Replica-Exchange Molecular Dynamics Simulations. 2008 , 4, 1119-28	64
1661	Modeling and biochemical analysis of the activity of antibiofilm agent Dispersin B. 2008, 59, 439-51	15
1660	Crystal structure of HAb18G/CD147: implications for immunoglobulin superfamily homophilic adhesion. 2008 , 283, 18056-65	98
1659	Molecular dynamics simulation of the structure, dynamics, and thermostability of the RNA hairpins uCACGg and cUUCGg. 2008 , 112, 134-42	45
1658	Aggregation of the hairy rod conjugated polyelectrolyte poly{1,4-phenylene-[9,9-bis(4-phenoxybutylsulfonate)]fluorene-2,7-diyl} in aqueous solution: an experimental and molecular modelling study. 2008 , 10, 4420-8	51

1657	Consistency of Ion Adsorption and Excess Surface Tension in Molecular Dynamics Simulations of Aqueous Salt Solutions. 2008 , 112, 19431-19442	36
1656	Solvation Effects on Molecules and Biomolecules. 2008,	49
1655	HLA-B27 subtypes differentially associated with disease exhibit conformational differences in solution. 2008 , 376, 798-810	50
1654	Salt-bridge dynamics control substrate-induced conformational change in the membrane transporter GlpT. 2008 , 378, 828-39	50
1653	Effects of familial Alzheimer's disease mutations on the folding nucleation of the amyloid beta-protein. 2008 , 381, 221-8	88
1652	A molecular dynamics study of the interaction of D-peptide amyloid inhibitors with their target sequence reveals a potential inhibitory pharmacophore conformation. 2008 , 383, 266-80	14
1651	Structural studies of human purine nucleoside phosphorylase: towards a new specific empirical scoring function. 2008 , 479, 28-38	30
1650	Crystal structure of a novel myotoxic Arg49 phospholipase A2 homolog (zhaoermiatoxin) from Zhaoermia mangshanensis snake venom: insights into Arg49 coordination and the role of Lys122 in the polarization of the C-terminus. 2008 , 51, 723-35	13
1649	Role of backbone-solvent interactions in determining conformational equilibria of intrinsically disordered proteins. 2008 , 130, 7380-92	171
1648	Site-directed mutagenesis of the conserved Ala348 and Gly350 residues at the putative active site of Bacillus kaustophilus leucine aminopeptidase. 2008 , 90, 811-9	8
1647	Role of phosphatidylglycerols in the stability of bacterial membranes. 2008 , 90, 930-8	83
1646	Effects of fluorescent probe NBD-PC on the structure, dynamics and phase transition of DPPC. A molecular dynamics and differential scanning calorimetry study. 2008 , 1778, 491-501	52
1645	Membrane curvature and surface area per lipid affect the conformation and oligomeric state of HIV-1 fusion peptide: a combined FTIR and MD simulation study. 2008 , 1778, 945-53	12
1644	Binding and interactions of L-BABP to lipid membranes studied by molecular dynamic simulations. 2008 , 1778, 1390-7	21
1643	P-LINCS: A Parallel Linear Constraint Solver for Molecular Simulation. 2008, 4, 116-22	2072
1642	Biomolecular simulations of membranes: physical properties from different force fields. 2008 , 128, 125103	227
1641	Mechanism of selectivity in aquaporins and aquaglyceroporins. 2008, 105, 1198-203	328
1640	Molecular dynamics simulations of cardiolipin bilayers. 2008 , 112, 11655-63	48

(2008-2008)

1639	Molecular dynamics simulations of rhodopsin point mutants at the cytoplasmic side of helices 3 and 6. 2008 , 25, 573-87	20
1638	Ab initio fragment molecular orbital study of molecular interactions in liganded retinoid X receptor: specification of residues associated with ligand inducible information transmission. 2008 , 112, 12081-94	46
1637	Unfolding and melting of DNA (RNA) hairpins: the concept of structure-specific 2D dynamic landscapes. 2008 , 10, 4227-39	28
1636	Molecular level structure of the liquid/liquid interface. Molecular dynamics simulation and ITIM analysis of the water-CCl4 system. 2008 , 10, 4754-64	46
1635	Implicit solvent models for micellization of ionic surfactants. 2008 , 112, 13783-92	51
1634	Combining Elastic Network Analysis and Molecular Dynamics Simulations by Hamiltonian Replica Exchange. 2008 , 4, 477-87	32
1633	Molecular dynamics study of triosephosphate isomerase from Trypanosoma cruzi in water/decane mixtures. 2008 , 112, 3529-39	23
1632	Theory and computer simulation of solute effects on the surface tension of liquids. 2008 , 112, 8975-84	27
1631	Molecular dynamics study to investigate the effect of chemical substitutions of methionine 35 on the secondary structure of the amyloid beta (Abeta(1-42)) monomer in aqueous solution. 2008 , 112, 2159-67	30
1630	Simulations of a protein crystal: explicit treatment of crystallization conditions links theory and experiment in the streptavidin-biotin complex. 2008 , 47, 12065-77	32
1629	Microscopic Picture of the Aqueous Solvation of Glutamic Acid. 2008, 4, 898-907	8
1628	Replacing the cholesterol hydroxyl group with the ketone group facilitates sterol flip-flop and promotes membrane fluidity. 2008 , 112, 1946-52	68
1627	Significance of cholesterol methyl groups. 2008 , 112, 2922-9	49
1626	Polyionic charge density plays a key role in differential recognition of mobile ions by biopolymers. 2008 , 112, 9135-45	20
1625	Molecular dynamic simulation of the Kv1.2 voltage-gated potassium channel in open and closed state conformations. 2008 , 112, 16966-74	10
1624	A comprehensive conformational analysis of bullacin B, a potent inhibitor of complex I. Molecular dynamics simulations and ab initio calculations. 2008 , 112, 7426-38	9
1623	Ab initio fragment molecular orbital study of molecular interactions between liganded retinoid X receptor and its coactivator; part II: influence of mutations in transcriptional activation function 2 activating domain core on the molecular interactions. 2008 , 112, 1986-98	37
1622	Antibody recognition and conformational flexibility of a plaque-specific beta-amyloid epitope modulated by non-native peptide flanking regions. 2008 , 51, 1150-61	4

1621	Molecular dynamics simulations for water and ions in protein crystals. 2008, 24, 4215-23	34
1620	Counterion binding in the aqueous solutions of bile acid salts, as studied by computer simulation methods. 2008 , 24, 10729-36	22
1619	Properties of free surface of water-methanol mixtures. Analysis of the truly interfacial molecular layer in computer simulation. 2008 , 112, 5428-38	61
1618	Investigation of Fullerene Solutions by the Molecular Dynamics Method. 2008 , 16, 555-562	5
1617	Coarse master equations for peptide folding dynamics. 2008 , 112, 6057-69	384
1616	Identification of phosphorylation sites of TOPORS and a role for serine 98 in the regulation of ubiquitin but not SUMO E3 ligase activity. 2008 , 47, 13887-96	8
1615	Protein structure and dynamics in ionic liquids. Insights from molecular dynamics simulation studies. 2008 , 112, 2566-72	182
1614	A temperature predictor for parallel tempering simulations. 2008 , 10, 2073-7	352
1613	Biophysical Techniques in Photosynthesis. 2008,	12
1612	Temperature dependence of dimerization and dewetting of large-scale hydrophobes: a molecular dynamics study. 2008 , 112, 8634-44	77
1611	Dielectric properties tangential to the interface in model insoluble monolayers: theoretical assessment. 2008 , 24, 4615-24	7
1610	Comparative molecular dynamics studies of wild-type and oxidized forms of full-length Alzheimer amyloid beta-peptides Abeta(1-40) and Abeta(1-42). 2008 , 112, 7123-31	55
1609	Sticking coefficient and processing of water vapor on organic-coated nanoaerosols. 2008, 112, 966-72	31
1608	Structural transitions in ion coordination driven by changes in competition for ligand binding. 2008 , 130, 15405-19	59
1607	Stable hairpins with beta-peptides: route to tackle protein-protein interactions. 2008, 112, 7581-91	8
1606	Role of the familial Dutch mutation E22Q in the folding and aggregation of the 15-28 fragment of the Alzheimer amyloid-beta protein. 2008 , 105, 6027-32	70
1605	Mutation of Gly-11 on the dimer interface results in the complete crystallographic dimer dissociation of severe acute respiratory syndrome coronavirus 3C-like protease: crystal structure with molecular dynamics simulations. 2008 , 283, 554-564	57
1604	Influence of cis double-bond parametrization on lipid membrane properties: how seemingly insignificant details in force-field change even qualitative trends. 2008 , 129, 105103	48

1603	NMR and MD studies of the temperature-dependent dynamics of RNA YNMG-tetraloops. 2008 , 36, 1928-40	50
1602	Computing the stability diagram of the Trp-cage miniprotein. 2008 , 105, 17754-9	133
1601	Molecular dynamics simulations of the Apo-, Holo-, and acyl-forms of Escherichia coli acyl carrier protein. 2008 , 283, 33620-9	38
1600	Spontaneous conformational change and toxin binding in alpha7 acetylcholine receptor: insight into channel activation and inhibition. 2008 , 105, 8280-5	41
1599	A molecular dynamics study of the motion of a nanodroplet of pure liquid on a wetting gradient. 2008 , 129, 164708	35
1598	Identification and rational redesign of peptide ligands to CRIP1, a novel biomarker for cancers. 2008 , 4, e1000138	42
1597	Effects of active site mutations in haemoglobin I from Lucina pectinata: a molecular dynamic study. 2008 , 34, 715-725	4
1596	Chromophore protonation state controls photoswitching of the fluoroprotein asFP595. 2008 , 4, e1000034	89
1595	The effect of salt on the melting of ice: A molecular dynamics simulation study. 2008, 129, 124504	36
1594	Functional and structural roles of conserved cysteine residues in the carboxyl-terminal domain of the follicle-stimulating hormone receptor in human embryonic kidney 293 cells. 2008 , 78, 869-82	36
1593	A diffusive anomaly of water in aqueous sodium chloride solutions at low temperatures. 2008 , 112, 1729-35	30
1592	Two amino acid substitutions within the first external loop of CCR5 induce human immunodeficiency virus-blocking antibodies in mice and chickens. 2008 , 82, 4125-34	19
1591	Test of the Gouy-Chapman theory for a charged lipid membrane against explicit-solvent molecular dynamics simulations. 2008 , 101, 038103	40
1590	Calculating free-energy profiles in biomolecular systems from fast nonequilibrium processes. 2008 , 78, 051913	29
1589	Biochemical and structural investigations of Bothropstoxin-II, a myotoxic Asp49 phospholipase A2 from Bothrops jararacussu venom. 2008 , 15, 1002-8	13
1588	In silico study on the effect of F19T mutation on amyloid-beta peptide (10-35). 2008 , 13, 3951-65	
1587	Electroporating fields target oxidatively damaged areas in the cell membrane. 2009, 4, e7966	99
1586	Molecular Dynamics Computations for Proteins: A Case Study in Membrane Ion Permeation. 2009,	

1585	Towards temperature-dependent coarse-grained potentials of side-chain interactions for protein folding simulations. I: molecular dynamics study of a pair of methane molecules in water at various temperatures. 2009 , 22, 547-52	20
1584	Adaptive anisotropic kernels for nonparametric estimation of absolute configurational entropies in high-dimensional configuration spaces. 2009 , 80, 011913	19
1583	Structural rearrangements of rhodopsin subunits in a dimer complex: a molecular dynamics simulation study. 2009 , 27, 127-47	40
1582	Desipramine induces disorder in cholesterol-rich membranes: implications for viral trafficking. 2009 , 6, 046004	9
1581	MOLECULAR DYNAMICS STUDY OF THE TRANSCRIPTIONAL RECOGNITION MECHANISM OF HEME ACTIVATE PROTEIN (HAP). 2009 , 08, 1-18	1
1580	Temperature-dependent wettability on a titanium dioxide surface. 2009 , 35, 31-37	38
1579	A MOLECULAR DYNAMICS SIMULATION STUDY OF CONFORMATIONAL CHANGES AND SOLVATION OF APPEPTIDE IN TRIFLUOROETHANOL AND WATER. 2009 , 08, 215-231	16
1578	Green tea catechins in chemoprevention of cancer: a molecular docking investigation into their interaction with glutathione S-transferase (GST P1-1). 2009 , 24, 287-95	19
1577	A kinetic model of trp-cage folding from multiple biased molecular dynamics simulations. 2009 , 5, e1000452	217
1576	Conformational effects of Lys191 in the human GnRH receptor: mutagenesis and molecular dynamics simulations studies. 2009 , 201, 297-307	13
1575	On violations of Le Chatelier's principle for a temperature change in small systems observed for short times. 2009 , 131, 214503	5
1574	Salt induced asymmetry in membrane simulations by partial restriction of ionic motion. 2009 , 130, 195105	14
1573	Conformational changes and slow dynamics through microsecond polarized atomistic molecular simulation of an integral Kv1.2 ion channel. 2009 , 5, e1000289	96
1572	Conformationally rigid nucleoside probes help understand the role of sugar pucker and nucleobase orientation in the thrombin-binding aptamer. 2009 , 37, 5589-601	33
1571	Molecular dynamic study of subtilisin Carlsberg in aqueous and nonaqueous solvents. 2009 , 35, 205-212	12
1570	Modeling signal propagation mechanisms and ligand-based conformational dynamics of the Hsp90 molecular chaperone full-length dimer. 2009 , 5, e1000323	125
1569	Removing systematic errors in interionic potentials of mean force computed in molecular simulations using reaction-field-based electrostatics. 2009 , 130, 104106	21
1568	Translational, rotational and internal dynamics of amyloid beta-peptides (Abeta40 and Abeta42) from molecular dynamics simulations. 2009 , 131, 155103	15

1567	Progress and challenges in the automated construction of Markov state models for full protein systems. 2009 , 131, 124101		303	
1566	Molecular dynamics calculations suggest a conduction mechanism for the M2 proton channel from influenza A virus. 2009 , 106, 1069-74		103	
1565	Differences in conformational dynamics of [Pt3(HPTAB)]6+-DNA adducts with various cross-linking modes. 2009 , 37, 5930-42		13	
1564	Protein contents in biological membranes can explain abnormal solvation of charged and polar residues. 2009 , 106, 15684-9		59	
1563	Insights into how nucleotide-binding domains power ABC transport. 2009 , 17, 1213-22		38	
1562	Synthesis, modelling, and antimitotic properties of tricyclic systems characterised by a 2-(5-Phenyl-1H-pyrrol-3-yl)-1,3,4-oxadiazole moiety. 2009 , 4, 998-1009		15	
1561	Discovery of plasmepsin inhibitors by fragment-based docking and consensus scoring. 2009 , 4, 1317-26		44	
1560	Probing the free energy landscape of the FBP28WW domain using multiple techniques. <i>Journal of Computational Chemistry</i> , 2009 , 30, 1059-68	3.5	6	
1559	GolP: an atomistic force-field to describe the interaction of proteins with Au(111) surfaces in water. Journal of Computational Chemistry, 2009 , 30, 1465-76	3.5	207	
1558	MILCH SHAKE: an efficient method for constraint dynamics applied to alkanes. <i>Journal of Computational Chemistry</i> , 2009 , 30, 2485-93	3.5	38	
1557	Molecular dynamics simulation study of association in trifluoroethanol/water mixtures. <i>Journal of Computational Chemistry</i> , 2010 , 31, 286-94	3.5	16	
1556	Assessment of biomolecular force fields for molecular dynamics simulations in a protein crystal. Journal of Computational Chemistry, 2010 , 31, 371-80	3.5	30	
1555	Efficient nonbonded interactions for molecular dynamics on a graphics processing unit. <i>Journal of Computational Chemistry</i> , 2010 , 31, 1268-72	3.5	88	
1554	Force field-dependent structural divergence revealed during long time simulations of Calbindin d9k. <i>Journal of Computational Chemistry</i> , 2010 , 31, 1864-72	3.5	12	
1553	Dioxygen and nitric oxide pathways and affinity to the catalytic site of rubredoxin:oxygen oxidoreductase from Desulfovibrio gigas. 2009 , 14, 853-62		16	
1552	Molecular modeling and dynamics studies of purine nucleoside phosphorylase from Bacteroides fragilis. 2009 , 15, 913-22		4	
1551	Evolutionarily evolved discriminators in the 3-TPR domain of the Toc64 family involved in protein translocation at the outer membrane of chloroplasts and mitochondria. 2009 , 15, 971-82		24	
1550	Parameterization of aromatic azido groups: application as photoaffinity probes in molecular dynamics studies. 2009 , 15, 1291-7		10	

1549	Molecular dynamics simulation of a mixed lipid emulsion model: Influence of the triglycerides on interfacial phospholipid organization. 2009 , 901, 174-185	16
1548	Islet neogenesis associated protein (ingap): structural and dynamical properties of its active pentadecapeptide. 2009 , 27, 701-5	4
1547	Conformational flexibility decreased due to Y67F and F82H mutations in cytochrome c: molecular dynamics simulation studies. 2009 , 28, 270-7	12
1546	?-SHAKE: An extension to SHAKE for the explicit treatment of angular constraints. 2009 , 180, 360-364	8
1545	Molecular dynamics study of the interaction between fatty acid binding proteins with palmitate mini-micelles. 2009 , 326, 29-33	10
1544	Calcium binding to the purple membrane: A molecular dynamics study. 2009 , 74, 669-81	5
1543	Molecular dynamics of amicyanin reveals a conserved dynamical core for blue copper proteins. 2009 , 74, 961-71	6
1542	An all-atom structure-based potential for proteins: bridging minimal models with all-atom empirical forcefields. 2009 , 75, 430-41	270
1541	Spontaneous beta-helical fold in prion protein: the case of PrP(82-146). 2009, 75, 964-76	5
1540	Inclusion of ionization states of ligands in affinity calculations. 2009 , 76, 138-50	9
1539	Conformational dynamics of the EGFR kinase domain reveals structural features involved in activation. 2009 , 76, 375-86	23
1538	Folding simulations of Trp-cage mini protein in explicit solvent using biasing potential replica-exchange molecular dynamics simulations. 2009 , 76, 448-60	48
1537	Different mechanisms of action of antimicrobial peptides: insights from fluorescence spectroscopy experiments and molecular dynamics simulations. 2009 , 15, 550-8	72
1536	Insights into the anthrax lethal factor-substrate interaction and selectivity using docking and molecular dynamics simulations. 2009 , 18, 1774-85	10
1535	Structures of the multicomponent Rieske non-heme iron toluene 2,3-dioxygenase enzyme system. 2009 , 65, 24-33	41
1534	Helical extension of the neuronal SNARE complex into the membrane. 2009 , 460, 525-8	311
1533	Water behavior in the neighborhood of hydrophilic and hydrophobic membranes: Lessons from molecular dynamics simulations. 2009 , 388, 4551-4559	8
1532	Prediction of partition coefficients and infinite dilution activity coefficients of 1-ethylpropylamine and 3-methyl-1-pentanol using force field methods. 2009 , 285, 19-23	13

1531	simulations: Spontaneous formation of elongated hemimicelles. 2009 , 329, 351-6	13
1530	High-ionic-strength electroosmotic flows in uncharged hydrophobic nanochannels. 2009 , 330, 194-200	17
1529	Rational design of Tamiflu derivatives targeting at the open conformation of neuraminidase subtype 1. 2009 , 28, 203-19	17
1528	Overhauser dynamic nuclear polarization and molecular dynamics simulations using pyrroline and piperidine ring nitroxide radicals. 2009 , 200, 137-41	20
1527	Wetting of hydrophobic substrates by nanodroplets of aqueous trisiloxane and alkyl polyethoxylate surfactant solutions. 2009 , 64, 4657-4667	37
1526	Molecular dynamics study of a phospholipid monolayer at a water/triglyceride interface: towards lipid emulsion modelling. 2009 , 157, 86-93	23
1525	Separation of amino acids in glucose isomerase crystal: insight from molecular dynamics simulations. 2009 , 1216, 5122-9	11
1524	Mapping of suramin binding sites on the group IIA human secreted phospholipase A2. 2009 , 37, 41-5	4
1523	Penetratin and derivatives acting as antifungal agents. 2009 , 44, 212-28	27
1522	Molecular modeling, dynamics and docking studies of purine nucleoside phosphorylase from Streptococcus pyogenes. 2009 , 142, 7-16	9
1521	Stability improvement of the fatty acid binding protein Sm14 from S. mansoni by Cys replacement: structural and functional characterization of a vaccine candidate. 2009 , 1794, 655-62	24
1520	Simulation of DNA double-strand dissociation and formation during replica-exchange molecular dynamics simulations. 2009 , 11, 10589-95	38
1519	Molecular dynamics simulation of water in cytochrome c oxidase reveals two water exit pathways and the mechanism of transport. 2009 , 1787, 1140-50	37
1518	Atypical mechanism of conduction in potassium channels. 2009 , 106, 16074-7	87
1517	Reaction pathway and free-energy barrier for reactivation of dimethylphosphoryl-inhibited human acetylcholinesterase. 2009 , 113, 16226-36	39
1516	Molecular dynamics simulations on binding models of Dervan-type polyamide + Cu(II) nuclease ligands to DNA. 2009 , 113, 839-48	16
1515	An elemental mercury diffusion coefficient for natural waters determined by molecular dynamics simulation. 2009 , 43, 3183-6	50
1514	Molecular binding of catechins to biomembranes: relationship to biological activity. 2009 , 57, 6720-8	116

1513	Structure of the Liquid Vapor Interface of Water Acetonitrile Mixtures As Seen from Molecular Dynamics Simulations and Identification of Truly Interfacial Molecules Analysis. 2009 , 113, 18173-18183	40
1512	Why is the sn-2 chain of monounsaturated glycerophospholipids usually unsaturated whereas the sn-1 chain is saturated? Studies of 1-stearoyl-2-oleoyl-sn-glycero-3-phosphatidylcholine (SOPC) and 1-oleoyl-2-stearoyl-sn-glycero-3-phosphatidylcholine (OSPC) membranes with and without	21
1511	Explicit- and Implicit-Solvent Molecular Dynamics Simulations of Complex Formation between Polycations and Polyanions. 2009 , 42, 8851-8863	41
1510	Ionic surfactant aggregates in saline solutions: sodium dodecyl sulfate (SDS) in the presence of excess sodium chloride (NaCl) or calcium chloride (CaCl(2)). 2009 , 113, 5863-70	173
1509	Chiral separation of racemic phenylglycines in thermolysin crystal: a molecular simulation study. 2009 , 113, 15851-7	12
1508	Molecular dynamics simulation study of the binding of purine bases to the aptamer domain of the guanine sensing riboswitch. 2009 , 37, 4774-86	69
1507	Low free energy barrier for ion permeation through double-helical gramicidin. 2009 , 113, 3195-202	13
1506	Characterization of the cationic DiC(14)-amidine bilayer by mixed DMPC/DiC(14)-amidine molecular dynamics simulations shows an interdigitated nonlamellar bilayer phase. 2009 , 25, 5230-8	9
1505	Hydrophobic Interactions and Dewetting between Plates with Hydrophobic and Hydrophilic Domains. 2009 , 113, 5244-5253	93
1504	Factors that affect the degree of twist in beta-sheet structures: a molecular dynamics simulation study of a cross-beta filament of the GNNQQNY peptide. 2009 , 113, 1728-37	54
1503	Structural and kinetic properties of alpha-tocopherol in phospholipid bilayers, a molecular dynamics simulation study. 2009 , 113, 16537-46	20
1502	Energy landscape of the trpzip2 peptide. 2009 , 113, 8288-95	24
1501	Molecular view of cholesterol flip-flop and chemical potential in different membrane environments. 2009 , 131, 12714-20	222
1500	Systematic coarse-graining of a multicomponent lipid bilayer. 2009 , 113, 1501-10	92
1499	Computational studies of Texas Red-1,2-dihexadecanoyl-sn-glycero-3-phosphoethanolamine-model building and applications. 2009 , 113, 8758-66	29
1498	Solubilization of poly{1,4-phenylene-[9,9-bis(4-phenoxy-butylsulfonate)]fluorene-2,7-diyl} in water by nonionic amphiphiles. 2009 , 25, 5545-56	34
1497	Interaction of the Tim44 C-terminal domain with negatively charged phospholipids. 2009 , 48, 11185-95	33
1496	Ion dynamics in cationic lipid bilayer systems in saline solutions. 2009 , 113, 9226-34	37

1495	Dynamics of the streptavidin-biotin complex in solution and in its crystal lattice: distinct behavior revealed by molecular simulations. 2009 , 113, 6971-85	30
1494	Relating the diffusion of small ligands in human neuroglobin to its structural and mechanical properties. 2009 , 113, 16257-67	41
1493	Exploring molecular mechanisms of ligand recognition by opioid receptors with metadynamics. 2009 , 48, 10020-9	71
1492	Creating conformational entropy by increasing interdomain mobility in ligand binding regulation: a revisit to N-terminal tandem PDZ domains of PSD-95. 2009 , 131, 787-96	48
1491	Binding ensemble profiling with photoaffinity labeling (BEProFL) approach: mapping the binding poses of HDAC8 inhibitors. 2009 , 52, 7003-13	39
1490	A solution NMR approach to the measurement of amphiphile immersion depth and orientation in membrane model systems. 2009 , 131, 6452-9	25
1489	Structure Prediction of Bis(amino acidato)copper(II) Complexes with a New Force Field for Molecular Modeling. 2009 , 5, 1940-54	22
1488	Experimental and simulation studies of a real-time polymerase chain reaction in the presence of a fullerene derivative. 2009 , 20, 415101	21
1487	Molecular Level Properties of the WaterDichloromethane Liquid/Liquid Interface, as Seen from Molecular Dynamics Simulation and Identification of Truly Interfacial Molecules Analysis. 2009 , 113, 19263-193	2 1 8
1486	Characterization of temperature dependent and substrate-binding cleft movements in Bacillus circulans family 11 xylanase: a molecular dynamics investigation. 2009 , 1790, 1301-6	24
1485	Alamethicin in lipid bilayers: combined use of X-ray scattering and MD simulations. 2009, 1788, 1387-97	85
1484	Membrane perturbation by the antimicrobial peptide PMAP-23: a fluorescence and molecular dynamics study. 2009 , 1788, 1523-33	58
1483	Mixed modes in opening of KcsA potassium channel from a targeted molecular dynamics simulation. 2009 , 388, 86-90	4
1482	SMase II, a new sphingomyelinase D from Loxosceles laeta venom gland: molecular cloning, expression, function and structural analysis. 2009 , 53, 743-53	31
1481	Design of novel histone-derived antimicrobial peptides. 2009 , 30, 2168-73	21
1480	Dynamics, energetics, and selectivity of the low-K+ KcsA channel structure. 2009 , 389, 637-45	35
1479	Microscopic factors that control beta-sheet registry in amyloid fibrils formed by fragment 11-25 of amyloid beta peptide: insights from computer simulations. 2009 , 389, 921-37	12
1478	Molecular simulation studies of monovalent counterion-mediated interactions in a model RNA kissing loop. 2009 , 390, 805-19	64

1477	SDS surfactants on carbon nanotubes: aggregate morphology. 2009 , 3, 595-602	221
1476	Thermodynamics of flip-flop and desorption for a systematic series of phosphatidylcholine lipids. 2009 , 5, 3295	97
1475	Titratable amino acid solvation in lipid membranes as a function of protonation state. 2009 , 113, 245-53	32
1474	Structural stability of electrosprayed proteins: temperature and hydration effects. 2009, 11, 8069-78	43
1473	Calcium binding and head group dipole angle in phosphatidylserine-phosphatidylcholine bilayers. 2009 , 25, 1020-7	72
1472	Determinants of water permeability through nanoscopic hydrophilic channels. 2009 , 96, 925-38	30
1471	Association of helical beta-peptides and their aggregation behavior from the potential of mean force in explicit solvent. 2009 , 96, 4349-62	13
1470	Molecular renormalization group coarse-graining of polymer chains: application to double-stranded DNA. 2009 , 96, 4044-52	70
1469	Molecular model of a cell plasma membrane with an asymmetric multicomponent composition: water permeation and ion effects. 2009 , 96, 4493-501	63
1468	Alternative mechanisms for the interaction of the cell-penetrating peptides penetratin and the TAT peptide with lipid bilayers. 2009 , 97, 40-9	143
1467	Molecular dynamics simulations of DNA-polycation complex formation. 2009, 97, 1971-83	78
1466	Secondary structure propensities in peptide folding simulations: a systematic comparison of molecular mechanics interaction schemes. 2009 , 97, 599-608	101
1465	Induced beta-barrel formation of the Alzheimer's Abeta25-35 oligomers on carbon nanotube surfaces: implication for amyloid fibril inhibition. 2009 , 97, 1795-803	76
1464	Common structural transitions in explicit-solvent simulations of villin headpiece folding. 2009 , 97, 2338-47	130
1463	Membrane binding by the endophilin N-BAR domain. 2009 , 97, 2746-53	50
1462	Undulation contributions to the area compressibility in lipid bilayer simulations. 2009 , 97, 2754-60	68
1461	Binding of the bacteriophage P22 N-peptide to the boxB RNA motif studied by molecular dynamics simulations. 2009 , 97, 3139-49	25
1460	Molecular dynamics simulations of threadlike cetyltrimethylammonium chloride micelles: effects of sodium chloride and sodium salicylate salts. 2009 , 113, 13697-710	89

1459	The role of lipid composition for insertion and stabilization of amino acids in membranes. 2009 , 130, 185101	56
1458	Staggered Mesh Ewald: An extension of the Smooth Particle-Mesh Ewald method adding great versatility. 2009 , 5, 2322	97
1457	Effect of headgroup size, charge, and solvent structure on polymer-micelle interactions, studied by molecular dynamics simulations. 2009 , 113, 15170-80	25
1456	On the possibility of the amphotericin B-sterol complex formation in cholesterol- and ergosterol-containing lipid bilayers: a molecular dynamics study. 2009 , 113, 15875-85	37
1455	Retardation of ice crystallization by short peptides. 2009 , 113, 4403-7	20
1454	Rational design of ion force fields based on thermodynamic solvation properties. 2009 , 130, 124507	197
1453	GM1 ganglioside embedded in a hydrated DOPC membrane: a molecular dynamics simulation study. 2009 , 113, 4876-86	20
1452	An insight into the thermostability of a pair of xylanases: the role of hydrogen bonds. 2009 , 107, 59-69	35
1451	Structure and dynamics of glyceride lipid formulations, with propylene glycol and water. 2009 , 6, 604-14	28
1450	Molecular dynamics simulations of ammonium surfactant monolayers at the heptane/water interface. 2009 , 113, 12680-6	20
1449	Combining an Elastic Network With a Coarse-Grained Molecular Force Field: Structure, Dynamics, and Intermolecular Recognition. 2009 , 5, 2531-43	397
1448	Steered molecular dynamics simulations reveal the likelier dissociation pathway of imatinib from its targeting kinases c-Kit and Abl. 2009 , 4, e8470	37
1447	Coarse-grained molecular dynamics simulation of ammonium surfactant self-assemblies: micelles and vesicles. 2009 , 113, 15010-6	49
1446	An improved united atom force field for simulation of mixed lipid bilayers. 2009 , 113, 2748-63	235
1445	Thermodynamic analysis of the effect of cholesterol on dipalmitoylphosphatidylcholine lipid membranes. 2009 , 131, 1972-8	133
1444	Molecular dynamics study of biomembrane/local anesthetics interactions. 2009, 107, 1437-1443	17
1443	Temperature-dependent mechanisms for the dynamics of protein-hydration waters: a molecular dynamics simulation study. 2009 , 113, 9386-92	35
1442	Synthesis, binding, and modeling studies of new cytisine derivatives, as ligands for neuronal nicotinic acetylcholine receptor subtypes. 2009 , 52, 4345-57	33

1441	Structural characterization on the gel to liquid-crystal phase transition of fully hydrated DSPC and DSPE bilayers. 2009 , 113, 8114-23	46
1440	Dynamic Behavior of Interfacial Water at the Silica Surface. 2009 , 113, 19591-19600	115
1439	Molecular renormalization group coarse-graining of electrolyte solutions: application to aqueous NaCl and KCl. 2009 , 113, 7785-93	68
1438	Encapsulation of myoglobin in a cetyl trimethylammonium bromide micelle in vacuo: a simulation study. 2009 , 48, 1006-15	32
1437	Dynamic nuclear polarization of water by a nitroxide radical: rigorous treatment of the electron spin saturation and comparison with experiments at 9.2 Tesla. 2009 , 11, 6638-53	40
1436	Dynamic nuclear polarization coupling factors calculated from molecular dynamics simulations of a nitroxide radical in water. 2009 , 11, 6626-37	69
1435	Self-assembling dipeptides: conformational sampling in solvent-free coarse-grained simulation. 2009 , 11, 2077-86	73
1434	Self-assembling dipeptides: including solvent degrees of freedom in a coarse-grained model. 2009 , 11, 2068-76	51
1433	A theoretical spin relaxation and molecular dynamics simulation study of the Gd(H2O)9(3+) complex. 2009 , 11, 10368-76	24
1432	A potential mechanism for Cu2+ reduction, beta-cleavage, and beta-sheet initiation within the N-terminal domain of the prion protein: insights from density functional theory and molecular dynamics calculations. 2009 , 72, 1040-59	15
1431	Conformational behaviour determines the low-relaxivity state of a conditional MRI contrast agent. 2009 , 11, 3943-50	12
1430	Are current semiempirical methods better than force fields? A study from the thermodynamics perspective. 2009 , 113, 11938-48	47
1429	Lipid Models for United-Atom Molecular Dynamics Simulations of Proteins. 2009 , 5, 615-26	209
1428	Detection of functional modes in protein dynamics. 2009 , 5, e1000480	107
1427	Water permeation through stratum corneum lipid bilayers from atomistic simulations. 2009 , 5, 4549	52
1426	Hydration structure on crystalline silica substrates. 2009 , 25, 8025-35	84
1425	Molecular dynamics study of the effect of cholesterol on the properties of lipid monolayers at low surface tensions. 2009 , 11, 1916-22	37
1424	Umbrella sampling simulations of biotin carboxylase: is a structure with an open ATP grasp domain stable in solution?. 2009 , 113, 10097-103	6

1423	Location, tilt, and binding: a molecular dynamics study of voltage-sensitive dyes in biomembranes. 2009 , 113, 15807-19	31
1422	In silico study of full-length amyloid beta 1-42 tri- and penta-oligomers in solution. 2009 , 113, 11710-9	79
1421	Curvature effects on the adsorption of aqueous sodium-dodecyl-sulfate surfactants on carbonaceous substrates: structural features and counterion dynamics. 2009 , 80, 021408	51
1420	How Does Solute-Polarization Affect the Hydrophobic Hydration of Methane?. 2009 , 223, 1091-1104	8
1419	Correlation of Static and Dynamic Heterogeneities in Supercooled Water by Means of Molecular Dynamics Simulations. 2009 , 223, 1001-1010	5
1418	Simulated tempering distributed replica sampling: A practical guide to enhanced conformational sampling. 2010 , 256, 012011	2
1417	On the Importance of LennardIlones Parameter Calibration in QM/MM Framework: Reaction Path Tracing via Free Energy Gradient Method for Ammonia Ionization Process in Aqueous Solution. 2010 , 83, 486-494	16
1416	The role of L-arginine in inclusion complexes of omeprazole with cyclodextrins. 2010 , 11, 233-40	29
1415	Dielectric Interpretation of Specificity of Ion Pairing in Water. 2010 , 1, 300-303	38
1414	Effects of Na+, K+, and Ca2+ on the structures of anionic lipid bilayers and biological implication. 2010 , 114, 16978-88	20
1413	Parametrization and application of a coarse grained force field for benzene/fullerene interactions with lipids. 2010 , 114, 16364-72	29
1412	Effect of the Integration Method on the Accuracy and Computational Efficiency of Free Energy Calculations Using Thermodynamic Integration. 2010 , 6, 1018-1027	71
1411	Effects of bundling on the properties of the SPC water model. 2010 , 125, 335-344	57
1410	Life cycle of an electropore: field-dependent and field-independent steps in pore creation and annihilation. 2010 , 236, 27-36	167
1409	Desolvation of polymers by ultrafast heating: Influence of hydrophilicity. 2010 , 101, 71-76	4
1408	Binding of curcumin with glyoxalase I: Molecular docking, molecular dynamics simulations, and kinetics analysis. 2010 , 147, 28-34	46
1407	Simulation studies of the insolubility of cellulose. 2010 , 345, 2060-6	135
1406	Direct calculation of FEster orientation factor of membrane probes by molecular simulation. 2010 , 946, 107-112	15

1405	Molecular modeling study on orphan human protein CYP4A22 for identification of potential ligand binding site. 2010 , 28, 524-32		15
1404	The solution structures of the cucumber mosaic virus and tomato aspermy virus coat proteins explored with molecular dynamics simulations. 2010 , 28, 569-76		7
1403	Insight into ligand selectivity in HCV NS5B polymerase: molecular dynamics simulations, free energy decomposition and docking. 2010 , 16, 49-59		18
1402	Probing ligand binding modes of Mycobacterium tuberculosis MurC ligase by molecular modeling, dynamics simulation and docking. 2010 , 16, 77-85		18
1401	Probing possible egress channels for multiple ligands in human CYP3A4: a molecular modeling study. 2010 , 16, 607-14		23
1400	Insight into the interaction sites between fatty acid binding proteins and their ligands. 2010 , 16, 929-38		11
1399	Molecular dynamics simulation of nanoscale liquid flows. 2010 , 9, 1011-1031		112
1398	Phosphorylation and ATP-binding induced conformational changes in the PrkC, Ser/Thr kinase from B. subtilis. 2010 , 24, 733-47		5
1397	How does heparin prevent the pH inactivation of cathepsin B? Allosteric mechanism elucidated by docking and molecular dynamics. 2010 , 11 Suppl 5, S5		21
1396	Unraveling the molecular mechanisms of nitrogenase conformational protection against oxygen in diazotrophic bacteria. 2010 , 11 Suppl 5, S7		12
1395	Molecular dynamics simulations of human and dog gastric lipases: insights into domain movements. 2010 , 584, 4599-605		21
1394	Molecular dynamics simulation of the adsorption of oxalic acid on an ice surface. 2010 , 11, 3971-9		13
1393	Adsorption of hydroxyacetone on pure ice surfaces. 2010 , 11, 3921-7		11
1392	Free energy profiles of amino acid side chain analogs near water-vapor interface obtained via MD simulations. <i>Journal of Computational Chemistry</i> , 2010 , 31, 204-16	3.5	11
1391	A new force field for simulating phosphatidylcholine bilayers. <i>Journal of Computational Chemistry</i> , 2010 , 31, 1117-25	3.5	261
1390	Atomistic insight into chondroitin-6-sulfate glycosaminoglycan chain through quantum mechanics calculations and molecular dynamics simulation. <i>Journal of Computational Chemistry</i> , 2010 , 31, 1670-80	3.5	9
1389	Polypeptide folding on a conformational-space network: dependence of network topology on the structural discretization procedure. <i>Journal of Computational Chemistry</i> , 2010 , 31, 1889-903	3.5	1
1388	Incorporation of deMon2k as a new parallel quantum mechanical code for the PUPIL system. <i>Journal of Computational Chemistry</i> , 2010 , 31, 2669-76	3.5	4

(2010-2010)

1387	New parameterization approaches of the LIE method to improve free energy calculations of PlmII-Inhibitors complexes. <i>Journal of Computational Chemistry</i> , 2010 , 31, 2723-34	14	
1386	VCD spectroscopic properties of the beta-hairpin forming miniprotein CLN025 in various solvents. 2010 , 93, 442-50	13	
1385	Conformational dynamics of active site loop in Escherichia coli phytase. 2010 , 93, 994-1002	11	
1384	Sugar treatment of human lipoprotein particles and their separation by capillary electrophoresis. 2010 , 33, 2528-35	5	
1383	Comparison of the complexation between methylprednisolone and different cyclodextrins in solution by 1H-NMR and molecular modeling studies. 2010 , 99, 3863-73	20	
1382	Computer simulation and ITIM analysis of the surface of waterthethanol mixtures containing traces of water. 2010 , 153, 88-93	23	
1381	Understanding the HIV-1 protease nelfinavir resistance mutation D30N in subtypes B and C through molecular dynamics simulations. 2010 , 29, 137-47	22	
1380	Tetrapyrrole binding affinity of the murine and human p22HBP heme-binding proteins. 2010 , 29, 396-405	9	
1379	Computational analysis of water residence on ceramide and sphingomyelin bilayer membranes. 2010 , 29, 461-9	12	
1378	Effects of commercial non-ionic alkyl oxyethylene and ionic biocompatible arginine-based surfactants on the photophysical behaviour of several poly(fluorene-1,4-phenylene)s. 2010 , 156, 18-27	10	
1377	Molecular simulation of the hydration Gibbs energy of barbiturates. 2010 , 289, 148-155	15	
1376	Molecular simulation of absolute hydration Gibbs energies of polar compounds. 2010 , 296, 110-115	16	
1375	Structure and conformation of HIV fusion inhibitor peptide T-1249 in presence of model membranes: A molecular dynamics study. 2010 , 946, 119-124	8	
1374	Analysis of binding modes of ligands to multiple conformations of CYP3A4. 2010 , 1804, 2036-45	24	
1373	Isoform-selective inhibition of chrysin towards human cytochrome P450 1A2. Kinetics analysis, molecular docking, and molecular dynamics simulations. 2010 , 20, 6008-12	22	
1372	End-point calculation of solvation free energy of amino-acid analogs by molecular theories of solution. 2010 , 496, 351-355	64	
1371	Phase solubility, 1H NMR and molecular modelling studies of bupivacaine hydrochloride complexation with different cyclodextrin derivates. 2010 , 500, 347-354	20	
1370	Prediction of microscopic structure and physical properties of complex fluid mixtures based on molecular simulation. 2010 , 296, 125-132	11	

1369	Investigation and improvement of DNA cleavage models of polyamide + Cu(II) nuclease + OOH-ligands bound to DNA. 2010 , 10, 35	3
1368	Conformational preference of ChaK1 binding peptides: a molecular dynamics study. 2010 , 3, 2	2
1367	Computational Modeling of Human Paraoxonase 1: Preparation of Protein Models, Binding Studies, and Mechanistic Insights. 2010 , 23, 357-369	17
1366	Molecular mechanism of allosteric communication in the human PPARalpha-RXRalpha heterodimer. 2010 , 78, 873-87	17
1365	Multi-scale characterization of the energy landscape of proteins with application to the C3D/Efb-C complex. 2010 , 78, 1004-14	5
1364	Studying pressure denaturation of a protein by molecular dynamics simulations. 2010 , 78, 1641-51	31
1363	Application of biasing-potential replica-exchange simulations for loop modeling and refinement of proteins in explicit solvent. 2010 , 78, 2809-19	27
1362	Molecular modeling-based evaluation of hTLR10 and identification of potential ligands in Toll-like receptor signaling. 2010 , 5, e12713	64
1361	Differential stability of 2'F-ANA*RNA and ANA*RNA hybrid duplexes: roles of structure, pseudohydrogen bonding, hydration, ion uptake and flexibility. 2010 , 38, 2498-511	58
1360	Enhanced sampling and applications in protein folding in explicit solvent. 2010 , 132, 244101	68
1359	Identification of specific lipid-binding sites in integral membrane proteins. 2010 , 285, 10519-26	29
1358	Infrared and Raman line shapes for ice Ih. I. Dilute HOD in H(2)O and D(2)O. 2010 , 132, 204505	80
1357	Molecular dynamics simulation and identification of the truly interfacial molecules (ITIM) analysis of the liquid-vapor interface of dimethyl sulfoxide. 2010 , 132, 134701	29
1356	Computer simulations of aqua metal ions for accurate reproduction of hydration free energies and structures. 2010 , 132, 104505	12
1355	Computational analysis of the binding free energy of H3K9me3 peptide to the tandem tudor domains of JMJD2A. 2010 ,	
1354	The multiscale coarse-graining method. VI. Implementation of three-body coarse-grained potentials. 2010 , 132, 164107	92
1353	Discriminating early stage A{beta}42 monomer structures using chirality-induced 2DIR spectroscopy in a simulation study. 2010 , 107, 15687-92	36
1352	Conformational transitions upon ligand binding: holo-structure prediction from apo conformations. 2010 , 6, e1000634	85

(2010-2010)

1351	Spontaneous quaternary and tertiary T-R transitions of human hemoglobin in molecular dynamics simulation. 2010 , 6, e1000774	48
1350	Distance and angular holonomic constraints in molecular simulations. 2010 , 133, 034114	14
1349	Puckering free energy of pyranoses: A NMR and metadynamics-umbrella sampling investigation. 2010 , 133, 095104	44
1348	Molecular level properties of the free water surface and different organic liquid/water interfaces, as seen from ITIM analysis of computer simulation results. 2010 , 22, 284112	38
1347	Serial tempering without exchange. 2010 , 133, 114113	3
1346	Free energy surfaces for the interaction of D-glucose with planar aromatic groups in aqueous solution. 2010 , 133, 155103	22
1345	Counterion Effects and Dynamics of Parathion in Anionic Lyomesophases. 2010 , 63, 68	1
1344	Binding of influenza A virus hemagglutinin to the sialoside receptor is not controlled by the homotropic allosteric effect. 2010 , 114, 15700-5	35
1343	Understanding the stabilization of liquid-phase-exfoliated graphene in polar solvents: molecular dynamics simulations and kinetic theory of colloid aggregation. 2010 , 132, 14638-48	234
1342	Role of the bile salt surfactant sodium cholate in enhancing the aqueous dispersion stability of single-walled carbon nanotubes: a molecular dynamics simulation study. 2010 , 114, 15616-25	117
1341	Biomolecular Structure and Modeling: Historical Perspective. 2010 , 1-40	
1340	Membrane/Toxin Interaction Energetics via Serial Multiscale Molecular Dynamics Simulations. 2010 , 6, 966-76	14
1339	Arginine-assisted solubilization system for drug substances: solubility experiment and simulation. 2010 , 114, 13455-62	69
1338	An iris-like mechanism of pore dilation in the CorA magnesium transport system. 2010 , 98, 784-92	72
1337	The behavior of the hydrophobic effect under pressure and protein denaturation. 2010 , 98, 1626-31	74
1336	Interactions between a voltage sensor and a toxin via multiscale simulations. 2010 , 98, 1558-65	24
1335	Putative active states of a prototypic g-protein-coupled receptor from biased molecular dynamics. 2010 , 98, 2347-55	52
1334	Protein thermostability calculations using alchemical free energy simulations. 2010 , 98, 2309-16	124

1333	Down-state model of the voltage-sensing domain of a potassium channel. 2010 , 98, 2857-66	29
1332	Atomistic simulations of bicelle mixtures. 2010 , 98, 2895-903	27
1331	RNA polymerase II with open and closed trigger loops: active site dynamics and nucleic acid translocation. 2010 , 99, 2577-86	49
1330	Interaction of salicylate and a terpenoid plant extract with model membranes: reconciling experiments and simulations. 2010 , 99, 3887-94	28
1329	The effects of perfluorination on carbohydrate-pi interactions: computational studies of the interaction of benzene and hexafluorobenzene with fucose and cyclodextrin. 2010 , 12, 7959-67	23
1328	Dynamics-Based Discovery of Allosteric Inhibitors: Selection of New Ligands for the C-terminal Domain of Hsp90. 2010 , 6, 2978-89	70
1327	Molecular Dynamics in Physiological Solutions: Force Fields, Alkali Metal Ions, and Ionic Strength. 2010 , 6, 2167-75	47
1326	Similarities and differences between cyclodextrin-sodium dodecyl sulfate host-guest complexes of different stoichiometries: molecular dynamics simulations at several temperatures. 2010 , 114, 12455-67	46
1325	Water replacement hypothesis in atomic details: effect of trehalose on the structure of single dehydrated POPC bilayers. 2010 , 26, 11118-26	51
1324	Structural and kinetic molecular dynamics study of electroporation in cholesterol-containing bilayers. 2010 , 114, 6855-65	67
1323	Kirkwood-Buff derived force field for alkali chlorides in simple point charge water. 2010 , 132, 024109	32
1322	Elucidation of interactions of Alzheimer amyloid beta peptides (Abeta40 and Abeta42) with insulin degrading enzyme: a molecular dynamics study. 2010 , 49, 3947-56	13
1321	Ion-specific effects under confinement: the role of interfacial water. 2010 , 4, 2035-42	120
1320	Membrane-induced conformational changes of kyotorphin revealed by molecular dynamics simulations. 2010 , 114, 11659-67	19
1319	Surface-Active cis-Pinonic Acid in Atmospheric Droplets: A Molecular Dynamics Study. 2010 , 1, 769-773	71
1318	A Critical Assessment of Methods for the Intrinsic Analysis of Liquid Interfaces: 2. Density Profiles. 2010 , 114, 18656-18663	56
1317	Congruency between biophysical data from multiple platforms and molecular dynamics simulation of the double-super helix model of nascent high-density lipoprotein. 2010 , 49, 7323-43	31
1316	Using molecular dynamics to probe the structural basis for enhanced stability in thermal stable cytochromes P450. 2010 , 49, 6680-6	23

(2010-2010)

1315	Sampling the conformation space of FAD in water-methanol mixtures through molecular dynamics and fluorescence measurements. 2010 , 114, 1017-22	14
1314	Stability and membrane orientation of the fukutin transmembrane domain: a combined multiscale molecular dynamics and circular dichroism study. 2010 , 49, 10796-802	23
1313	Atomistic simulation of hydrophobic matching effects on lipid composition near a helical peptide embedded in mixed-lipid bilayers. 2010 , 114, 8076-80	19
1312	Vibrational Stark effect spectroscopy at the interface of Ras and Rap1A bound to the Ras binding domain of RalGDS reveals an electrostatic mechanism for protein-protein interaction. 2010 , 114, 15331-44	56
1311	Comparative kinetics of cofactor association and dissociation for the human and trypanosomal S-adenosylhomocysteine hydrolases. 3. Role of lysyl and tyrosyl residues of the C-terminal extension. 2010 , 49, 8434-41	5
1310	Driving forces for adsorption of amphiphilic peptides to the air-water interface. 2010 , 114, 11093-101	19
1309	Amino acids at water-vapor interfaces: surface activity and orientational ordering. 2010, 114, 13005-10	5
1308	Multiple N-methylation of MT-II backbone amide bonds leads to melanocortin receptor subtype hMC1R selectivity: pharmacological and conformational studies. 2010 , 132, 8115-28	75
1307	Understanding the protonation behavior of linear polyethylenimine in solutions through Monte Carlo simulations. 2010 , 11, 29-38	131
1306	Computational Studies on Polarization Effects and Selectivity in K+ Channels. 2010 , 6, 3780-3792	21
1305	Disordered versus fibril-like amyloid (25-35) dimers in water: structure and thermodynamics. 2010 , 114, 15288-95	26
1304	A new coarse-grained model for water: the importance of electrostatic interactions. 2010 , 114, 10524-9	150
1303	Which one among aspartyl protease, metallopeptidase, and artificial metallopeptidase is the most efficient catalyst in peptide hydrolysis?. 2010 , 114, 10860-75	19
1302	Toward an improved understanding of the dissociation mechanism of gas phase protein complexes. 2010 , 114, 11646-53	16
1301	Insights into the sliding movement of the lac repressor nonspecifically bound to DNA. 2010 , 114, 2238-45	25
1300	Melting of a beta-hairpin peptide using isotope-edited 2D IR spectroscopy and simulations. 2010 , 114, 10913-24	93
1299	Active-site dynamics and large-scale domain motions of sulfite oxidase: a molecular dynamics study. 2010 , 114, 3266-75	22
1298	Chemical basis for the selectivity of the von Hippel Lindau tumor suppressor pVHL for prolyl-hydroxylated HIF-1alpha. 2010 , 49, 6936-44	14

1297	Long-range effects of confinement on water structure. 2010 , 114, 4246-51	6
1296	Molecular dynamics analysis of the conformations of a beta-hairpin miniprotein. 2010 , 114, 3028-37	22
1295	CCMA: A Robust, Parallelizable Constraint Method for Molecular Simulations. 2010 , 6, 434-437	46
1294	A Critical Assessment of Methods for the Intrinsic Analysis of Liquid Interfaces. 1. Surface Site Distributions. 2010 , 114, 11169-11179	81
1293	Class I phospho-inositide-3-kinases (PI3Ks) isoform-specific inhibition study by the combination of docking and molecular dynamics simulation. 2010 , 50, 136-45	25
1292	Molecular dynamics study of the electric and dielectric properties of model DPPC and dicaprin insoluble monolayers: size effect. 2010 , 26, 8093-105	5
1291	Fusion-relevant changes in lipid shape of hydrated cholesterol hemisuccinate induced by pH and counterion species. 2010 , 114, 14941-6	11
1290	Effects of the RGTFEGKF inhibitor on the structures of the transmembrane fragment 70-86 of glycophorin A: an all-atom molecular dynamics study. 2010 , 114, 1004-9	3
1289	Binding sites of the E. Coli DNA recombinase protein to the ssDNA: a computational study. 2010 , 27, 407-28	17
1288	Potentials of mean force and permeabilities for carbon dioxide, ammonia, and water flux across a Rhesus protein channel and lipid membranes. 2010 , 132, 13251-63	78
1287	Dynamics and structural changes induced by ATP binding in SAV1866, a bacterial ABC exporter. 2010 , 114, 15948-57	39
1286	Insights into the molecular mechanism of an ABC transporter: conformational changes in the NBD dimer of MJ0796. 2010 , 114, 5486-96	29
1285	Crystal structure and molecular modeling study of N-carbamoylsarcosine amidase Ta0454 from Thermoplasma acidophilum. 2010 , 169, 304-11	13
1284	A dynamic model of HIV integrase inhibition and drug resistance. 2010 , 397, 600-15	52
1283	The membrane complex between transducin and dark-state rhodopsin exhibits large-amplitude interface dynamics on the sub-microsecond timescale: insights from all-atom MD simulations. 2010 , 398, 161-73	19
1282	A transmembrane polar interaction is involved in the functional regulation of integrin alpha L beta 2. 2010 , 398, 569-83	11
1281	Membrane docking geometry and target lipid stoichiometry of membrane-bound PKCEC2 domain: a combined molecular dynamics and experimental study. 2010 , 402, 301-10	43
1280	Membrane simulations mimicking acidic pH reveal increased thickness and negative curvature in a bilayer consisting of lysophosphatidylcholines and free fatty acids. 2010 , 1798, 938-46	40

1279	Molecular simulation of the water meniscus in dip-pen nanolithography. 2010 , 32, 2-8	12
1278	Molecular dynamics of DNA: comparison of force fields and terminal nucleotide definitions. 2010 , 114, 9882-93	67
1277	On the Validation of Molecular Dynamics Simulations of Saturated and cis-Monounsaturated Phosphatidylcholine Lipid Bilayers: A Comparison with Experiment. 2010 , 6, 325-36	232
1276	Effect of pH and ibuprofen on the phospholipid bilayer bending modulus. 2010 , 114, 8061-6	54
1275	Adsorption of poly(ethylene oxide) at the free water surface. A computer simulation study. 2010 , 114, 10995-1001	16
1274	The role of nonbonded interactions in the conformational dynamics of organophosphorous hydrolase adsorbed onto functionalized mesoporous silica surfaces. 2010 , 114, 531-40	33
1273	Transferability of Nonbonded Interaction Potentials for Coarse-Grained Simulations: Benzene in Water. 2010 , 6, 2434-44	62
1272	Poly(styrenesulfonate) P oly(diallyldimethylammonium) Mixtures: Toward the Understanding of Polyelectrolyte Complexes and Multilayers via Atomistic Simulations. 2010 , 43, 7828-7838	40
1271	Capture and manipulation of hybrid DNAs by carbon nanotube bundles. 2010 , 21, 195301	4
1270	On the self-assembly of a highly selective benzothiazole-based TIM inhibitor in aqueous solution. 2010 , 26, 16681-9	7
1269	Dynamical properties of supercooled water close to the liquid-liquid coexistence lines, and their relation to those at ambient conditions. 2010 , 22, 284105	5
1268	Molecular dynamics simulations of Zn(2+) coordination in protein binding sites. 2010 , 132, 205101	11
1267	Infrared and Raman line shapes for ice Ih. II. H2O and D2O. 2010 , 133, 244504	77
1266	Can salting-in/salting-out ions be classified as chaotropes/kosmotropes?. 2010 , 114, 643-50	130
1265	Equilibrium study of protein denaturation by urea. 2010 , 132, 2338-44	218
1264	Molecular simulations of lipid flip-flop in the presence of model transmembrane helices. 2010 , 49, 7665-73	31
1263	Systematic design of unimolecular star copolymer micelles using molecular dynamics simulations. 2010 , 6, 5491	27
1262	Inclusion of terpenoid plant extracts in lipid bilayers investigated by molecular dynamics simulations. 2010 , 114, 15825-31	36

1261	Consensus modes, a robust description of protein collective motions from multiple-minima normal mode analysisapplication to the HIV-1 protease. 2010 , 12, 2850-9	28
1260	Properties of the LiquidNapor Interface of WaterDimethyl Sulfoxide Mixtures. A Molecular Dynamics Simulation and ITIM Analysis Study. 2010 , 114, 12207-12220	28
1259	C12E6 and SDS surfactants simulated at the vacuum-water interface. 2010 , 26, 5462-74	51
1258	Lateral confinement effects on the structural properties of surfactant aggregates: SDS on graphene. 2010 , 12, 13137-43	45
1257	Atomistic simulations of the wetting behavior of nanodroplets of water on homogeneous and phase separated self-assembled monolayers. 2010 , 6, 1297	19
1256	Insulin dimer dissociation and unfolding revealed by amide I two-dimensional infrared spectroscopy. 2010 , 12, 3579-88	64
1255	A comparative analysis of the role of water in the binding pockets of ionotropic glutamate receptors. 2010 , 12, 14057-66	12
1254	Lateral pressure profiles in lipid monolayers. 2010 , 144, 393-409; discussion 445-81	46
1253	Sequence-dependent interaction of the ptides with membranes. 2010 , 114, 13585-92	27
1252	Experimental test of the thermodynamic model of protein cooperativity using temperature-induced unfolding of a Ubq-UIM fusion protein. 2010 , 49, 8455-67	7
1251	Modelling the binding of HIV-reverse transcriptase and nevirapine: an assessment of quantum mechanical and force field approaches and predictions of the effect of mutations on binding. 2010 , 12, 7117-25	26
1250	Dynamics and energetics of solute permeation through the Plasmodium falciparum aquaglyceroporin. 2010 , 12, 10246-54	22
1249	Crystallographic controls on uranyl binding at the quartz/water interface. 2011 , 13, 7845-51	12
1248	Rectification of the current in alpha-hemolysin pore depends on the cation type: the alkali series probed by MD simulations and experiments. 2011 , 115, 4255-4264	59
1247	Conformational variability of organophosphorus hydrolase upon soman and paraoxon binding. 2011 , 115, 15389-98	7
1246	Influence of water-protein hydrogen bonding on the stability of Trp-cage miniprotein. A comparison between the TIP3P and TIP4P-Ew water models. 2011 , 13, 19840-7	63
1245	Study of the antimicrobial peptide indolicidin and mutants in eukaryotic modelled membrane by molecular dynamics simulations. 2011 , 109, 289-300	O
1244	An atomistic study of a poly(styrene sulfonate)/poly(diallyldimethylammonium) bilayer: the role of surface properties and charge reversal. 2011 , 13, 16336-42	19

(2011-2011)

1243	Predicting hydration Gibbs energies of alkyl-aromatics using molecular simulation: a comparison of current force fields and the development of a new parameter set for accurate solvation data. 2011 , 13, 17384-94	19
1242	A Kirkwood-Buff force field for the aromatic amino acids. 2011 , 13, 18154-67	33
1241	Fast flexible modeling of RNA structure using internal coordinates. 2011 , 8, 1247-57	49
1240	Atomistic molecular dynamics simulations of the interactions of oleic and 2-hydroxyoleic acids with phosphatidylcholine bilayers. 2011 , 115, 11727-38	19
1239	Molecular Dynamics Study of Water Interacting with Siloxane Surface Modified by Poly(ethylene oxide) Chains. 2011 , 115, 18740-18751	8
1238	Molecular Mechanics Investigation of an Adenine-Adenine Non-Canonical Pair Conformational Change. 2011 , 7, 3779-3792	12
1237	A molecular dynamics approach for the association of apolipoproteinB-100 and chondroitin-6-sulfate. 2011 , 115, 4818-25	5
1236	Structural dynamics of the S4 voltage-sensor helix in lipid bilayers lacking phosphate groups. 2011 , 115, 8732-8	15
1235	Coarse-grained molecular dynamics simulations of the sphere to rod transition in surfactant micelles. 2011 , 27, 6628-38	112
1234	Proline 68 enhances photoisomerization yield in photoactive yellow protein. 2011 , 115, 6668-77	17
1233	Enhanced Lipid Diffusion and Mixing in Accelerated Molecular Dynamics. 2011 , 7, 3199-3207	57
1232	Solvation Free Energy Profile of the SCNIIon across the WaterII,2-Dichloroethane Liquid/Liquid Interface. A Computer Simulation Study. 2011 , 115, 11140-11146	14
1231	Influence of chloroform in liquid-ordered and liquid-disordered phases in lipid membranes. 2011 , 115, 2527-35	24
1230	Simulative Analysis of a Truncated Octahedral DNA Nanocage Family Indicates the Single-Stranded Thymidine Linkers as the Major Player for the Conformational Variability. 2011 , 115, 16819-16827	14
1229	Driving force for hydrophobic interaction at different length scales. 2011 , 115, 2303-11	58
1228	Driving Force for the Association of Amphiphilic Molecules. 2011 , 2, 2391-2395	26
1227	Characterizing the dynamics and ligand-specific interactions in the human leukocyte elastase through molecular dynamics simulations. 2011 , 51, 1690-702	8
1226	Interaction of 7-nitrobenz-2-oxa-1,3-diazol-4-yl-labeled fatty amines with 1-palmitoyl, 2-oleoyl-sn-glycero-3-phosphocholine bilayers: a molecular dynamics study. 2011 , 115, 10109-19	25

1225	Implementation of Accelerated Molecular Dynamics in NAMD. 2011 , 4,	105
1224	The key residues of active sites on the catalytic fragment for paclitaxel interacting with poly (ADP-ribose) polymerase. 2011 , 28, 881-93	10
1223	Behavior of the Eigen form of hydronium at the air/water interface. 2011 , 115, 5881-6	29
1222	Constant pH Molecular Dynamics in Explicit Solvent with EDynamics. 2011 , 7, 1962-1978	130
1221	Hydrogenated/fluorinated catanionic surfactants as potential templates for nanostructure design. 2011 , 27, 9719-28	14
1220	Nanopore analysis of individual RNA/antibiotic complexes. 2011 , 5, 9345-53	58
1219	Dewetting transitions in the self-assembly of two amyloidogenic	26
1218	Unfolding the conformational behavior of peptide dendrimers: insights from molecular dynamics simulations. 2011 , 133, 5042-52	30
1217	Simulation analysis of the temperature dependence of lignin structure and dynamics. 2011 , 133, 20277-87	100
1216	Membrane insertion of a voltage sensor helix. 2011 , 100, 410-9	14
1216 1215	Membrane insertion of a voltage sensor helix. 2011 , 100, 410-9 Backbone and side-chain contributions in protein denaturation by urea. 2011 , 100, 1526-33	91
1215		
1215	Backbone and side-chain contributions in protein denaturation by urea. 2011 , 100, 1526-33	91
1215 1214	Backbone and side-chain contributions in protein denaturation by urea. 2011 , 100, 1526-33 Acyl-chain methyl distributions of liquid-ordered and -disordered membranes. 2011 , 100, 1455-62	91
1215 1214 1213	Backbone and side-chain contributions in protein denaturation by urea. 2011 , 100, 1526-33 Acyl-chain methyl distributions of liquid-ordered and -disordered membranes. 2011 , 100, 1455-62 Mechanism of membrane curvature sensing by amphipathic helix containing proteins. 2011 , 100, 1271-9 3Ehelix conformation facilitates the transition of a voltage sensor S4 segment toward the down	91 60 147
1215 1214 1213 1212	Backbone and side-chain contributions in protein denaturation by urea. 2011 , 100, 1526-33 Acyl-chain methyl distributions of liquid-ordered and -disordered membranes. 2011 , 100, 1455-62 Mechanism of membrane curvature sensing by amphipathic helix containing proteins. 2011 , 100, 1271-9 3Ehelix conformation facilitates the transition of a voltage sensor S4 segment toward the down state. 2011 , 100, 1446-54	91 60 147 40
1215 1214 1213 1212 1211	Backbone and side-chain contributions in protein denaturation by urea. 2011, 100, 1526-33 Acyl-chain methyl distributions of liquid-ordered and -disordered membranes. 2011, 100, 1455-62 Mechanism of membrane curvature sensing by amphipathic helix containing proteins. 2011, 100, 1271-9 3Ehelix conformation facilitates the transition of a voltage sensor S4 segment toward the down state. 2011, 100, 1446-54 Extension of a three-helix bundle domain of myosin VI and key role of calmodulins. 2011, 100, 2964-73	91 60 147 40

1207	Multiscale ensemble modeling of intrinsically disordered proteins: p53 N-terminal domain. 2011 , 101, 1450-8	72
1206	Gating at the selectivity filter of ion channels that conduct Na+ and K+ ions. 2011 , 101, 1623-31	18
1205	Carbon nanotube inhibits the formation of	140
1204	Modeling the binding of three toxins to the voltage-gated potassium channel (Kv1.3). 2011 , 101, 2652-60	45
1203	The effect of environment on the recognition and binding of vancomycin to native and resistant forms of lipid II. 2011 , 101, 2684-92	28
1202	High temperatures enhance cooperative motions between CBM and catalytic domains of a thermostable cellulase: mechanism insights from essential dynamics. 2011 , 13, 13709-20	33
1201	Using molecular dynamics to study liquid phase behavior: simulations of the ternary sodium laurate/sodium oleate/water system. 2011 , 27, 11381-93	28
1200	The orientation and charge of water at the hydrophobic oil droplet-water interface. 2011 , 133, 10204-10	175
1199	A molecular dynamics study of water nucleation using the TIP4P/2005 model. 2011 , 135, 244505	27
1198	Simulation studies of protein folding/unfolding equilibrium under polar and nonpolar confinement. 2011 , 133, 15157-64	48
1197	Molecular Dynamics Studies of Interfacial Water at the Alumina Surface. 2011 , 115, 2038-2046	119
1196	Implicit-solvent models for micellization: nonionic surfactants and temperature-dependent properties. 2011 , 115, 990-1001	29
1195	NMR-NOE and MD simulation study on phospholipid membranes: dependence on membrane diameter and multiple time scale dynamics. 2011 , 115, 9106-15	13
1194	Molecular insights into the surface morphology, layering structure, and aggregation kinetics of surfactant-stabilized graphene dispersions. 2011 , 133, 12810-23	128
1193	Atomistic Study of Surface Effects on Polyelectrolyte Adsorption: Case Study of a Poly(styrenesulfonate) Monolayer. 2011 , 44, 1707-1718	28
1192	Aqueous NaCl Solutions within Charged Carbon-Slit Pores: Partition Coefficients and Density Distributions from Molecular Dynamics Simulations. 2011 , 115, 13786-13795	64
1191	Bridging the Atomic and Coarse-Grained Descriptions of Collective Motions in Proteins. 2011 , 159-178	
1190	Simulations of the confinement of ubiquitin in self-assembled reverse micelles. 2011 , 134, 225101	52

1189	First-principles-based multiscale, multiparadigm molecular mechanics and dynamics methods for describing complex chemical processes. 2012 , 307, 1-42	8
1188	Identifying low variance pathways for free energy calculations of molecular transformations in solution phase. 2011 , 135, 034114	61
1187	Frontier residues lining globin internal cavities present specific mechanical properties. 2011 , 133, 8753-61	20
1186	Analysis of twisting of cellulose nanofibrils in atomistic molecular dynamics simulations. 2011 , 115, 3747-55	103
1185	Effect of high pressure on fully hydrated DPPC and POPC bilayers. 2011 , 115, 1038-44	26
1184	Competitive adsorption of surfactants and polymers at the free water surface. A computer simulation study of the sodium dodecyl sulfate-poly(ethylene oxide) system. 2011 , 115, 933-44	29
1183	Water adsorption around oxalic acid aggregates: a molecular dynamics simulation of water nucleation on organic aerosols. 2011 , 13, 19830-9	20
1182	The CLN025 decapeptide retains a thairpin conformation in urea and guanidinium chloride. 2011 , 115, 4971-81	12
1181	Atomistic simulation of ion solvation in water explains surface preference of halides. 2011 , 108, 6838-6842	171
1180	Transferability of Coarse Grained Potentials: Implicit Solvent Models for Hydrated Ions. 2011 , 7, 1916-27	48
1179	Properties and behaviour of tetracyclic allopsoralen derivatives inside a DPPC lipid bilayer model. 2011 , 13, 10174-82	5
1178	Nonequilibrium water transport in a nonionic microemulsion system. 2011 , 115, 6503-8	1
1177	Interactions of A費5-35 助arrel-like oligomers with anionic lipid bilayer and resulting membrane leakage: an all-atom molecular dynamics study. 2011 , 115, 1165-74	44
1176	Disruption and formation of surface salt bridges are coupled to DNA binding by the integration host factor: a computational analysis. 2011 , 50, 266-75	10
1175	Zeolitic imidazolate framework-8 as a reverse osmosis membrane for water desalination: insight from molecular simulation. 2011 , 134, 134705	153
1174	Protonation/deprotonation effects on the stability of the Trp-cage miniprotein. 2011 , 13, 17056-63	18
1173	Role of the closing base pair for d(GCA) hairpin stability: free energy analysis and folding simulations. 2011 , 39, 8271-80	11
1172	Conformational states of nucleic acidpeptide complexes monitored by acoustic wave propagation and molecular dynamics simulation. 2011 , 2, 237-255	12

1171	A theoretical study of the physicochemical mechanisms associated with DNA recognition modulation in artificial zinc-finger proteins. 2011 , 115, 4774-80	10
1170	Combined experimental and computational study of cis-trans isomerism in bis(L-valinato)copper(II). 2011 , 50, 3632-44	26
1169	Computational modeling of substrate specificity and catalysis of the Becretase (BACE1) enzyme. 2011 , 50, 4337-49	41
1168	Surface Hydroxyl Identity and Reactivity in Akaganlie. 2011 , 115, 17036-17045	28
1167	References. 557-640	
1166	Quantum Corrections to Classical Molecular Dynamics Simulations of Water and Ice. 2011 , 7, 2903-9	25
1165	Molecular Dynamics Simulation Study of Chlorophyll a in Different Organic Solvents. 2011, 7, 1131-40	30
1164	Experimental and molecular dynamics investigation into the amphiphilic nature of sulforhodamine B. 2011 , 115, 1394-402	18
1163	Nature of halide binding to the molybdenum site of sulfite oxidase. 2011 , 50, 9406-13	8
1162	Dynamics of noncovalent interactions in all-由nd all-社lass proteins: implications for the stability of amyloid aggregates. 2011 , 51, 3208-16	7
1161	A New Coarse-Grained Force Field for Membrane-Peptide Simulations. 2011 , 7, 3793-802	70
1160	Molecular binding of black tea theaflavins to biological membranes: relationship to bioactivities. 2011 , 59, 3780-7	60
1159	Origin of the Difference in Structural Behavior of Poly(acrylic acid) and Poly(methacrylic acid) in Aqueous Solution Discerned by Explicit-Solvent Explicit-Ion MD Simulations. 2011 , 50, 11785-11796	64
1158	Computational study of drug binding to the membrane-bound tetrameric M2 peptide bundle from influenza A virus. 2011 , 1808, 530-7	33
1157	Exploring the conformational dynamics and membrane interactions of PorB from C. glutamicum: a multi-scale molecular dynamics simulation study. 2011 , 1808, 1746-52	6
1156	Amphipathic-Lipid-Packing-Sensor interactions with lipids assessed by atomistic molecular dynamics. 2011 , 1808, 2119-27	20
1155	Statistical Convergence of Equilibrium Properties in Simulations of Molecular Solutes Embedded in Lipid Bilayers. 2011 , 7, 4175-88	162
1154	lons and the protein surface revisited: extensive molecular dynamics simulations and analysis of protein structures in alkali-chloride solutions. 2011 , 115, 9213-23	30

1153	Water Defect and Pore Formation in Atomistic and Coarse-Grained Lipid Membranes: Pushing the Limits of Coarse Graining. 2011 , 7, 2981-8	101
1152	Simulations of micellization of sodium hexyl sulfate. 2011 , 115, 1403-10	39
1151	Molecular dynamics simulations reveal insights into key structural elements of adenosine receptors. 2011 , 50, 4194-208	60
1150	Atomistic simulation of cholesterol effects on miscibility of saturated and unsaturated phospholipids: implications for liquid-ordered/liquid-disordered phase coexistence. 2011 , 133, 3625-34	41
1149	Structure and dynamics of the kinase IKK-#A key regulator of the NF-kappa B transcription factor. 2011 , 176, 133-42	11
1148	Atomic-level characterization of the ensemble of the At 1-42) monomer in water using unbiased molecular dynamics simulations and spectral algorithms. 2011 , 405, 570-83	179
1147	Selectivity and permeation of alkali metal ions in K+-channels. 2011 , 409, 867-78	26
1146	Subunit interface dynamics in hexadecameric rubisco. 2011 , 411, 1083-98	29
1145	Comparison of SARS and NL63 papain-like protease binding sites and binding site dynamics: inhibitor design implications. 2011 , 414, 272-88	17
1144	Dynamical behaviour of the human #-adrenoceptor under agonist binding. 2011 , 37, 907-913	7
1143	Size and sequence and the volume change of protein folding. 2011 , 133, 6020-7	93
1142	Structure and orientation of interfacial water determine atomic force microscopy results: insights from molecular dynamics simulations. 2011 , 5, 2215-23	59
1141	Keep It Flexible: Driving Macromolecular Rotary Motions in Atomistic Simulations with GROMACS. 2011 , 7, 1381-1393	33
1140	Molecular dynamics simulation studies of caffeine aggregation in aqueous solution. 2011 , 115, 10957-66	58
1140	Molecular dynamics simulation studies of caffeine aggregation in aqueous solution. 2011 , 115, 10957-66 High-performance scalable molecular dynamics simulations of a polarizable force field based on classical Drude oscillators in NAMD. 2011 , 2, 87-92	58 191
	High-performance scalable molecular dynamics simulations of a polarizable force field based on	
1139	High-performance scalable molecular dynamics simulations of a polarizable force field based on classical Drude oscillators in NAMD. 2011 , 2, 87-92	191

1135	Application of molecular dynamics simulations in molecular property prediction II: diffusion coefficient. <i>Journal of Computational Chemistry</i> , 2011 , 32, 3505-19	3.5	91	
1134	Is DNA's rigidity dominated by electrostatic or nonelectrostatic interactions?. 2011 , 133, 19290-3		53	
1133	Algorithm improvements for molecular dynamics simulations. 2011 , 1, 93-108		26	
1132	Application of Molecular Dynamics Simulations in Molecular Property Prediction I: Density and Heat of Vaporization. 2011 , 7, 2151-2165		85	
1131	Effect of poly(ethylene glycol) (PEG) spacers on the conformational properties of small peptides: a molecular dynamics study. 2011 , 27, 296-303		28	
1130	The cages, dynamics, and structuring of incipient methane clathrate hydrates. 2011 , 13, 19951-9		99	
1129	Collective dynamics of supercooled water close to the liquid-liquid coexistence lines. 2011 , 13, 19823-9		6	
1128	The dynamics of Ca2+ ions within the solvation shell of calbindin D9k. 2011 , 6, e14718		3	
1127	Mapping the conformational dynamics and pathways of spontaneous steric zipper Peptide oligomerization. 2011 , 6, e19129		38	
1126	Effects of single nucleotide polymorphisms on human N-acetyltransferase 2 structure and dynamics by molecular dynamics simulation. 2011 , 6, e25801		27	
1125	An #b mutation in patients with Glanzmann thrombasthenia located in the N-terminus of blade 1 of the #propeller (Asn2Asp) disrupts a calcium binding site in blade 6. 2011 , 9, 192-200		14	
1124	Binding site analysis of CCR2 through in silico methodologies: docking, CoMFA, and CoMSIA. 2011 , 78, 161-74		16	
1123	Molecular mimicry and ligand recognition in binding and catalysis by the histone demethylase LSD1-CoREST complex. 2011 , 19, 212-20		72	
1122	Multiscale simulation of microbe structure and dynamics. 2011 , 107, 200-17		26	
1121	Molecular dynamics simulations of T-20 HIV fusion inhibitor interacting with model membranes. 2011 , 159, 275-86		10	
1120	The impact of Texas red on lipid bilayer properties. 2011 , 115, 8500-5		50	
1119	Replica exchange and expanded ensemble simulations as Gibbs sampling: simple improvements for enhanced mixing. 2011 , 135, 194110		118	
1118	Cholesterol effect on water permeability through DPPC and PSM lipid bilayers: a molecular dynamics study. 2011 , 115, 15241-50		89	

1117	Nanoscale carbon particles and the stability of lipid bilayers. 2011 , 7, 1139-1146	41
1116	Indenyl ring slippage in crown thioether complexes [IndMo(CO)2L]+ and C-S activation of trithiacyclononane: experimental and theoretical studies. 2011 , 40, 10513-25	17
1115	Communication: Free-energy analysis of hydration effect on protein with explicit solvent: equilibrium fluctuation of cytochrome c. 2011 , 134, 041105	42
1114	Molecular-dynamic simulation of DPPC bilayer in different phase state: Hydration and electric field distribution in the presence of Be2+ cations. 2011 , 5, 370-378	3
1113	Atomic-level study of adsorption, conformational change, and dimerization of an Helical peptide at graphene surface. 2011 , 115, 9813-22	74
1112	Methane Hydrate Nucleation Rates from Molecular Dynamics Simulations: Effects of Aqueous Methane Concentration, Interfacial Curvature, and System Size. 2011 , 115, 21241-21248	142
1111	Structural-dynamical investigation of the ZnuA histidine-rich loop: involvement in zinc management and transport. 2011 , 25, 181-94	14
1110	Molecular dynamics simulations of pro-apoptotic BH3 peptide helices in aqueous medium: relationship between helix stability and their binding affinities to the anti-apoptotic protein Bcl-X(L). 2011 , 25, 413-26	20
1109	Effect of human serum albumin on the kinetics of 4-methylumbelliferyl-#D-N-N'-N? Triacetylchitotrioside hydrolysis catalyzed by hen egg white lysozyme. 2011 , 30, 367-73	10
1108	Water Dynamics at Interfaces and Solutes: Disentangling Free Energy and Diffusivity Contributions. 2011 , 145, 240-252	34
1107	Lipid bilayer coated Al(2)O(3) nanopore sensors: towards a hybrid biological solid-state nanopore. 2011 , 13, 671-82	47
1106	Binding selectivity of RecA to a single stranded DNA, a computational approach. 2011 , 17, 133-50	2
1105	Trajectory NG: portable, compressed, general molecular dynamics trajectories. 2011 , 17, 2669-85	12
1104	Effect of atom- and group-based truncations on biomolecules simulated with reaction-field electrostatics. 2011 , 17, 2883-93	11
1103	Molecular dynamics simulation of the Staphylococcus aureus YsxC protein: molecular insights into ribosome assembly and allosteric inhibition of the protein. 2011 , 17, 3129-49	4
1102	Investigating the effect of different positioning of lysine residues along the peptide chain of mastoparans for their secondary structures and biological activities. 2011 , 40, 77-90	25
1101	The effect of membrane curvature on the conformation of antimicrobial peptides: implications for binding and the mechanism of action. 2011 , 40, 545-53	46
1100	How do carbon nanotubes serve as carriers for gemcitabine transport in a drug delivery system?. 2011 , 29, 591-6	109

1099	Comprehensive structural and functional characterization of Mycobacterium tuberculosis UDP-NAG enolpyruvyl transferase (Mtb-MurA) and prediction of its accurate binding affinities with inhibitors. 2011 , 3, 204-16		20	
1098	Conformational and functional analysis of molecular dynamics trajectories by self-organising maps. 2011 , 12, 158		33	
1097	Revealing the functionality of hypothetical protein KPN00728 from Klebsiella pneumoniae MGH78578: molecular dynamics simulation approaches. 2011 , 12 Suppl 13, S11		6	
1096	Molecular mechanism of 略heet self-organization at water-hydrophobic interfaces. 2011 , 79, 1-22		42	
1095	A computational investigation on the role of glycosylation in the binding of alpha1 nicotinic acetylcholine receptor with two alpha-neurotoxins. 2011 , 79, 142-52		5	
1094	Behavior of the ATP grasp domain of biotin carboxylase monomers and dimers studied using molecular dynamics simulations. 2011 , 79, 622-32		5	
1093	Conformational changes induced by ATP-hydrolysis in an ABC transporter: a molecular dynamics study of the Sav1866 exporter. 2011 , 79, 1977-90		53	
1092	Conformational dynamics of L-lysine, L-arginine, L-ornithine binding protein reveals ligand-dependent plasticity. 2011 , 79, 2097-108		15	
1091	In silico predictions of LH2 ring sizes from the crystal structure of a single subunit using molecular dynamics simulations. 2011 , 79, 2306-15		1	
1090	Structural determinants of ligand imprinting: a molecular dynamics simulation study of subtilisin in aqueous and apolar solvents. 2011 , 20, 379-86		12	
1089	Structural consequences of ATP hydrolysis on the ABC transporter NBD dimer: molecular dynamics studies of HlyB. 2011 , 20, 1220-30		36	
1088	Early stages of the recovery stroke in myosin II studied by molecular dynamics simulations. 2011 , 20, 2013-22		11	
1087	Structural analysis of zinc-finger (TTK) + [Cu(BPA)]2+ /[Cu(IDB)]2+ + DNA complexes: an investigation by molecular dynamics simulation. 2011 , 24, 981-94		5	
1086	Conformation of the tridimensional structure of 1,2,3,4,6-pentagalloyl-即-glucopyranose (PGG) by (1)H NMR, NOESY and theoretical study and membrane interaction in a simulated phospholipid bilayer: a first insight. 2011 , 49, 132-6		20	
1085	Control of Nanoscale Environment to Improve Stability of Immobilized Proteins on Diamond Surfaces. 2011 , 21, 1040-1050		28	
1084	Interaction identification of Zif268 and TATA(ZF) proteins with GC-/AT-rich DNA sequence: A theoretical study. <i>Journal of Computational Chemistry</i> , 2011 , 32, 416-28	3.5	25	
1083	On easy implementation of a variant of the replica exchange with solute tempering in GROMACS. Journal of Computational Chemistry, 2011 , 32, 1228-34	3.5	113	
1082	Combination of the CHARMM27 force field with united-atom lipid force fields. <i>Journal of Computational Chemistry</i> , 2011 , 32, 1400-10	3.5	57	

1081	Optimization of parameters for molecular dynamics simulation using smooth particle-mesh Ewald in GROMACS 4.5. <i>Journal of Computational Chemistry</i> , 2011 , 32, 2031-40	3.5	153
1080	Toward a new approach for determination of solute's charge distribution to analyze interatomic electrostatic interactions in quantum mechanical/molecular mechanical simulations. <i>Journal of Computational Chemistry</i> , 2011 , 32, 3092-104	3.5	6
1079	Applying efficient implicit nongeometric constraints in alchemical free energy simulations. <i>Journal of Computational Chemistry</i> , 2011 , 32, 3423-32	3.5	32
1078	Transmembrane peptides used to investigate the homo-oligomeric interface and binding hotspot of latent membrane protein 1. 2011 , 95, 772-84		14
1077	Investigation of the binding of a carbohydrate-mimetic peptide to its complementary anticarbohydrate antibody by STD-NMR spectroscopy and molecular-dynamics simulations. 2011 , 17, 11446-55		20
1076	Design and synthesis of sphingomyelin-cholesterol conjugates and their formation of ordered membranes. 2011 , 17, 8568-75		8
1075	WaterLOGSY NMR experiments in conjunction with molecular-dynamics simulations identify immobilized water molecules that bridge peptide mimic MDWNMHAA to anticarbohydrate antibody SYA/J6. 2011 , 17, 11438-45		11
1074	An MD2 hot-spot-mimicking peptide that suppresses TLR4-mediated inflammatory response in vitro and in vivo. 2011 , 12, 1827-31		11
1073	Wetting transition of water on graphite and boron-nitride surfaces: A molecular dynamics study. 2011 , 302, 310-315		58
1072	Prediction of thermodynamic, transport and vaporliquid equilibrium properties of binary mixtures of ethylene glycol and water. 2011 , 301, 137-144		15
1071	Synthesis and topoisomerase I inhibitory activity of a novel diazaindeno[2,1-b]phenanthrene analogue of Lamellarin D. 2011 , 19, 4971-84		29
1070	Structural investigation into the inhibitory mechanisms of indomethacin and its analogues towards human glyoxalase I. 2011 , 21, 4243-7		2
1069	Comparing the structural properties of human and rat islet amyloid polypeptide by MD computer simulations. 2011 , 156, 43-50		41
1068	On the accurate calculation of the dielectric constant from molecular dynamics simulations: The case of SPC/E and SWM4-DP water. 2011 , 507, 80-83		79
1067	Molecular dynamics studies on the mutational structures of a nylon-6 byproduct-degrading enzyme. 2011 , 507, 157-161		12
1066	Penetratin analogues acting as antifungal agents. 2011 , 46, 370-7		14
1065	System size and trajectory length dependence of the static structure factor and the diffusion coefficient as calculated from molecular dynamics simulations: The case of SPC/E water. 2011 , 161, 36-4	10	14
1064	Molecular aspects of the interaction between plants sterols and DPPC bilayers: an experimental and theoretical approach. 2011 , 358, 192-201		33

1063	Crossover between tetrahedral and hexagonal structures in liquid water. 2011 , 375, 572-576	11
1062	Novel cytotoxity exhibition mode of polybia-CP, a novel antimicrobial peptide from the venom of the social wasp Polybia paulista. 2011 , 288, 27-33	23
1061	Ionic solvation studied by image-charge reaction field method. 2011 , 134, 044105	20
1060	A Mixed Heuristic Algorithm for Traveling Salesman Problem. 2011 ,	
1059	Perturbation analyses of intermolecular interactions. 2011 , 84, 026704	3
1058	Towards computational specificity screening of DNA-binding proteins. 2011 , 39, 8281-90	17
1057	Exploring platelet chemokine antimicrobial activity: nuclear magnetic resonance backbone dynamics of NAP-2 and TC-1. 2011 , 55, 2074-83	19
1056	Recognition of 5-hydroxymethylcytosine by the Uhrf1 SRA domain. 2011 , 6, e21306	147
1055	Robust three-body water simulation model. 2011 , 134, 184501	105
1054	Torsional elasticity and energetics of F1-ATPase. 2011 , 108, 7408-13	41
1053	Effects of backbone substitutions on the conformational behavior of Shigella flexneri O-antigens: implications for vaccine strategy. 2011 , 21, 109-21	29
1052	Engineering bifunctional laccase-xylanase chimeras for improved catalytic performance. 2011 , 286, 43026-38	42
1051	Molecular dynamics simulations of vapor/liquid coexistence using the nonpolarizable water models. 2011 , 134, 124708	50
1050	Dynamical reweighting: improved estimates of dynamical properties from simulations at multiple temperatures. 2011 , 134, 244107	50
1049	Inter-domain communication mechanisms in an ABC importer: a molecular dynamics study of the MalFGK2E complex. 2011 , 7, e1002128	28
1048	Ligand-induced modulation of the free-energy landscape of G protein-coupled receptors explored by adaptive biasing techniques. 2011 , 7, e1002193	63
1047	Collagenolytic activities of the major secreted cathepsin L peptidases involved in the virulence of the helminth pathogen, Fasciola hepatica. 2011 , 5, e1012	51
1046	Quantifying intramolecular binding in multivalent interactions: a structure-based synergistic study on Grb2-Sos1 complex. 2011 , 7, e1002192	15

1045	Temperature effects on structure and dynamics of the psychrophilic protease subtilisin S41 and its thermostable mutants in solution. 2011 , 24, 533-44	24
1044	Proton transport in a binary biomimetic solution revealed by molecular dynamics simulation. 2011 , 135, 114502	7
1043	Polymorph specific RMSD local order parameters for molecular crystals and nuclei: 日 貝 and Eglycine. 2011 , 135, 134101	17
1042	A role for both conformational selection and induced fit in ligand binding by the LAO protein. 2011 , 7, e1002054	172
1041	Molecular dynamics simulations of forced unbending of integrin (♣v) #2011 , 7, e1001086	47
1040	A multiscale approach to characterize the early aggregation steps of the amyloid-forming peptide GNNQQNY from the yeast prion sup-35. 2011 , 7, e1002051	68
1039	Ensemble-based computational approach discriminates functional activity of p53 cancer and rescue mutants. 2011 , 7, e1002238	28
1038	On conduction in a bacterial sodium channel. 2012 , 8, e1002476	69
1037	Surface properties of the polarizable Baranyai-Kiss water model. 2012 , 136, 114706	11
1036	Molecular dynamics simulation of HIV fusion inhibitor T-1249: insights on peptide-lipid interaction. 2012 , 2012, 151854	7
1035	Water and ion distributions in a silicon nanochannel: a molecular dynamics study. 2012 , 226, 31-34	О
1034	Corresponding functional dynamics across the Hsp90 Chaperone family: insights from a multiscale analysis of MD simulations. 2012 , 8, e1002433	82
1033	Molecular dynamics simulation of palmitate ester self-assembly with diclofenac. 2012, 13, 9572-83	18
1032	A computational investigation on the connection between dynamics properties of ribosomal proteins and ribosome assembly. 2012 , 8, e1002530	16
1031	Regulation of the H4 tail binding and folding landscapes via Lys-16 acetylation. 2012, 109, 17857-62	66
1030	Mechanism of enhanced mechanical stability of a minimal RNA kissing complex elucidated by nonequilibrium molecular dynamics simulations. 2012 , 109, E1530-9	22
1029	Pharmacological enhancement of Eglucosidase by the allosteric chaperone N-acetylcysteine. 2012 , 20, 2201-11	72
1028	Estimating statistical distributions using an integral identity. 2012 , 136, 204113	3

1027	Water-induced ethanol dewetting transition. 2012 , 137, 024703	15
1026	Dynamics of two-dimensional monolayer water confined in hydrophobic and charged environments. 2012 , 137, 114510	12
1025	Bovine pancreatic trypsin inhibitor crystals with different morphologies: a molecular dynamics simulation study. 2012 , 38, 112-118	O
1024	Molecular simulation of rapid translocation of cholesterol, diacylglycerol, and ceramide in model raft and nonraft membranes. 2012 , 53, 421-429	70
1023	An improvement in quantum mechanical description of solute-solvent interactions in condensed systems via the number-adaptive multiscale quantum mechanical/molecular mechanical-molecular dynamics method: application to zwitterionic glycine in aqueous solution. 2012 , 137, 024501	22
1022	Nanopore-Based Technology. 2012 ,	2
1021	Structure and dynamics of nano-sized raft-like domains on the plasma membrane. 2012, 136, 015103	12
1020	The multiscale coarse-graining method. IX. A general method for construction of three body coarse-grained force fields. 2012 , 136, 194114	47
1019	POSITIONING OF FtzE1 DOMAIN AFFECTS ON THE ACTIVITY OF HUMAN LRH-1: MOLECULAR DYNAMICS STUDY ON HUMAN LRH-1-DNA COMPLEXES. 2012 , 11, 329-359	3
1018	Protein kinase A (PKA) phosphorylation of Na+/K+-ATPase opens intracellular C-terminal water pathway leading to third Na+-binding site in molecular dynamics simulations. 2012 , 287, 15959-65	21
1017	Hydration repulsion between biomembranes results from an interplay of dehydration and depolarization. 2012 , 109, 14405-9	107
1016	Effect of secondary structure on the self-assembly of amphiphilic molecules: a multiscale simulation study. 2012 , 136, 084902	11
1015	Liquid-to-glass transition of tetrahydrofuran and 2-methyltetrahydrofuran. 2012, 21, 086402	11
1014	Zeolitic imidazolate framework-7 as an ultra-selective nanofilter for H2 purification: atomistic simulation study. 2012 , 38, 830-837	3
1013	Local order parameters for use in driving homogeneous ice nucleation with all-atom models of water. 2012 , 137, 194504	80
1012	A molecular dynamics approach to ligand-receptor interaction in the aspirin-human serum albumin complex. 2012 , 2012, 642745	10
1011	Conformational relaxations of human serum albumin studied by molecular dynamics simulations with pressure jumps. 2012 , 28, 486-492	5
1010	A sugar isomerization reaction established on various (#barrel scaffolds is based on substrate-assisted catalysis. 2012 , 25, 751-60	6

1009	Counteracting effects operating on Src homology 2 domain-containing protein-tyrosine phosphatase 2 (SHP2) function drive selection of the recurrent Y62D and Y63C substitutions in Noonan syndrome. 2012 , 287, 27066-77	18
1008	Insights into the modulation of optimum pH by a single histidine residue in arginine deiminase from Pseudomonas aeruginosa. 2012 , 393, 1013-24	5
1007	The Effects of Ions and Surface Charge Density on Water Distribution in Silicon Nanochannel. 2012,	
1006	Proteome-wide analysis of lysine acetylation suggests its broad regulatory scope in Saccharomyces cerevisiae. 2012 , 11, 1510-22	200
1005	Multiscale, Multiparadigm Modeling for Nanosystems Characterization and Design. 2012, 935-982	
1004	Structural determinants for the membrane insertion of the transmembrane peptide of hemagglutinin from influenza virus. 2012 , 52, 3001-12	8
1003	How to distinguish methyl-cytosine from cytosine with high fidelity. 2012 , 424, 215-24	7
1002	Lateral distribution of NBD-PC fluorescent lipid analogs in membranes probed by molecular dynamics-assisted analysis of Fister Resonance Energy Transfer (FRET) and fluorescence quenching. 2012 , 13, 14545-64	17
1001	Structural insight into the mechanism of epothilone A bound to beta-tubulin and its mutants at Arg282Gln and Thr274Ile. 2012 , 30, 559-73	11
1000	Molecular dynamics investigations of PRODAN in a DLPC bilayer. 2012 , 116, 2713-21	26
1000 999	Molecular dynamics investigations of PRODAN in a DLPC bilayer. 2012 , 116, 2713-21 Dynamic behavior of acrylic acid clusters as quasi-mobile nodes in a model of hydrogel network. 2012 , 137, 244908	26 7
	Dynamic behavior of acrylic acid clusters as quasi-mobile nodes in a model of hydrogel network.	
999	Dynamic behavior of acrylic acid clusters as quasi-mobile nodes in a model of hydrogel network. 2012, 137, 244908 Photodynamic efficiency of cationic meso-porphyrins at lipid bilayers: insights from molecular	7
999 998	Dynamic behavior of acrylic acid clusters as quasi-mobile nodes in a model of hydrogel network. 2012, 137, 244908 Photodynamic efficiency of cationic meso-porphyrins at lipid bilayers: insights from molecular dynamics simulations. 2012, 116, 14618-27 Molecular Structure and Dynamics in Thin Water Films at Metal Oxide Surfaces: Magnesium,	7 29
999 998 997	Dynamic behavior of acrylic acid clusters as quasi-mobile nodes in a model of hydrogel network. 2012, 137, 244908 Photodynamic efficiency of cationic meso-porphyrins at lipid bilayers: insights from molecular dynamics simulations. 2012, 116, 14618-27 Molecular Structure and Dynamics in Thin Water Films at Metal Oxide Surfaces: Magnesium, Aluminum, and Silicon Oxide Surfaces. 2012, 116, 15962-15973 Develop and test a solvent accessible surface area-based model in conformational entropy	7 29 94
999 998 997 996	Dynamic behavior of acrylic acid clusters as quasi-mobile nodes in a model of hydrogel network. 2012, 137, 244908 Photodynamic efficiency of cationic meso-porphyrins at lipid bilayers: insights from molecular dynamics simulations. 2012, 116, 14618-27 Molecular Structure and Dynamics in Thin Water Films at Metal Oxide Surfaces: Magnesium, Aluminum, and Silicon Oxide Surfaces. 2012, 116, 15962-15973 Develop and test a solvent accessible surface area-based model in conformational entropy calculations. 2012, 52, 1199-212	7 29 94 70
999 998 997 996	Dynamic behavior of acrylic acid clusters as quasi-mobile nodes in a model of hydrogel network. 2012, 137, 244908 Photodynamic efficiency of cationic meso-porphyrins at lipid bilayers: insights from molecular dynamics simulations. 2012, 116, 14618-27 Molecular Structure and Dynamics in Thin Water Films at Metal Oxide Surfaces: Magnesium, Aluminum, and Silicon Oxide Surfaces. 2012, 116, 15962-15973 Develop and test a solvent accessible surface area-based model in conformational entropy calculations. 2012, 52, 1199-212 The Catalytic Machinery of Rhomboid Proteases: Combined MD and QM Simulations. 2012, 8, 4663-71 Revisiting Molecular Dynamics on a CPU/GPU system: Water Kernel and SHAKE Parallelization.	7 29 94 70

(2012-2012)

991	New insights into the mechanism of the Schiff base hydrolysis catalyzed by type I dehydroquinate dehydratase from S. enterica: a theoretical study. 2012 , 10, 7037-44	12
990	First-principles molecular dynamics simulations of NH4(+) and CH3COO(-) adsorption at the aqueous quartz interface. 2012 , 137, 224702	20
989	Phase transitions in coarse-grained lipid bilayers containing cholesterol by molecular dynamics simulations. 2012 , 103, 2125-33	47
988	Molecular dynamics simulation of HIV-1 fusion domain-membrane complexes: Insight into the N-terminal gp41 fusion mechanism. 2012 , 170, 9-16	12
987	Derivation and systematic validation of a refined all-atom force field for phosphatidylcholine lipids. 2012 , 116, 3164-79	394
986	Copper, BDNF and Its N-terminal domain: inorganic features and biological perspectives. 2012 , 18, 15618-31	31
985	Toward detection of DNA-bound proteins using solid-state nanopores: insights from computer simulations. 2012 , 33, 3466-79	12
984	Side-chain hydrophobicity and the stability of A E aggregates. 2012 , 21, 1837-48	37
983	Homology modeling of the human 5-HT1A, 5-HT 2A, D1, and D2 receptors: model refinement with molecular dynamics simulations and docking evaluation. 2012 , 18, 3639-55	24
982	Structural insights into interacting mechanism of ID1 protein with an antagonist ID1/3-PA7 and agonist ETS-1 in treatment of ovarian cancer: molecular docking and dynamics studies. 2012 , 18, 4865-84	6
981	Extensive structural change of the envelope protein of dengue virus induced by a tuned ionic strength: conformational and energetic analyses. 2012 , 26, 1311-25	7
980	Molecular dynamics re-refinement of two different small RNA loop structures using the original NMR data suggest a common structure. 2012 , 53, 321-39	22
979	Characterization and molecular modeling of the inclusion complexes of 2-(2-nitrovinyl) furan (G-0) with cyclodextrines. 2012 , 439, 275-85	10
978	Molecular recognition of esterase plays a major role on the removal of fatty soils during detergency. 2012 , 161, 228-34	5
977	Nonselective conduction in a mutated NaK channel with three cation-binding sites. 2012, 103, 2106-14	16
976	Peptide salt bridge stability: from gas phase via microhydration to bulk water simulations. 2012 , 137, 185101	14
975	Artificial Intelligence Applications and Innovations. 2012,	
974	Ligand selection from the analysis of protein conformational substates: new leads targeting the N-terminal domain of Hsp90. 2012 , 2, 4268	7

973	Structural controls on OH site availability and reactivity at iron oxyhydroxide particle surfaces. 2012 , 14, 2579-86	36
972	Screening for the Location of RNA using the Chloride Ion Distribution in Simulations of Virus Capsids. 2012 , 8, 2474-83	19
971	Proton transport in a membrane protein channel: two-dimensional infrared spectrum modeling. 2012 , 116, 6336-45	8
970	Molecular Dynamics Simulations of PAAPMA Polyelectrolyte Copolymers in Dilute Aqueous Solution: Chain Conformations and Hydration Properties. 2012 , 51, 10833-10839	28
969	Anesthetic molecules embedded in a lipid membrane: a computer simulation study. 2012 , 14, 12956-69	23
968	Modeling Triple Conformational Disorder in a New Crystal Polymorph of cis-Aquabis(l-isoleucinato)copper(II). 2012 , 12, 4116-4129	9
967	Atomistic simulations of a multicomponent asymmetric lipid bilayer. 2012 , 116, 13403-10	29
966	Interaction of counterions with subtilisin in acetonitrile: insights from molecular dynamics simulations. 2012 , 116, 5838-48	7
965	Molecular dynamics simulation of the spherical electrical double layer of a soft nanoparticle: effect of the surface charge and counterion valence. 2012 , 137, 174701	18
964	Exploring the mineralization of hydrophobins at a liquid interface. 2012 , 8, 11343	10
963	Properties of water in the interfacial region of a polyelectrolyte bilayer adsorbed onto a substrate studied by computer simulations. 2012 , 14, 11425-32	12
962	Interaction of naphthalene derivatives with lipids in membranes studied by the 1H-nuclear Overhauser effect and molecular dynamics simulation. 2012 , 14, 14049-60	6
961	Organic molecules on the surface of water dropletsan energetic perspective. 2012 , 14, 9537-45	43
960	Mixing Atomistic and Coarse Grain Solvation Models for MD Simulations: Let WT4 Handle the Bulk. 2012 , 8, 3880-94	37
959	Aqueous NaCl and CsCl solutions confined in crystalline slit-shaped silica nanopores of varying degree of protonation. 2012 , 28, 1256-66	71
958	Mechanism for Variable Selectivity and Conductance in Mutated NaK Channels. 2012 , 3, 2887-2891	6
957	Oriented confined water induced by cationic lipids. 2012 , 28, 4712-22	9
956	Analysis of solute-solvent interactions in the fragment molecular orbital method interfaced with effective fragment potentials: theory and application to a solvated griffithsin-carbohydrate complex. 2012 , 116, 9088-99	18

955	Conserved functional surface of antimammalian scorpion # oxins. 2012 , 116, 4796-800	19
954	Molecular modeling study for conformational changes of Sirtuin 2 due to substrate and inhibitor binding. 2012 , 30, 235-54	15
953	Water Structure and Hydrogen Bonding at Goethite/Water Interfaces: Implications for Proton Affinities. 2012 , 116, 4714-4724	49
952	Toward a detailed description of the pathways of allosteric communication in the GroEL chaperonin through atomistic simulation. 2012 , 51, 1707-18	8
951	Three-dimensional structure of human tefensin 28 via homology modelling and molecular dynamics. 2012 , 38, 90-101	4
950	Confinement-induced states in the folding landscape of the Trp-cage miniprotein. 2012 , 116, 11872-80	31
949	Interaction of water vapor with the surfaces of imidazolium-based ionic liquid nanoparticles and thin films. 2012 , 116, 11255-65	16
948	Nonintercalating nanosubstrates create asymmetry between bilayer leaflets. 2012 , 28, 2842-8	10
947	Insights into intrastrand cross-link lesions of DNA from QM/MM molecular dynamics simulations. 2012 , 134, 2111-9	57
946	Influence of protonation on substrate and inhibitor interactions at the active site of human monoamine oxidase-A. 2012 , 52, 1213-21	10
945	Second-contact shell mutation diminishes streptavidin-biotin binding affinity through transmitted effects on equilibrium dynamics. 2012 , 51, 597-607	7
944	Toward temperature-dependent coarse-grained potentials of side-chain interactions for protein folding simulations. II. Molecular dynamics study of pairs of different types of interactions in water at various temperatures. 2012 , 116, 6844-53	7
943	Hydration force between mica surfaces in aqueous KCl electrolyte solution. 2012, 28, 5339-49	77
942	Elements of nucleotide specificity in the Trypanosoma brucei mitochondrial RNA editing enzyme RET2. 2012 , 52, 1308-18	7
941	Development of polarizable models for molecular mechanical calculations. 4. van der Waals parametrization. 2012 , 116, 7088-101	44
940	Detection of allosteric signal transmission by information-theoretic analysis of protein dynamics. 2012 , 26, 868-81	86
939	Molecular dynamics simulation of the behaviour of the charged nanodroplet in electrospray. 2012 , 7, 1001-1004	2
938	Adsorption, folding, and packing of an amphiphilic peptide at the air/water interface. 2012 , 116, 2198-207	11

937	Theory and Simulation of Multicomponent Osmotic Systems. 2012, 8, 3493-3503	19
936	Kepler Predictor-Corrector Algorithm: Scattering Dynamics with One-Over-R Singular Potentials. 2012 , 8, 24-35	2
935	Dimerization of the full-length Alzheimer amyloid 即eptide (A畢2) in explicit aqueous solution: a molecular dynamics study. 2012 , 116, 4405-16	45
934	Efficient Algorithms for Langevin and DPD Dynamics. 2012 , 8, 3637-49	157
933	Binding modes and functional surface of anti-mammalian scorpion £toxins to sodium channels. 2012 , 51, 7775-82	21
932	Free energy of separation of structure II clathrate hydrate in water and a light oil. 2012 , 116, 5933-40	5
931	Molecular dynamics simulation study of the effect of DMSO on structural and permeation properties of DMPC lipid bilayers. 2012 , 116, 1299-308	23
930	Quantitative assessment of protein interaction with methyl-lysine analogues by hybrid computational and experimental approaches. 2012 , 7, 150-4	38
929	Nature of protein-CO2 interactions as elucidated via molecular dynamics. 2012 , 116, 11578-93	6
928	Characterization of a disordered protein during micellation: interactions of	14
927	Interaction of C70 fullerene with the Kv1.2 potassium channel. 2012 , 14, 12526-33	14
926	Assessing polyglutamine conformation in the nucleating event by molecular dynamics simulations. 2012 , 116, 10259-65	26
925	An Extension and Further Validation of an All-Atomistic Force Field for Biological Membranes. 2012 , 8, 2938-48	325
924	Peptide friction in water nanofilm on mica surface. 2012 , 21, 026801	3
923	Molecular dynamics study of anhydrous lamellar structures of synthetic glycolipids: effects of chain branching and disaccharide headgroup. 2012 , 116, 11626-34	17
922	Insights on P-Glycoprotein's Efflux Mechanism Obtained by Molecular Dynamics Simulations. 2012 , 8, 1853-64	79
921	Comparative molecular dynamics simulation study of crystal environment effect on protein structure. 2012 , 116, 6810-8	16
920	Sodium dodecyl sulfate at water-hydrophobic interfaces: a simulation study. 2012 , 116, 11936-42	28

(2012-2012)

919	A transporter converted into a sensor, a phototaxis signaling mutant of bacteriorhodopsin at $3.0\mathrm{I}$ 2012 , 415, 455-63	18
918	The role of hydration in protein stability: comparison of the cold and heat unfolded states of Yfh1. 2012 , 417, 413-24	42
917	Driving forces and structural determinants of steric zipper peptide oligomer formation elucidated by atomistic simulations. 2012 , 421, 390-416	55
916	Functional and conformational changes in the aspartic protease cardosin A induced by TFE. 2012 , 50, 323-30	3
915	Structural effect of the L16Q, K50E, and R53P mutations on homeodomain of pituitary homeobox protein 2. 2012 , 51, 305-13	9
914	Insight into NSAID-induced membrane alterations, pathogenesis and therapeutics: characterization of interaction of NSAIDs with phosphatidylcholine. 2012 , 1821, 994-1002	85
913	Water wires in atomistic models of the Hv1 proton channel. 2012 , 1818, 286-93	58
912	Mechanism of structural transformations induced by antimicrobial peptides in lipid membranes. 2012 , 1818, 194-204	42
911	Structure, dynamics, and hydration of POPC/POPS bilayers suspended in NaCl, KCl, and CsCl solutions. 2012 , 1818, 609-16	86
910	Comparative molecular dynamics simulations of the antimicrobial peptide CM15 in model lipid bilayers. 2012 , 1818, 1402-9	63
909	Coupling between the voltage-sensing and pore domains in a voltage-gated potassium channel. 2012 , 1818, 1726-36	17
908	Size-controlled nanopores in lipid membranes with stabilizing electric fields. 2012 , 423, 325-30	48
907	1-(2,6-Dibenzyloxybenzoyl)-3-(9H-fluoren-9-yl)-urea: a novel cyclophilin A allosteric activator. 2012 , 425, 938-43	2
906	Solvent Boundary Potentials for Hybrid QM/MM Computations Using Classical Drude Oscillators: A Fully Polarizable Model. 2012 , 8, 4527-38	98
905	Lipid Bilayers: The Effect of Force Field on Ordering and Dynamics. 2012, 8, 4807-17	66
904	Competitive binding of cations to duplex DNA revealed through molecular dynamics simulations. 2012 , 116, 12946-54	77
903	Why does the G117H mutation considerably improve the activity of human butyrylcholinesterase against sarin? Insights from quantum mechanical/molecular mechanical free energy calculations. 2012 , 51, 8980-92	27
902	Study on molecular cavity of oligoamide macrocycles by using scanning tunneling microscopy. 2012 , 13, 3598-604	7

901	The mechanism of the converter domain rotation in the recovery stroke of myosin motor protein. 2012 , 80, 2701-10	10
900	Flexible connection of the N-terminal domain in ClpB modulates substrate binding and the aggregate reactivation efficiency. 2012 , 80, 2758-68	15
899	Desolvation of macromolecules by ultrafast heating: A molecular-dynamics study. 2012 , 35, 99	1
898	Enhancing the effectiveness of virtual screening by using the ChemBioServer: Application to the discovery of PI3K#nhibitors. 2012 ,	1
897	Molecular dynamics approach to water structure of H(II) mesophase of monoolein. 2012, 136, 074509	8
896	Self-diffusion and viscosity in electrolyte solutions. 2012 , 116, 12007-13	117
895	Binding of hanatoxin to the voltage sensor of Kv2.1. 2012 , 4, 1552-64	12
894	Simple liquid models with corrected dielectric constants. 2012 , 116, 6936-44	54
893	All-atom stability and oligomerization simulations of polyglutamine nanotubes with and without the 17-amino-acid N-terminal fragment of the Huntingtin protein. 2012 , 116, 12168-79	11
892	A GROMOS Parameter Set for Vicinal Diether Functions: Properties of Polyethyleneoxide and Polyethyleneglycol. 2012 , 8, 3943-63	56
891	New Soft-Core Potential Function for Molecular Dynamics Based Alchemical Free Energy Calculations. 2012 , 8, 2373-82	69
890	Molecular dynamics simulations of membranes composed of glycolipids and phospholipids. 2012 , 116, 244-52	31
889	Understanding the pH-dependent behavior of graphene oxide aqueous solutions: a comparative experimental and molecular dynamics simulation study. 2012 , 28, 235-41	442
888	Insight into the structural deformations of beta-cyclodextrin caused by alcohol cosolvents and guest molecules. 2012 , 116, 3880-9	31
887	Force field development for actinyl ions via quantum mechanical calculations: an approach to account for many body solvation effects. 2012 , 116, 10885-97	35
886	Withaferin A binds covalently to the N-terminal domain of annexin A2. 2012 , 393, 1151-63	18
885	Dynamics of metastable 即airpin structures in the folding nucleus of amyloid 即rotein. 2012 , 116, 6311-25	23
884	Structural insights of rohu TLR3, its binding site analysis with fish reovirus dsRNA, poly I:C and zebrafish TRIF. 2012 , 51, 531-43	27

(2012-2012)

883	Structural Properties of Nonionic Tween80 Micelle in Water Elucidated by Molecular Dynamics Simulation. 2012 , 3, 287-297	33
882	In silico and in vitro characterization of phospholipase Allsoforms from soybean (Glycine max). 2012 , 94, 2608-19	14
881	Binding modes of Econotoxin to the bacterial sodium channel (NaVAb). 2012 , 102, 483-8	32
880	A theoretical model for calculating voltage sensitivity of ion channels and the application on Kv1.2 potassium channel. 2012 , 102, 1815-25	1
879	Hydrophobic mismatch and lipid sorting near OmpA in mixed bilayers: atomistic and coarse-grained simulations. 2012 , 102, 2279-87	15
878	Role of 即airpin formation in aggregation: the self-assembly of the amyloid-t25-35) peptide. 2012 , 103, 576-586	85
877	Elucidating the locking mechanism of peptides onto growing amyloid fibrils through transition path sampling. 2012 , 103, 1296-304	33
876	Simulations of HIV capsid protein dimerization reveal the effect of chemistry and topography on the mechanism of hydrophobic protein association. 2012 , 103, 1363-9	11
875	Constraint force design method for topology optimization of planar rigid-body mechanisms. 2012 , 44, 1277-1296	15
874	Theoretical study of the reaction mechanism of Mycobacterium tuberculosis type II dehydroquinate dehydratase. 2012 , 1001, 60-66	5
873	Proton-coupled dynamics in lactose permease. 2012 , 20, 1893-904	46
872	In silico identification of novel hevein-like peptide precursors. 2012 , 38, 127-36	40
871	Insights into buforin II membrane translocation from molecular dynamics simulations. 2012, 38, 357-62	10
870	Membrane binding and self-association of the epsin N-terminal homology domain. 2012 , 423, 800-17	44
869	Temperature dependence of the lateral hydrogen bonded clusters of molecules at the free water surface. 2012 , 176, 33-38	8
868	Optimization of the molecular dynamics method for simulations of DNA and ion transport through biological nanopores. 2012 , 870, 165-86	16
867	Molecular dynamics study of the interaction of arginine with phosphatidylcholine and phosphatidylethanolamine bilayers. 2012 , 116, 4476-83	12
866	SUMO1 modification of PTEN regulates tumorigenesis by controlling its association with the plasma membrane. 2012 , 3, 911	138

865	Facet Selectivity of Binding on Quartz Surfaces: Free Energy Calculations of Amino-Acid Analogue Adsorption. 2012 , 116, 2933-2945	38
864	Charge Transfer between Water Molecules As the Possible Origin of the Observed Charging at the Surface of Pure Water. 2012 , 3, 107-111	86
863	A Chemically Accurate Implicit-Solvent Coarse-Grained Model for Polystyrenesulfonate Solutions. 2012 , 45, 2551-2561	31
862	Conformational free-energy landscapes for a peptide in saline environments. 2012 , 103, 2513-20	5
861	Cationic dimyristoylphosphatidylcholine and dioleoyloxytrimethylammonium propane lipid bilayers: atomistic insight for structure and dynamics. 2012 , 116, 269-76	22
860	Interpretation of IR and Raman line shapes for H2O and D2O ice Ih. 2012 , 116, 13821-30	84
859	Optimal pairwise and non-pairwise alchemical pathways for free energy calculations of molecular transformation in solution phase. 2012 , 136, 124120	36
858	Multiple templates-based homology modeling and docking analysis of angiotensin II type 1 receptor. 2012 , 19, 3033-3039	1
857	Optimization of the additive CHARMM all-atom protein force field targeting improved sampling of the backbone [Iland side-chain (11) and (12) dihedral angles. 2012 , 8, 3257-3273	2511
856	Molecular dynamics properties of varying amounts of the anticancer drug gemcitabine inside an open-ended single-walled carbon nanotube. 2012 , 550, 99-103	19
855	Nonequilibrium molecular dynamics simulations of the thermal conductivity of water: a systematic investigation of the SPC/E and TIP4P/2005 models. 2012 , 137, 074503	66
854	Correlations in liquid water for the TIP3P-Ewald, TIP4P-2005, TIP5P-Ewald, and SWM4-NDP models. 2012 , 136, 064518	37
853	Mimicking the biomolecular control of calcium oxalate monohydrate crystal growth: effect of contiguous glutamic acids. 2012 , 28, 12182-90	17
852	Lateral dynamics of surfactants at the free water surface: a computer simulation study. 2012 , 28, 14944-53	34
851	Sitting at the edge: how biomolecules use hydrophobicity to tune their interactions and function. 2012 , 116, 2498-503	166
850	Large influence of cholesterol on solute partitioning into lipid membranes. 2012 , 134, 5351-61	124
849	Variable interactions between protein crowders and biomolecular solutes are important in understanding cellular crowding. 2012 , 116, 599-605	104
848	The Multiscale Coarse-Graining Method. 2012 , 47-81	17

847	Computational Drug Discovery and Design. 2012 ,	19
846	Calcium and phosphatidylserine inhibit lipid electropore formation and reduce pore lifetime. 2012 , 245, 599-610	29
845	Ss-bCNGa: a unique member of the bacterial cyclic nucleotide gated (bCNG) channel family that gates in response to mechanical tension. 2012 , 41, 1003-13	10
844	Analyzing the molecular basis of enzyme stability in ethanol/water mixtures using molecular dynamics simulations. 2012 , 52, 465-73	36
843	Structural coupling between the Rho-insert domain of Cdc42 and the geranylgeranyl binding site of RhoGDI. 2012 , 51, 715-23	8
842	Dynamic changes in the secondary structure of ECE-1 and XCE account for their different substrate specificities. 2012 , 13, 285	4
841	Molecular origin of piezo- and pyroelectric properties in collagen investigated by molecular dynamics simulations. 2012 , 116, 1901-7	20
840	Modeling the Structure and Dynamics of Polyelectrolyte Multilayers. 2012 , 121-166	3
839	Mechanism of inhibition of calcium oxalate crystal growth by an osteopontin phosphopeptide. 2012 , 8, 1226-1233	26
838	Engineering a potent and specific blocker of voltage-gated potassium channel Kv1.3, a target for autoimmune diseases. 2012 , 51, 1976-82	20
837	Virus capsid dissolution studied by microsecond molecular dynamics simulations. 2012 , 8, e1002502	53
836	Cupricyclins, novel redox-active metallopeptides based on conotoxins scaffold. 2012 , 7, e30739	6
835	Exploring protein dynamics space: the dynasome as the missing link between protein structure and function. 2012 , 7, e33931	65
834	Disulfide bridges remain intact while native insulin converts into amyloid fibrils. 2012 , 7, e36989	56
833	Structural basis of the selective block of Kv1.2 by maurotoxin from computer simulations. 2012 , 7, e47253	18
832	Engineering tocopherol selectivity in ETTP: a combined in vitro/in silico study. 2012 , 7, e49195	10
831	Simulation of Intramolecular Hydrogen Bond Dynamics in Manzamine A as a Sensitive Test for Charge Distribution Quality. 2012 , 7, 1934578X1200700	
830	Catalytic and Molecular Properties of Rabbit Liver Carboxylesterase Acting on 1,8-Cineole Derivatives. 2012 , 7, 1934578X1200700	

829	Effects of point mutations in pVHL on the binding of HIF-1⊞ 2012 , 80, 733-46	14
828	Molecular modeling of hair keratin/peptide complex: Using MM-PBSA calculations to describe experimental binding results. 2012 , 80, 1409-17	13
827	Interactions between relay helix and Src homology 1 (SH1) domain helix drive the converter domain rotation during the recovery stroke of myosin II. 2012 , 80, 1569-81	3
826	Mimicking the action of folding chaperones by Hamiltonian replica-exchange molecular dynamics simulations: application in the refinement of de novo models. 2012 , 80, 1744-54	12
825	Exploring the essential collective dynamics of interacting proteins: application to prion protein dimers. 2012 , 80, 1847-65	13
824	Attraction between like-charged monovalent ions. 2012 , 136, 184501	22
823	Routine Microsecond Molecular Dynamics Simulations with AMBER on GPUs. 1. Generalized Born. 2012 , 8, 1542-1555	1186
822	Molecular dynamics study of MspA arginine mutants predicts slow DNA translocations and ion current blockades indicative of DNA sequence. 2012 , 6, 6960-8	58
821	On Atomistic and Coarse-Grained Models for C60 Fullerene. 2012 , 8, 1370-8	107
820	Coherent microscopic picture for urea-induced denaturation of proteins. 2012 , 116, 8856-62	26
820 819	Coherent microscopic picture for urea-induced denaturation of proteins. 2012 , 116, 8856-62 Molecular dynamics simulations of the TrkH membrane protein. 2012 , 51, 1559-65	26
819	Molecular dynamics simulations of the TrkH membrane protein. 2012 , 51, 1559-65	20
819 818	Molecular dynamics simulations of the TrkH membrane protein. 2012 , 51, 1559-65 Salt effects on water/hydrophobic liquid interfaces: a molecular dynamics study. 2012 , 24, 124109 Effect of the thermostat in the molecular dynamics simulation on the folding of the model protein	20
819 818 817	Molecular dynamics simulations of the TrkH membrane protein. 2012, 51, 1559-65 Salt effects on water/hydrophobic liquid interfaces: a molecular dynamics study. 2012, 24, 124109 Effect of the thermostat in the molecular dynamics simulation on the folding of the model protein chignolin. 2012, 18, 2785-94	20 17 7
819 818 817	Molecular dynamics simulations of the TrkH membrane protein. 2012, 51, 1559-65 Salt effects on water/hydrophobic liquid interfaces: a molecular dynamics study. 2012, 24, 124109 Effect of the thermostat in the molecular dynamics simulation on the folding of the model protein chignolin. 2012, 18, 2785-94 Membrane Protein Simulations Using AMBER Force Field and Berger Lipid Parameters. 2012, 8, 948-58 Mechanistic Insights into the Hydrolysis of Organophosphorus Compounds by Paraoxonase-1:	20 17 7 115
819 818 817 816 815	Molecular dynamics simulations of the TrkH membrane protein. 2012, 51, 1559-65 Salt effects on water/hydrophobic liquid interfaces: a molecular dynamics study. 2012, 24, 124109 Effect of the thermostat in the molecular dynamics simulation on the folding of the model protein chignolin. 2012, 18, 2785-94 Membrane Protein Simulations Using AMBER Force Field and Berger Lipid Parameters. 2012, 8, 948-58 Mechanistic Insights into the Hydrolysis of Organophosphorus Compounds by Paraoxonase-1: Exploring the Limits of Substrate Tolerance in a Promiscuous Enzyme. 2012, 25, 1247-1260 Comparison of selected polarizable and nonpolarizable water models in molecular dynamics	20 17 7 115

811	Folding helical proteins in explicit solvent using dihedral-biased tempering. 2012, 109, 8139-44	25
810	Hybrid QM/MM Molecular Dynamics Study of Benzocaine in a Membrane Environment: How Does a Quantum Mechanical Treatment of Both Anesthetic and Lipids Affect Their Interaction. 2012 , 8, 2197-203	13
809	Molecular dynamics simulation studies on structural and conformational changes in tyrosine-67 nitrated cytochrome c. 2012 , 38, 459-467	2
808	Chemical details on nucleolipid supramolecular architecture: molecular modeling and physicochemical studies. 2012 , 28, 7452-60	10
807	Estimation of the mutual orientation and intermolecular interaction of C12Ex from molecular dynamics simulations. 2012 , 116, 4879-88	4
806	Comparison of Cellulose Isimulations with Three Carbohydrate Force Fields. 2012 , 8, 735-48	101
805	Searching the "biologically relevant"conformation of dopamine: a computational approach. 2012 , 52, 99-112	42
804	Testing the semi-explicit assembly solvation model in the SAMPL3 community blind test. 2012 , 26, 563-8	19
803	Thermodynamic integration to predict host-guest binding affinities. 2012 , 26, 569-76	18
802	3D-QSAR studies of triazolopyrimidine derivatives of Plasmodium falciparum dihydroorotate dehydrogenase inhibitors using a combination of molecular dynamics, docking, and genetic algorithm-based methods. 2012 , 5, 91-103	11
801	New insights into the mechanism of the Schiff base formation catalyzed by type I dehydroquinate dehydratase from S. enterica. 2012 , 131, 1	5
800	Hot or not? Discovery and characterization of a thermostable alditol oxidase from Acidothermus cellulolyticus 11B. 2012 , 95, 389-403	17
799	Structural features of [NiFeSe] and [NiFe] hydrogenases determining their different properties: a computational approach. 2012 , 17, 543-55	24
798	Conformation analysis of a surface loop that controls active site access in the GH11 xylanase A from Bacillus subtilis. 2012 , 18, 1473-9	14
797	Accurate prediction of the binding free energy and analysis of the mechanism of the interaction of replication protein A (RPA) with ssDNA. 2012 , 18, 2761-83	3
796	Theoretical prediction of the binding free energy for mutants of replication protein A. 2012, 18, 3035-49	3
795	3D-QSAR studies of JNK1 inhibitors utilizing various alignment methods. 2012 , 79, 53-67	9
794	Molecular dynamics simulations of the interaction of glucose with imidazole in aqueous solution. 2012 , 349, 73-7	16

793	Synthesis and characterization of a paramagnetic sialic acid conjugate as probe for magnetic resonance applications. 2012 , 354, 21-31	5	
792	Oligoarginine vectors for intracellular delivery: role of arginine side-chain orientation in chain length-dependent destabilization of lipid membranes. 2012 , 165, 89-96	5	
791	Molecular dynamics studies of thairpin folding with the presence of the sodium ion. 2012 , 38, 1-9	2	
790	Architecture, implementation and parallelisation of the GROMOS software for biomolecular simulation. 2012 , 183, 890-903	246	
789	Properties of oxidized phospholipid monolayers: An atomistic molecular dynamics study. 2012 , 519-520, 93-99	24	
788	Rapid flip-flop motions of diacylglycerol and ceramide in phospholipid bilayers. 2012 , 522, 96-102	39	
787	The number-adaptive multiscale QM/MM molecular dynamics simulation: Application to liquid water. 2012 , 524, 56-61	46	
786	Structure and dynamics of <code>Hactoglobulin</code> in complex with dodecyl sulfate and laurate: a molecular dynamics study. 2012 , 165-166, 79-86	33	
785	Molecular mechanism of the allosteric enhancement of the umami taste sensation. 2012 , 279, 3112-20	66	
7 ⁸ 4	Free energy calculations on snake venom metalloproteinase BaP1. 2012 , 79, 990-1000	4	
783	The molecular dynamics of Trypanosoma brucei UDP-galactose 4'-epimerase: a drug target for African sleeping sickness. 2012 , 80, 173-81	12	
782	Molecular docking and dynamics simulation, receptor-based hypothesis: application to identify novel sirtuin 2 inhibitors. 2012 , 80, 315-27	12	
781	Molecular dynamics simulations of peptide inhibitors complexed with Trypanosoma cruzi trypanothione reductase. 2012 , 80, 561-71	8	
780	Thermodynamics and kinetics of large-time-step molecular dynamics. <i>Journal of Computational Chemistry</i> , 2012 , 33, 475-83	10	
779	Enabling grand-canonical Monte Carlo: extending the flexibility of GROMACS through the GromPy python interface module. <i>Journal of Computational Chemistry</i> , 2012 , 33, 1207-14	2	
778	Structure of micelle-bound adrenomedullin: a first step toward the analysis of its interactions with receptors and small molecules. 2012 , 97, 45-53	28	
777	Study and design of stability in GH5 cellulases. 2012 , 109, 31-44	81	
776	Probing the oligomeric state and interaction surfaces of Fukutin-I in dilauroylphosphatidylcholine bilayers. 2012 , 41, 199-207	13	

(2021-2012)

775	The molecular basis for the inhibition of human cytochrome P450 1A2 by oroxylin and wogonin. 2012 , 41, 297-306		12
774	Tetrahydroisoquinolines acting as dopaminergic ligands. A molecular modeling study using MD simulations and QM calculations. 2012 , 18, 419-31		23
773	Molecular dynamics simulation and density functional theory studies on the active pocket for the binding of paclitaxel to tubulin. 2012 , 18, 377-91		15
772	A morphometric approach for the accurate solvation thermodynamics of proteins and ligands. <i>Journal of Computational Chemistry</i> , 2013 , 34, 1969-74	3.5	8
771	Molecular mechanism of membrane binding of the GRP1 PH domain. 2013, 425, 3073-90		46
770	Improving the Efficiency of Free Energy Calculations in the Amber Molecular Dynamics Package. 2013 , 9,		72
769	Nanoscale, electric field-driven water bridges in vacuum gaps and lipid bilayers. 2013 , 246, 793-801		17
768	Improved Parameterization of Protein DNA Interactions for Molecular Dynamics Simulations of PCNA Diffusion on DNA.		
767	The binding of palonosetron and other antiemetic drugs to the serotonin 5-HT3 receptor.		1
766	Unifying the Ambivalent Mechanisms of Protein-Stabilising Osmolytes.		
765	A buried glutamate in the cross-thore renders then dorphin fibrils reversible. 2021 , 13, 19593-19603		2
764	An allosteric interaction controls the activation mechanism of SHP2 tyrosine phosphatase.		
763	Structural Determinants of Phosphopeptide Binding to the N-Terminal Src Homology 2 Domain of the SHP2 Phosphatase.		0
762	Induced Polarization in MD Simulations of the 5HT3 Receptor Channel.		
761	Structures of metabotropic GABABreceptor.		
760	In silico design of Multi-epitope-based peptide vaccine against SARS-CoV-2 using its spike protein.		5
759	Simulating Multiple Substrate Binding Events by EGlutamyltransferase using Accelerated Molecular Dynamics.		
758	Scaffold Searching of FDA and EMA-Approved Drugs Identifies Lead Candidates for Drug Repurposing in Alzheimer's Disease. 2021 , 9, 736509		1

757	Conformational Flexibilities and Solvation Properties of Insulin in Aromatic Amino Acid Solutions: A Molecular Dynamics Study Using CHARMM Drude Polarizable Model. 1-14	О
756	Structure Determination of Inactive-State GPCRs with a Universal Nanobody.	2
755	Zn(II) binding causes interdomain changes in the structure and flexibility of the human prion protein. 2021 , 11, 21703	1
754	A surface-promoted redox reaction occurs spontaneously on solvating inorganic aerosol surfaces. 2021 , 374, 747-752	6
753	Stable Cell Clones Harboring Self-Replicating SARS-CoV-2 RNAs for Drug Screen.	0
752	Modulating the pro-apoptotic activity of cytochrome c at a biomimetic electrified interface. 2021 , 7, eabg4119	O
751	Plasticity in Ligand Recognition at Somatostatin Receptors.	3
75°	Atomistic description of molecular binding processes based on returning probability theory. 2021 , 155, 204503	Ο
749	Multiple rereads of single proteins at single-amino acid resolution using nanopores. 2021 , eabl4381	48
748	Rhenium nanoparticles for the delivery of HSP 90 inhibitors: A new drug delivery platform designed by molecular dynamics simulation. 2021 , 347, 117995	1
747	Alpha-synuclein[in PreNAC(46-56) Fibril B [En f] Molekler Dinamik Simlasyon Yfitemi ile Konformasyonel Defirlendirmesi.	
746	Tyrosine Nitration Contributes to Nitric OxideBtimulated Degradation of CYP2B6. 2020 , 98, 267-279	1
745	Structure and dynamics of the quaternary hunchback mRNA translation repression complex.	
744	Stability of Human Serum Amyloid A Fibrils.	
743	A joint reaction coordinate for computing the free energy landscape of pore nucleation and pore expansion in lipid membranes.	
742	Insights into G-Quadruplex⊞emin Dynamics Using Atomistic Simulations: Implications for Reactivity and Folding.	
741	Structure of HIV-1 gp41 with its membrane anchors targeted by neutralizing antibodies.	
740	The loops of the N-SH2 binding cleft do not serve as allosteric switch in SHP2 activation.	

739	Forever Young: Structural Stability of Telomeric Guanine-Quadruplexes in Presence of Oxidative DNA Lesions.	
738	Computational NMR Study of Ion Pairing of 1-Decyl-3-methyl-imidazolium Chloride in Molecular Solvents. 2020 , 124, 10776-10786	3
737	The Molecular Dynamics Study on the stability of Elk Prion Protein. 2020,	
736	The Molecular Dynamics Study on the PATHOGENICITy of Cystatin C Mutant. 2020,	
735	Hydrophobic fluorinated graphene templated molecular sieving for high efficiency seawater desalination. 2022 , 523, 115452	О
734	Axonal plasma membrane-mediated toxicity of cholesterol in Alzheimer's disease: A microsecond molecular dynamics study. 2021 , 281, 106718	O
733	Ferrocene-modified dendrimers as support of copper nanoparticles: evaluation of the catalytic activity for the decomposition of ammonium perchlorate. 2022 , 23, 100631	О
732	Computational design of a hydrogenated porous graphene membrane for anion selective transport. 2021 ,	О
731	Investigation of Marine-Derived Natural Products as Raf Kinase Inhibitory Protein (RKIP)-Binding Ligands. 2021 , 19, 581	1
730	Computational Insights into the Unfolding of a Destabilized Superoxide Dismutase 1 Mutant 2021 , 10,	
729	Structural Variations of Metallothionein with or without Zinc Ions Elucidated by All-Atom Molecular Dynamics Simulations. 2021 , 125, 12712-12717	О
728	Structural basis of the regulation of the normal and oncogenic methylation of nucleosomal histone H3 Lys36 by NSD2. 2021 , 12, 6605	2
727	A Thermostat-Consistent Fully Coupled Molecular Dynamics Generalized Fluctuating Hydrodynamics Model for Non-Equilibrium Flows. 2100360	
726	The C. albicans virulence factor Candidalysin polymerizes in solution to form membrane pores and damage epithelial cells.	
725	Fast Equilibration of Water between Buried Sites and the Bulk by Molecular Dynamics with Parallel Monte Carlo Water Moves on Graphical Processing Units. 2021 ,	1
724	Computational and Experimental Models of Type III Lipid-Based Formulations of Loratadine Containing Complex Nonionic Surfactants. 2021 , 18, 4354-4370	
723	Resolving isomeric posttranslational modifications using a nanopore.	0
722	Histone H3 Inhibits Ubiquitin-Ubiquitin Intermolecular Interactions to Enhance Binding to DNA Methyl Transferase 1. 2021 , 434, 167371	O

721	Structure and Undulations of Escin Adsorption Layer at Water Surface Studied by Molecular Dynamics. 2021 , 26,	О
720	Interplay of - and -Interactions of Glycolipids in Membrane Adhesion. 2021 , 8, 754654	1
719	Paratope states in solution improve structure prediction and docking. 2021,	2
718	study of cox protein from P2 type enteric bacteriophages based on sequence, structure and dynamics to understand its functional integrity. 2021 , 1-16	O
717	Reaction-Controlled Phase-Transfer Process of Polyoxometalate-Based Catalyst for Cellulose Esterification: A Molecular Dynamics Study. 2021 , 125, 25478-25487	0
716	Phenotypic and studies for a series of synthetic thiosemicarbazones as New Delhi metallo-beta-lactamase carbapenemase inhibitors. 2021 , 1-13	1
715	Structural mechanism for regulation of Rab7 by site-specific monoubiquitination. 2021,	О
714	Structure-based screening combined with computational and biochemical analyses identified the inhibitor targeting the binding of DNA Ligase 1 to UHRF1. 2021 , 52, 116500	3
713	Interactions of Urea-Based Inhibitors with Prostate-Specific Membrane Antigen for Boron Neutron Capture Therapy 2021 , 6, 33354-33369	
712	N-Terminal-Driven Binding Mechanism of an Antigen Peptide to Human Leukocyte Antigen-A*2402 Elucidated by Multicanonical Molecular Dynamic-Based Dynamic Docking and Path Sampling Simulations. 2021 ,	O
711	Residue Folding Degree-Relationship to Secondary Structure Categories and Use as Collective Variable. 2021 , 22,	0
710	Charge neutralization of lysine via carbamylation reveals hidden aggregation hot-spots in tau protein flanking regions. 2021 ,	О
709	The computational analyses, molecular dynamics of fatty-acid transport mechanism to the CD36 receptor. 2021 , 11, 23207	0
708	Metabolic interactions of benzodiazepines with oxycodone ex vivo and toxicity depending on usage patterns in an animal model. 2021 ,	1
707	Recharging your fats: CHARMM36 parameters for neutral lipids triacylglycerol and diacylglycerol 2021 , 1, None	0
706	Molecular Dynamics Simulation Study of Covalently Bound Hybrid Coagulants (CBHyC): Molecular Structure and Coagulation Mechanisms.	
705	The molecular origin of the electrostatic gating of single-molecule field-effect biosensors investigated by molecular dynamics simulations 2022 ,	О
704	Mechanism of Alkaline Surfactant Polymer in Oil-Water Interface: Physicochemical of Fluid Rheology, Interfacial Tension and Molecular Dynamics Simulation. 2021 , 147-155	1

703	Binding free energy of protein/ligand complexes calculated using dissociation Parallel Cascade Selection Molecular Dynamics and Markov state model 2021 , 18, 305-316	1
702	Thermodynamic solubility of celecoxib in organic solvents.	
701	SARS-Cov-2 Spike binding to ACE2 is stronger and longer ranged due to glycan interaction. 2021 ,	3
700	Deconvoluting the Directed Evolution Pathway of Engineered Acyltransferase LovD. e202101349	O
699	The Systems of Naringenin with Solubilizers Expand Its Capability to Prevent Neurodegenerative Diseases 2022 , 23,	1
698	Molecular dynamics investigation of the liquid-gas interface behavior: Simulations of the sodium oleate/sodium abietate/water system. 2022 , 635, 128086	Ο
697	Exploring the permeation of fluoroquinolone metalloantibiotics across outer membrane porins by combining molecular dynamics simulations and a porin-mimetic in vitro model 2021 , 1864, 183838	1
696	Insights into the binding of morin to human D -crystallin 2021 , 282, 106750	1
695	Molecular dynamics simulations of the flexibility and inhibition of SARS-CoV-2 NSP 13 helicase 2022 , 112, 108122	
694	Volumetric Properties for the Binding of 1,4-Dioxane to Amide Naphthotubes in Water. 2020 , 124, 9175-9181	4
693	Unraveling the Influence of K280 Acetylation on the Conformational Features of Tau Core Fragment: A Molecular Dynamics Simulation Study 2021 , 8, 801577	3
692	Anchoring of Amyloid-Bonto Polyunsaturated Phospholipid Membranes 2021, 1-11	
691	Design, Synthesis, Biological Evaluation, and Molecular Modeling of 2-Difluoromethylbenzimidazole Derivatives as Potential PI3K nhibitors 2022 , 27,	
690	Impact of deep eutectic solvents (DESs) and individual DES components on alcohol dehydrogenase catalysis: connecting experimental data and molecular dynamics simulations. 2022 , 24, 1120-1131	5
689	The Molecular Mechanism of Human Voltage-Dependent Anion Channel 1 Blockade by the Metallofullerenol Gd@C(OH): An In Silico Study 2022 , 12,	O
688	Structure and Interaction Based Design of Anti-SARS-CoV-2 Aptamers 2022 ,	1
687	Structural Ramifications of Spike Protein D614G Mutation in SARS-CoV-2.	1
686	Evaluation of Docking Machine Learning and Molecular Dynamics Methodologies for DNA-Ligand Systems 2022 , 15,	2

685	Protein allostery and ligand design: Computational design meets experiments to discover novel chemical probes 2022 , 167468	2
684	Microsecond molecular dynamics studies of cholesterol-mediated myelin sheath degeneration in early Alzheimer's disease. 2021 ,	O
683	Dynamics of molecular associates in methanol/water mixtures 2022,	0
682	Dynamics of 5R-Tg Base Flipping in DNA Duplexes Based on Simulations-Agreement with Experiments and Beyond 2022 , 62, 386-398	O
681	Dissipative Particle Dynamics Simulation of Ultrasound Propagation through Liquid Water 2022,	1
680	Molecular mechanisms of direct and indirect interplay between amyloid #2 oligomer and characteristic lipids. 2022 ,	
679	Autophagy and evasion of immune system by SARS-CoV-2. Structural features of the Non-structural protein 6 from Wild Type and Omicron viral strains interacting with a model lipid bilayer.	
678	'C-type' closed state and gating mechanisms of K2P channels revealed by conformational changes of the TREK-1 channel 2022 ,	O
677	Specific Ion Effects in Lanthanide-Amphiphile Structures at the Air-Water Interface and Their Implications for Selective Separation 2022 , 14, 7504-7512	2
676	A Model for the Signal Initiation Complex Between Arrestin-3 and the Src Family Kinase Fgr 2021 , 434, 167400	1
675	Construction of a Humanized Artificial VHH Library Reproducing Structural Features of Camelid VHHs for Therapeutics 2022 , 11,	1
674	A Computer-Aided Approach for the Discovery of D-Peptides as Inhibitors of SARS-CoV-2 Main Protease 2021 , 8, 816166	3
673	Degradation of pesticides diazinon and diazoxon by phosphotriesterase: insight into divergent mechanisms from QM/MM and MD simulations 2021 ,	2
672	Development of OPLS-AA/M Parameters for Simulations of G Protein-Coupled Receptors and Other Membrane Proteins.	1
671	RNA Triplex Structures Revealed by WAXS-Driven MD Simulations.	
670	The phase behaviour of cetyltrimethylammonium chloride surfactant aqueous solutions at high concentrations: an all-atom molecular dynamics simulation study 2022 ,	O
669	A bioactivated in vivo assembly nanotechnology fabricated NIR probe for small pancreatic tumor intraoperative imaging 2022 , 13, 418	4
668	Peptide Isomerization is Suppressed at the Air-Water Interface 2022 , 574-579	1

667	CDR loop interactions can determine heavy and light chain pairing preferences in bispecific antibodies 2022 , 14, 2024118	O
666	Comparing Antibody Interfaces to Inform Rational Design of New Antibody Formats 2022 , 9, 812750	O
665	Oligosaccharide Presentation Modulates the Molecular Recognition of Glycolipids by Galectins on Membrane Surfaces 2022 , 15,	1
664	The effects of molecular weight and orientation on the membrane permeation and partitioning of polycyclic aromatic hydrocarbons: a computational study 2022 ,	O
663	Mechanistic insight into the destabilization of p53TD tetramer by cancer-related R337H mutation: a molecular dynamics study 2022 ,	1
662	Residue-Residue Contact Changes during Functional Processes Define Allosteric Communication Pathways 2022 ,	3
661	Exploring Toxins for Hunting SARS-CoV-2 Main Protease Inhibitors: Molecular Docking, Molecular Dynamics, Pharmacokinetic Properties, and Reactome Study 2022 , 15,	6
660	Stable Cell Clones Harboring Self-Replicating SARS-CoV-2 RNAs for Drug Screen 2022 , jvi0221621	1
659	In Silico and Experimental ADAM17 Kinetic Modeling as Basis for Future Screening System for Modulators 2022 , 23,	0
658	Docking-guided rational engineering of a macrolide glycosyltransferase glycodiversifies epothilone B 2022 , 5, 100	1
657	Fluorinated graphene nanomaterial causes potential mechanical perturbations to a biomembrane 2022 , 28, 49	
656	Substrate specificity and proposed structure of the proofreading complex of T7 DNA polymerase 2022 , 101627	O
655	A multiple-step screening protocol to identify allosteric inhibitors of Spike-hACE2 binding 2022,	2
654	Data Mining Guided Molecular Investigations on the Coalescence of Water-in-Oil Droplets.	O
653	Salting-Up of Surfactants at the Surface of Saline Water as Detected by Tensiometry and SFG and Supported by Molecular Dynamics Simulation 2022 ,	3
652	Study on the interaction of ethylene glycol with trypsin: Binding ability, activity, and stability. 2022 , 350, 118542	2
651	Field-enhanced water transport in sub-nanometer graphene nanopores. 2022 , 528, 115610	2
650	Insights into Sorption and Molecular Transport of Aqueous Glucose into Zeolite Nanopores 2022 ,	

649	Effects of interlayer spacing and oxidation degree of graphene oxide nanosheets on water permeation: a molecular dynamics study 2022 , 28, 57	2
648	Ion Permeation, Selectivity, and Electronic Polarization in Fluoride Channels 2022,	1
647	Protein-protein interaction of RdRp with its co-factor NSP8 and NSP7 to decipher the interface hotspot residues for drug targeting: A comparison between SARS-CoV-2 and SARS-CoV 2022 , 1257, 132602	2
646	Strigolactone Analogs: Two New Potential Bioactiphores for Glioblastoma 2022,	
645	Predictions of Skin Permeability Using Molecular Dynamics Simulation from Two-Dimensional Sampling of Spatial and Alchemical Perturbation Reaction Coordinates.	2
644	Modulation of slippage at brineBil interfaces by surfactants: The effects of surfactant density and tail length. 2022 , 34, 022106	O
643	SPCS1-Dependent E2-p7 processing determines HCV Assembly efficiency 2022 , 18, e1010310	1
642	DNA opening during transcription initiation by RNA polymerase II in atomic detail.	
641	Exploring the Structural Rearrangements of the Human Insulin-Degrading Enzyme through Molecular Dynamics Simulations 2022 , 23,	О
640	Accurate Simulations of Lipid Monolayers Require a Water Model with Correct Surface Tension 2022 ,	2
639	Conformational transitions and ligand-binding to a muscle-type nicotinic acetylcholine receptor 2022 ,	1
638	Investigating the Broad Matrix-Gate Network in the Mitochondrial ADP/ATP Carrier through Molecular Dynamics Simulations 2022 , 27,	2
637	Conformational Change from U- to I-Shape of Ion Transporters Facilitates K Transport across Lipid Bilayers 2022 ,	0
636	In silico study of substrate chemistry effect on the tethering of engineered antibodies for SARS-CoV-2 detection: Amorphous silica vs gold 2022 , 213, 112400	
635	Broadly neutralizing antibodies target a hemagglutinin anchor epitope 2021,	7
634	Src activates retrograde membrane traffic through phosphorylation of GBF1. 2021 , 10,	2
633	Identification of functional substates of KRas during GTP hydrolysis with enhanced sampling simulations 2022 ,	3
632	The Role of Structural Order in Heterogeneous Ice Nucleation.	1

631	Computational Models for the Study of Protein Aggregation 2022 , 2340, 51-78	
630	Investigation of the pH-dependent aggregation mechanisms of GCSF using low resolution protein characterization techniques and advanced molecular dynamics simulations 2022 , 20, 1439-1455	0
629	Lipid bilayers as potential ice nucleating agents 2022,	
628	Molecular Dynamics Simulation Study of Covalently Bound Hybrid Coagulants (Cbhyc): Molecular Structure and Coagulation Mechanisms.	
627	Non-Covalent Hybridization of Carbon Nanotube by Single-Stranded DNA Homodecamers: in-silico Approach. 2022 , 96, 145-151	
626	Characterization of Amyloidogenic Peptide Aggregability in Helical Subspace 2022 , 2340, 401-448	o
625	Approach to Study pH-Dependent Protein Association Using Constant-pH Molecular Dynamics: Application to the Dimerization of 配actoglobulin 2022 ,	1
624	Plasticity in ligand recognition at somatostatin receptors 2022,	2
623	Investigation of the Molecular Details of the Interactions of Selenoglycosides and Human Galectin-3 2022 , 23,	1
622	Interactions of Co, Cu, and non-metal phthalocyanines with external structures of SARS-CoV-2 using docking and molecular dynamics 2022 , 12, 3316	1
621	HNF1A POU Domain Mutations Found in Japanese Liver Cancer Patients Cause Downregulation of Promoter Activity with Possible Disruption in Transcription Networks 2022 , 13,	0
620	Naturally occurring plant-based anticancerous candidates as prospective ABCG2 inhibitors: an in silico drug discovery study 2022 , 1	3
619	Visualizing RNA Structures by SAXS-Driven MD Simulations. 2022 , 2,	1
618	A Method for Detection of Water Permeation Events in Molecular Dynamics Simulations of Lipid Bilayers. 2022 , 52, 1	1
617	Differences in Ion-RNA binding modes due to charge density variations explain the stability of RNA in monovalent salts.	
616	Structure-based discovery of orally efficient inhibitors via unique interactions with H-pocket of PDE8 for the treatment of vascular dementia. 2022 ,	0
615	Molecular mechanisms of spontaneous curvature and softening in complex lipid bilayer mixtures.	0
614	Computational Investigation of Structural Basis for Enhanced Binding of Isoflavone Analogues with Mitochondrial Aldehyde Dehydrogenase 2022 , 7, 8115-8127	1

613	Molecular Interactions of Tannic Acid with Proteins Associated with SARS-CoV-2 Infectivity 2022 , 23,	1
612	Discovery of the Xenon-Protein Interactome Using Large-Scale Measurements of Protein Folding and Stability 2022 ,	0
611	Virtual screening of small natural compounds against NS1 protein of DENV, YFV and ZIKV 2022, 1-11	3
610	Ligand Binding Path Sampling Based on Parallel Cascade Selection Molecular Dynamics: LB-PaCS-MD 2022 , 15,	O
609	Reorienting Mechanism of Harderoheme in Coproheme Decarboxylase-A Computational Study 2022 , 23,	1
608	DNA-functionalized Gold Nanorods for Targeted Triple-modal Optical Imaging and Photothermal Therapy of Triple-negative Breast Cancer.	
607	Interdisciplinary Study of the Effects of Dipeptidyl-Peptidase III Cancer Mutations on the KEAP1-NRF2 Signaling Pathway 2022 , 23,	1
606	Osteocalcin binds to the GPRC6A Venus fly trap allosteric site to positively modulate GPRC6A signaling.	
605	Protective Mechanism of a Layer-by-Layer-Assembled Artificial Cell Wall on Probiotics 2022,	0
604	Structure, mechanism and lipid-mediated remodeling of the mammalian Na/H exchanger NHA2 2022 , 29, 108-120	2
603	Design and Characterization of Myristoylated and Non-Myristoylated Peptides Effective against spp. Clinical Isolates 2022 , 23,	1
602	Effect of an amyloidogenic SARS-COV-2 protein fragment on Bynuclein monomers and fibrils 2022 ,	1
601	Synthesis, anti-TB activities, and molecular docking studies of 4-(1,2,3-triazoyl)arylmethanone derivatives 2022 , e22998	
600	Coexistence of Ammonium Transporter and Channel Mechanisms in Amt-Mep-Rh Twin-His Variants Impairs the Filamentation Signaling Capacity of Fungal Mep2 Transceptors 2022 , e0291321	O
599	RNA triplex structures revealed by WAXS-driven MD simulations.	
598	Atomistic Simulation of Lysozyme in Solutions Crowded by Tetraethylene Glycol: Force Field Dependence 2022 , 27,	
597	Poly-L-Arginine Molecule Properties in Simple Electrolytes: Molecular Dynamic Modeling and Experiments 2022 , 19,	1
596	Three-body aggregation of guest molecules as a key step in methane hydrate nucleation and growth. 2022 , 5,	6

595	Linking Alzheimer's Disease and Type 2 Diabetes: Characterization and Inhibition of Cytotoxic All and IAPP Hetero-Aggregates 2022 , 9, 842582		O
594	The oxytocin signaling complex reveals a molecular switch for cation dependence 2022,		4
593	Free Energy Prediction of Ion-Induced Nucleation of Aqueous Aerosols 2022,		O
592	Standard Binding Free Energy and Membrane Desorption Mechanism for a Phospholipase C 2022,		1
591	Monosaccharide induced temporal delay in cholesterol self-aggregation 2022, 1-13		О
590	SenseNet, a tool for analysis of protein structure networks obtained from molecular dynamics simulations 2022 , 17, e0265194		O
589	Thermodynamic stabilization of the von Willebrand Factor A1 domain due to loss-of-function disease-related mutations.		
588	Conformations and binding pockets of HRas and its guanine nucleotide exchange factors complexes in the guanosine triphosphate exchange process <i>Journal of Computational Chemistry</i> , 2022 ,	3.5	5
587	Repurposing of existing antibiotics for the treatment of diabetes mellitus 2022, 10, 4		
586	Sequence Modulates Polypeptoid Hydration Water Structure and Dynamics 2022,		1
585	Dissociation Pathways of the p53 DNA Binding Domain from DNA and Critical Roles of Key Residues Elucidated by dPaCS-MD/MSM 2022 ,		O
584	Computational Study of Ion Permeation Through Claudin-4 Paracellular Channels.		
583	Computational identification of host genomic biomarkers highlighting their functions, pathways and regulators that influence SARS-CoV-2 infections and drug repurposing 2022 , 12, 4279		8
582	Computational Assessment of Different Structural Models for Claudin-5 Complexes in Blood-Brain-Barrier Tight-Junctions.		
581	The Role of ATP in Solubilizing RNA-binding Protein Fused in Sarcoma 2022,		4
580	The inherent flexibility of receptor binding domains in SARS-CoV-2 spike protein 2022 , 11,		3
579	Mechano-redox control of Mac-1 de-adhesion from ICAM-1 by protein disulfide isomerase promotes directional movement of neutrophils under flow.		
578	Solubility of Gases in Choline Chloride-Based Deep Eutectic Solvents from Molecular Dynamics Simulation. 2022 , 61, 4659-4671		O

577	In-silico analysis of non-synonymous single nucleotide polymorphisms in human 毗efensin type 1 gene reveals their impact on protein-ligand binding sites 2022 , 98, 107669	0
576	Multivalent Cations Reverse the Twist-Stretch Coupling of RNA 2022 , 128, 108103	3
575	Discovery, Topo I inhibitory activity and mechanism evaluation of two novel cytisine-type alkaloid dimers from the seeds of Sophora alopecuroides L 2022 , 116723	
574	Distribution and Structure Analysis of Fibril-Forming Peptides Focusing on Concentration Dependency 2022 , 7, 10012-10021	
573	Transcription factor protein interactomes reveal genetic determinants in heart disease 2022,	3
572	The importance of atomic partial charges in the reproduction of intermolecular interactions for the triacetin - a model of glycerol backbone 2022 , 105203	
571	Structural basis of lipopolysaccharide maturation by the O-antigen ligase 2022,	1
57°	Mechanistic insights into multiple-step transport of mitochondrial ADP/ATP carrier 2022 , 20, 1829-1840	2
569	Amorphous Inclusion Complexes: Molecular Interactions of Hesperidin and Hesperetin with HP-ECD and Their Biological Effects 2022 , 23,	4
568	Formation of non-base-pairing DNA microgels using directed phase transition of amphiphilic monomers 2022 ,	O
567	Path to Actinorhodin: Regio- and Stereoselective Ketone Reduction by a Type II Polyketide Ketoreductase Revealed in Atomistic Detail 2022 , 2, 972-984	0
566	Computational design of a thermolabile uracil-DNA glycosylase of Escherichia coli 2022,	O
565	Selective Anticancer Therapy Based on a HA-CD44 Interaction Inhibitor Loaded on Polymeric Nanoparticles 2022 , 14,	1
564	Peptide Permeation across a Phosphocholine Membrane: An Atomically Detailed Mechanism Determined through Simulations and Supported by Experimentation 2022 ,	1
563	Length-dependent collective vibrational dynamics in alpha-helices 2022,	
562	Bioinformatics Screening of Potential Biomarkers from mRNA Expression Profiles to Discover Drug Targets and Agents for Cervical Cancer 2022 , 23,	4
561	Synthetic peptides bioinspired in temporin-PTa with antibacterial and antibiofilm activity 2022,	1
560	Microscopic mechanism for electrocoalescence of water droplets in water-in-oil emulsions containing surfactant: A molecular dynamics study. 2022 , 289, 120756	1

559	Interfacial tension reduction mechanism by alkaline-surfactant-polymer at oil-water interface from experimental and molecular dynamics approaches. 2022 , 356, 119006	О
558	Design and various in silico studies of the novel curcumin derivatives as potential candidates against COVID-19 -associated main enzymes 2022 , 98, 107657	O
557	How can the cisplatin analogs with different amine act on DNA during cancer treatment theoretically?. 2021 , 28, 2	1
556	Dynamic Coupling of Tyrosine 185 with the Bacteriorhodopsin Photocycle, as Revealed by Chemical Shifts, Assisted AF-QM/MM Calculations and Molecular Dynamic Simulations 2021 , 22,	
555	Wavefunction-Based Electrostatic-Embedding QM/MM Using CFOUR through MiMiC 2021,	1
554	Critical Packing Density of Water-Mediated Nonstick Self-Assembled Monolayer Coatings 2021 ,	
553	Organic Host Encapsulation Effects on Nitrosobenzene MonomerDimer Distribution and CNO Bond Rotation in an Aqueous Solution. 2022 , 2, 175-185	О
552	Small Molecules Targeting the Disordered Transactivation Domain of the Androgen Receptor Induce the Formation of Collapsed Helical States.	О
551	Enhanced Conformational Sampling of Nanobody CDR H3 Loop by Generalized Replica-Exchange with Solute Tempering 2021 , 11,	0
550	IgG1-b12-HIV-gp120 Interface in Solution: A Computational Study 2021 ,	
549	Regioselectivity mechanism of the Thunbergia alata 🛭 -16:0-acyl carrier protein desaturase. 2021 ,	O
548	Response of Hydrated Lipid Bilayers to RF EM Fields: Molecular Dynamics Investigations. 2021 ,	
547	Disruption of Water Networks is the Cause of Human/Mouse Species Selectivity in Urokinase Plasminogen Activator (uPA) Inhibitors Derived from Hexamethylene Amiloride (HMA) 2021 ,	1
546	Ion Permeation, Selectivity, and Electronic Polarization in Fluoride Channels.	
545	How Much Entropy Is Contained in NMR Relaxation Parameters?. 2021,	O
544	Precise Binding Free Energy Calculations for Multiple Molecules Using an Optimal Measurement Network of Pairwise Differences. 2021 ,	1
543	Pyranose Ring Puckering Thermodynamics for Glycan Monosaccharides Associated with Vertebrate Proteins 2021 , 23,	2

541	The Prion Protein Octarepeat Domain Forms Transient		O
540	Taking the Monte-Carlo gamble: How not to buckle under the pressure!. <i>Journal of Computational Chemistry</i> , 2021 ,	3.5	1
539	Design of a protein-targeted DNA aptamer using atomistic simulation 2021, 1-9		1
538	Never cared for what they do. High structural stability of Guanine-quadruplexes in presence of strand-break damages.		
537	Rational Design of Nonbonded Point Charge Models for Monovalent Ions with Lennard-Jones 12-6 Potential. 2021 ,		2
536	QM/MM and MM MD simulations on decontamination of the V-type nerve agent VX by phosphotriesterase: toward a comprehensive understanding of steroselectivity and activity 2022 ,		O
535	Electronic polarization effects on membrane translocation of anti-cancer drugs 2022,		0
534	Autism-associated mutation in Hevin/Sparcl1 induces endoplasmic reticulum stress through structural instability.		O
533	Mechanistic Insights into Passive Membrane Permeability of Drug-like Molecules from a Weighted Ensemble of Trajectories 2022 ,		O
532	Hijacking of Cellular Functions by SARS-CoV-2. Permeabilization and Polarization of the Host Lipid Membrane by Viroporins.		
531	Reorganization free energy of copper proteins in solution, in vacuum, and on metal surfaces 2022 , 156, 175101		2
530	Molecular Dynamics Studies on Effective Surface-Active Additives: Toward Hard Water-Resistant Chemical Flooding for Enhanced Oil Recovery 2022 ,		
529	Estimating ruggedness of free-energy landscapes of small globular proteins from principal component analysis of molecular dynamics trajectories 2022 , 105, 044404		1
528	Effect of Ethanol and Urea as Solvent Additives on PSS-PDADMA Polyelectrolyte Complexation 2022 , 55, 3140-3150		O
527	The tethered peptide activation mechanism of adhesion GPCRs 2022,		4
526	Systematic Evaluation of Ion Diffusion and Water Exchange 2022,		O
525	Enhancement of Rebaudioside M Production by Structure-Guided Engineering of Glycosyltransferase UGT76G1 2022 ,		О
524	Hydroxychloroquine Does Not Function as a Direct Zinc Ionophore. 2022 , 14, 899		O

(2019-2022)

523	Assessing the Mobility of Severe Acute Respiratory Syndrome Coronavirus-2 Spike Protein Glycans by Structural and Computational Methods 2022 , 13, 870938	
522	Single-molecule biophysics experiments: Toward a physical model of a replisome 2022 , 25, 104264	
521	Novel US-CpHMD Protocol to Study the Protonation-Dependent Mechanism of the ATP/ADP Carrier 2022 ,	O
520	Distal Mutations Shape Substrate-Binding Sites during Evolution of a Metallo-Oxidase into a Laccase. 5022-5035	
519	AKT mutant allele-specific activation dictates pharmacologic sensitivities 2022, 13, 2111	2
518	Atomic-level insights into the mechanism of saline-regulated montmorillonite (001)-salt droplet interface wetting: A molecular dynamics study. 2022 , 224, 106513	O
517	Chapter 10. Novel Insights into Membrane Transport from Computational Methodologies. 247-280	1
516	Image_1.pdf. 2020 ,	
515	Data_Sheet_1.pdf. 2020 ,	
514	Table_1.docx. 2020 ,	
513	Data_Sheet_1.docx. 2019 ,	
512	Image_1.tif. 2019 ,	
511	Table_1.pdf. 2019 ,	
510	Table_2.pdf. 2019 ,	
509	Data_Sheet_1.docx. 2020 ,	
508	Data_Sheet_1.docx. 2019 ,	
507	Data_Sheet_1.PDF. 2019 ,	
506	Data_Sheet_2.PDF. 2019 ,	

505	Table_1.DOCX. 2019 ,	
504	Table_1.DOCX. 2020 ,	
503	Data_Sheet_1.PDF. 2020 ,	
502	Table_1.DOCX. 2020 ,	
501	Data_Sheet_1.docx. 2020 ,	
500	Table_1.docx. 2019 ,	
499	Data_Sheet_1.pdf. 2018 ,	
498	Computational Analysis on the Allostery of Tryptophan Synthase: Relationship between 無 igand Binding and Distal Domain Closure 2022 ,	1
497	The CD3D daptor structure determines functional differences between human and mouse CD16 Fc receptor signaling 2022 , 219,	2
496	Omicron-included mutation-induced changes in epitopes of SARS-CoV-2 spike protein and effectiveness assessments of current antibodies 2022 , 3, 12	o
495	Bacterial Membranes Are More Perturbed by the Asymmetric Versus Symmetric Loading of Amphiphilic Molecules 2022 , 12,	1
494	PknG R242P Mutation Results in Structural Changes with Enhanced Virulence in the Mouse Model of Infection 2022 , 10,	2
493	Using molecular dynamics simulations to interrogate T cell receptor non-equilibrium kinetics. 2022 , 20, 2124-2133	1
492	Theoretical Study of the Hydrogen-Bond Interactions of CO2 in the Organic Absorbent 1,3-Diphenylguanidine.	
491	Identification of the probable structure of the sAPPEGABAR1a complex and theoretical solutions for such cases 2022 ,	2
490	Autophagy and evasion of the immune system by SARS-CoV-2. Structural features of the non-structural protein 6 from wild type and Omicron viral strains interacting with a model lipid bilayer.	1
489	Volume viscosity and ultrasonic relaxation of ethanol-water mixtures studied by molecular dynamics simulations 2022 ,	О
488	Functional and molecular characterization of a cold-active lipase from Psychrobacter celer PU3 with potential a*ntibiofilm property 2022 ,	O

487	Applying polypharmacology approach for drug repurposing for SARS-CoV2 2022 , 134, 57		1
486	Interaction of Compounds with Lactoferrin and SARS-CoV-2: Insights from Molecular Simulations 2022 , 19,		1
485	Alchemical free energy simulations without speed limits. A generic framework to calculate free energy differences independent of the underlying molecular dynamics program <i>Journal of Computational Chemistry</i> , 2022 ,	3.5	0
484	Practical Protocols for Efficient Sampling of Kinase-Inhibitor Binding Pathways Using Two-Dimensional Replica-Exchange Molecular Dynamics 2022 , 9, 878830		О
483	New Insights into the Biophysical Behavior of an Old Molecule: Experimental and Theoretical Studies of the Interaction Between 1,10-Phenanthroline and Model Phospholipid Membranes. 2022 , 52,		
482	Study of the dynamic behavior of the cruzain enzyme in free and complexed forms with competitive and noncovalent benzimidazole inhibitors 2022 , 1-15		
481	Nearest-Neighbor dsDNA Stability Analysis Using Alchemical Free-Energy Simulations 2022,		
480	Orientation and Conformation of Hydrophobin at the Oil-Water Interface: Insights from Molecular Dynamics Simulations 2022 ,		1
479	Exploring Natural Product Activity and Species Source Candidates for Hunting ABCB1 Transporter Inhibitors: An In Silico Drug Discovery Study. 2022 , 27, 3104		2
478	The Val34Met, Thr164Ile and Ser220Cys Polymorphisms of the 🛭 -Adrenergic Receptor and Their Consequences on the Receptor Conformational Features: A Molecular Dynamics Simulation Study. 2022 , 23, 5449		
477	Conformational dynamics of the membrane enzyme LspA upon antibiotic and substrate binding 2022 ,		2
476	Conducting the RBD of SARS-CoV-2 Omicron Variant with Phytoconstituents from to Repudiate the Binding of Spike Glycoprotein Using Computational Molecular Search and Simulation Approach 2022 , 27,		1
475	Structural dynamics of SARS-CoV-2 nucleocapsid protein induced by RNA binding 2022 , 18, e1010121		3
474	The Effects of Flexibility on dsDNAdsDNA Interactions. 2022 , 12, 699		
473	Grotthuss Molecular Dynamics Simulations for Modeling Proton Hopping in Electrosprayed Water Droplets 2022 ,		O
472	Merging bioresponsive release of insulin-like growth factor I with 3D printable thermogelling hydrogels 2022 ,		O
471	Mechanistic insights into the size-dependent effects of nanoparticles on inhibiting and accelerating amyloid fibril formation 2022 , 622, 804-818		3
470	Geometrically Induced Selectivity and Unidirectional Electroosmosis in Uncharged Nanopores 2022 ,		2

469	Enhancing Ligand and Protein Sampling Using Sequential Monte Carlo 2022,		0
468	Integrated Approach to Interaction Studies of Pyrene Derivatives with Bovine Serum Albumin: Insights from Theory and Experiment 2022 ,		
467	Effect of an Amyloidogenic SARS-COV-2 Protein Fragment on Esynuclein Monomers and Fibrils 2022 ,		3
466	Hijacking of Cellular Functions by Severe Acute Respiratory Syndrome Coronavirus-2. Permeabilization and Polarization of the Host Lipid Membrane by Viroporins 2022 , 4642-4649		
465	Chiral emergence in multistep hierarchical assembly of achiral conjugated polymers 2022, 13, 2738		3
464	Doxorubicin-peptide-gold nanoparticle conjugate as a functionalized drug delivery system: exploring the limits.		O
463	Ultralong recovery time in nanosecond electroporation systems enabled by orientational-disordering processes.		0
462	Consistent Picture of PhosphateDivalent Cation Binding from Models with Implicit and Explicit Electronic Polarization.		
461	Not so rigid capsids based on cyclodextrin complexes: keys to design. 2022,		
460	Transmembrane Phosphate/Chloride Antiport Activities of 2-Benzimidazolylthiourea Receptors.		
459	py-MCMD: Python Software for Performing Hybrid Monte Carlo/Molecular Dynamics Simulations with GOMC and NAMD.		3
458	Structure of the malaria vaccine candidate Pfs48/45 and its recognition by transmission blocking antibodies.		
457	In silico folding of hydrophobic peptides that form thairpin structures in solution.		
456	The Bood, Ithe Bad, Iand the Bidden In neutron scattering and molecular dynamics of ionic aqueous solutions. 2022 , 156, 194505		1
455	Binding behavior of ibuprofen-based ionic liquids with bovine serum albumin: Thermodynamic and molecular modeling studies. 2022 , 360, 119367		2
454	Adsorption Characteristics of Peptides on the Functionalized Self-assembled Monolayers: A Molecular Dynamics Study.		O
453	Evaluating the conformational space of the active site of D 2 dopamine receptor. Scope and limitations of the standard docking methods. <i>Journal of Computational Chemistry</i> ,	3.5	0
452	Identification of Novel Nontoxic Mutants of Diphtheria Toxin Unable to ADP-ribosylate EF2 Using Molecular Dynamics Simulations and Free Energy Calculations. 2022 , 19,		

 $_{\rm 451}$ $\,$ Structure-based discovery of selective histone deacetylase (HDAC) 3 and 4 inhibitors.

450	The Ability of Chlorophyll to Trap Carcinogen Aflatoxin B1: A Theoretical Approach. 2022 , 23, 6068	2
449	In-silico study of the interactions between acylated glucagon like-peptide-1 analogues and the native receptor. 1-15	0
448	Never Cared for What They Do: High Structural Stability of Guanine-Quadruplexes in the Presence of Strand-Break Damage. 2022 , 27, 3256	O
447	Phenol Sensing in Nature Modulated via a Conformational Switch Governed by Dynamic Allostery.	
446	Atomistic-Level Description of the Covalent Inhibition of SARS-CoV-2 Papain-like Protease. 2022 , 23, 5855	O
445	Unraveling the Molecular Interface and Boundary Problems in an Electrical Double Layer and Electroosmotic Flow.	O
444	Influence of ion specificity and concentration on the conformational transition of intrinsically disordered sheep prion peptide.	1
443	Chitosan characteristics in electrolyte solutions: Combined molecular dynamics modeling and slender body hydrodynamics. 2022 , 119676	0
442	Modified Poisson B oltzmann theory for polyelectrolytes in monovalent salt solutions with finite-size ions. 2022 , 156, 214906	1
441	Automated protein-protein structure prediction of the T cell receptor-peptide major histocompatibility complex.	
440	Quaternary structure independent folding of voltage-gated ion channel pore domain subunits.	1
439	CelS-Catalyzed Processive Cellulose Degradation and Cellobiose Extraction for the Production of Bioethanol.	1
438	Adsorption Energetics of Amino Acid Analogs on Polymer/Water Interfaces Studied by All-Atom Molecular Dynamics Simulation and a Theory of Solutions.	
437	Anion-kinetics-selective graphene anode and cation-energy-selective MXene cathode for high-performance capacitive deionization. 2022 , 50, 395-406	3
436	Structural view on the role of TRD loop in regulating DNMT3A activity: a molecular dynamics study.	
435	ALS-associated A315E and A315pT variants exhibit distinct mechanisms in inducing irreversible aggregation of TDP-43312-317 peptide.	3
434	Activation of Atg7-dependent autophagy by a novel inhibitor of the Keap1-Nrf2 protein-protein interaction from Penthorum chinense Pursh. attenuates 6-hydroxydopamine-induced ferroptosis in zebrafish and dopaminergic neurons.	1

433	Impacts of targeting different hydration free energy references in the development of ion potentials.	
432	Dual Functional Amphiphilic Sugar-Coated AIE-Active Fluorescent Organic Nanoparticles for the Monitoring and Inhibition of Insulin Amyloid Fibrillation Based on Carbohydrate-Protein Interactions.	O
431	Modified Hamiltonian in FEP Calculations for Reducing the Computational Cost of Electrostatic Interactions. 2022 , 62, 2846-2856	0
430	DNA-Functionalized Gold Nanorods for Perioperative Optical Imaging and Photothermal Therapy of Triple-Negative Breast Cancer.	O
429	Phosphorylation Induced Conformational Transitions in DNA Polymerase ₹9,	
428	Structural basis of human ACE2 higher binding affinity to currently circulating Omicron SARS-CoV-2 sub-variants BA.2 and BA.1.1. 2022 ,	7
427	Development of OPLS-AA/M Parameters for Simulations of G Protein-Coupled Receptors and Other Membrane Proteins.	O
426	Binding of DEP domain to phospholipid membranes: More than just electrostatics. 2022 , 183983	
425	A new hypothesis for cavitation nucleation in gas saturated solutions: clustering of gas molecules lowers significantly the surface tension. 2022 ,	O
424	Studying the Dynamics of a Complex G-Quadruplex System: Insights into the Comparison of MD and NMR Data.	1
423	Molecular Mechanism of D1135E-Induced Discriminated CRISPR-Cas9 PAM Recognition.	3
422	Improvement of saccharification of native grass, Pennisetum sp. using cellulase from isolated Aspergillus fumigatus for bioethanol production: an insight into in silico molecular modelling, docking and dynamics studies.	O
421	Optimization of an in Silico Protocol Using Probe Permeabilities to Identify Membrane Pan-Assay Interference Compounds.	2
420	Development of coarse-grained potential of silica species. 1-13	1
419	Archaeal Lipids Regulating the Trimeric Structure Dynamics of Bacteriorhodopsin for Efficient Proton Release and Uptake. 2022 , 23, 6913	O
418	G-quadruplex recognition by DARPIns through epitope/paratope analogy.	
417	Temperature Sensitive Contacts in Disordered Loops Tune Enzyme I Activity.	
416	Electronic Polarization at the Interface between the p53 Transactivation Domain and Two Binding Partners.	

415	Nonmonotonic Relationship between the Oxidation State of Graphene-Based Materials and Its Cell Membrane Damage Effects.	1
414	Reshaping the dynamics of follicle-stimulant hormone receptor models in polyunsaturated lipid bilayers. Calculation of conformational free energy landscapes of Helical domains from all-atom MD simulations	
413	Assessment of the Components of the Electrostatic Potential of Proteins in Solution: Comparing Experiment and Theory. 2022 , 126, 4543-4554	2
412	Symmetric Molecular Dynamics.	O
411	Effect of methanol as an amphiphile on water structuring around a hydrate forming gas molecule: Insights from molecular dynamics simulations. 2022 , 361, 119628	O
410	Foreseeing the future of green Technology. Molecular dynamic investigation on passive membrane penetration by the products of the CO2 and 1,3-butadiene reaction. 2022 , 361, 119581	
409	Towards the correct microscopic structure of aqueous CsCl solutions with a comparison of classical interatomic potential models. 2022 , 361, 119660	1
408	Probing effects of the SARS-CoV-2 E protein on membrane curvature and intracellular calcium. 2022 , 1864, 183994	1
407	Breakthrough pressure of oil displacement by water through the ultra-narrow kerogen pore throat from the Young[aplace equation and molecular dynamic simulations.	O
406	Structural basis for defective membrane targeting of mutant enzyme in human VLCAD deficiency. 2022 , 13,	О
405	A molecular dynamics investigation of N-glycosylation effects on T-cell receptor kinetics. 1-10	
404	Ion-Dependent Conformational Plasticity of Telomeric G-Hairpins and G-Quadruplexes. 2022 , 7, 23368-23379	1
403	Membrane lipid reshaping underlies oxidative stress sensing by the mitochondrial proteins UCP1 and ANT1.	
402	Crystal Growth of Urea and Its Modulation by Additives as Analyzed by All-Atom MD Simulation and Solution Theory.	
401	Analysis of amyloidogenic transthyretin mutations using continuum solvent free energy calculations.	O
400	Exploring CRD mobility during RAS/RAF engagement at the membrane. 2022 ,	O
399	Cryo neutron crystallography demonstrates influence of RNA 2?-OH orientation on conformation, sugar pucker and water structure.	
398	Hidden Markov Modeling of Molecular Orientations and Structures from High-Speed Atomic Force Microscopy Time-Series Images.	

397	Topological bio-scaling analysis as a universal measure of protein folding. 2022 , 9,	
396	Long-range communication between transmembrane- and nucleotide-binding domains does not depend on drug binding to mutant P-glycoprotein.	
395	Computational Assessment of Protein Protein Binding Specificity within a Family of Synaptic Surface Receptors.	1
394	Induction of beige-like adipocyte markers and functions in 3T3-L1 cells by Clk1 and PKC# inhibitory molecules.	
393	Autism-associated mutation in Hevin/Sparcl1 induces endoplasmic reticulum stress through structural instability. 2022 , 12,	1
392	Thermodynamic stabilization of von Willebrand Factor A1 domain induces protein loss of function.	
391	Conformational entropy limits the transition from nucleation to elongation in amyloid aggregation. 2022 ,	
390	Effect of material surface on the formation and dissociation of gas hydrate in restricted space between two parallel substrates. 2022 , 138120	1
389	Ionic Liquid Decelerates Single-Stranded DNA Transport through Molybdenum Disulfide Nanopores.	0
388	Computational analysis uncovers the deleterious SNPs along with the mutational spectrum of p53 gene and its differential expression pattern in pan-cancer. 2022 , 46,	
387	Predicting Antigenic Peptides from Rocio Virus NS1 Protein for Immunodiagnostic Testing Using Immunoinformatics and Molecular Dynamics Simulation. 2022 , 23, 7681	0
386	Structural and thermodynamics properties of pure phase alkanes, monoamides and alkane/monoamide mixtures with an ab initio based force-field model. 2022 , 119797	
385	Computational study of ion permeation through claudin-4 paracellular channels.	0
384	Allosteric Enhancement of the BCR-Abl1 Kinase Inhibition Activity of Nilotinib by Co-Binding of Asciminib. 2022 , 102238	1
383	Computational Assessment of Different Structural Models for Claudin-5 Complexes in Blood ${f B}$ rain Barrier Tight Junctions.	0
382	Solution Structural Studies of Pre-amyloid Oligomer States of the Biofilm Protein Aap. 2022 , 434, 167708	O
381	Structural dynamics and in silico design of pyrazolopyran-based inhibitors against Plasmodium serine hydroxymethyltransferases. 2022 , 362, 119737	
380	Discovery and evaluation of cytisine N-isoflavones as novel EGFR/HER2 dual inhibitors. 2022 , 127, 105868	O

379	The roles of functional groups of antifreeze protein in inhibition of hydrate growth. 2022 , 327, 125060	0
378	In silico analysis of SARS-CoV-2 spike protein N501Y and N501T mutation effects on human ACE2 binding. 2022 , 116, 108260	
377	Molecular dynamics simulations of cRGD-conjugated PEGylated TiO2 nanoparticles for targeted photodynamic therapy. 2022 , 627, 126-141	1
376	Revisit the adsorption of aromatic compounds on graphene oxide: Roles of oxidized debris. 2022 , 450, 137996	O
375	RNA Electrostatics: How Ribozymes Engineer Active Sites to Enable Catalysis.	1
374	Exploring the Interaction of G-quadruplex Binders with a (3 + 1) Hybrid G-quadruplex Forming Sequence within the PARP1 Gene Promoter Region. 2022 , 27, 4792	
373	Arresting Aqueous Swelling of Layered Graphene-Oxide Membranes with H3O+ and OHIlons.	0
372	Naturally Occurring 8[1] 3Ekaur-15-en-17-al and Anti-Malarial Activity from Podocarpus polystachyus Leaves. 2022 , 15, 902	O
371	Asynchronous Reciprocal Coupling of Martini 2.2 Coarse-Grained and CHARMM36 All-Atom Simulations in an Automated Multiscale Framework.	О
370	Polymer affinity with quartz (1 0 1) surface in saline solutions: A molecular dynamics study. 2022 , 186, 107750	1
369	Comparative analysis of hydration layer reorientation dynamics of antifreeze protein and protein cytochrome P450. 2022 , 35, 509-515	
368	Extending the Martini 3 Coarse-Grained Force Field to Carbohydrates. 2022 , 18, 5089-5107	1
367	Role of Enzyme and Active Site Conformational Dynamics in the Catalysis by Amylase Explored with QM/MM Molecular Dynamics. 2022 , 62, 3638-3650	О
366	Design of Peptides that Fold and Self-Assemble on Graphite.	О
365	Molecular Insights into Factors Affecting the Generation Behaviors, Dynamic Properties, and Interfacial Structures of Methane Gas Bubbles. 2022 , 14, 2327	
364	Differences in ion-RNA binding modes due to charge density variations explain the stability of RNA in monovalent salts. 2022 , 8,	1
363	Structural Analysis of the Poly(thymidine)Melamine Assembly.	
362	Leveraging the Sampling Efficiency of RE-EDS in OpenMM Using a Shifted Reaction-Field With an Atom-Based Cutoff.	1

361	Identification of a HTT-specific binding motif in DNAJB1 essential for suppression and disaggregation of HTT. 2022 , 13,	
360	Perforin-2 clockwise hand-over-hand pre-pore to pore transition mechanism. 2022 , 13,	O
359	Design, synthesis, acetylcholinesterase, butyrylcholinesterase, and amyloid-軸ggregation inhibition studies of substituted 4,4?-diimine/4,4?-diazobiphenyl derivatives.	
358	JM-20, a Benzodiazepine-Dihydropyridine Hybrid Molecule, Inhibits the Formation of Alpha-Synuclein-Aggregated Species.	O
357	Molecular Dynamics of CYFIP2 Protein and Its R87C Variant Related to Early Infantile Epileptic Encephalopathy. 2022 , 23, 8708	
356	Enhanced Water Evaporation from Escale Graphene Nanopores.	О
355	Resolving Isomeric Posttranslational Modifications Using a Biological Nanopore as a Sensor of Molecular Shape.	О
354	Phenol sensing in nature is modulated via a conformational switch governed by dynamic allostery. 2022 , 102399	O
353	Modeling the Enzymatic Mechanism of the SARS-CoV-2 RNA-Dependent RNA Polymerase by DFT/MM-MD: An Unusual Active Site Leading to High Replication Rates.	2
352	Molecular mechanisms of spontaneous curvature and softening in complex lipid bilayer mixtures. 2022 ,	O
351	G-Quadruplex Recognition by DARPIns through Epitope/Paratope Analogy**.	
350	Highly efficient production of rebaudioside D enabled by structure-guided engineering of bacterial glycosyltransferase YojK. 10,	1
349	Tachykinin Neuropeptides and Amyloid ₹25B5) Assembly: Friend or Foe?. 2022 , 144, 14614-14626	O
348	The volume changes of unfolding of dsDNA. 2022 ,	О
347	Identification of new small molecule monoamine oxidase-B inhibitors through pharmacophore-based virtual screening, molecular docking and molecular dynamics simulation studies. 1-22	О
346	The two enantiomers of 2-hydroxyglutarate differentially regulate cytotoxic T cell function.	
345	Capturing Concentration-Induced Aggregation of Nucleobases on a Graphene Surface through Polarizable Force Field Simulations. 2022 , 126, 13122-13131	О
344	Investigation of the Second Harmonic Generation at the WaterNacuum Interface by Using Multi-Scale Modeling Methods.	

343	Carbon Nanodots from an In Silico Perspective. 2022, 122, 13709-13799	2
342	Dynamic Disulfide Bond Topologies in von-Willebrand-Factor⊞ C4-Domain Undermine Platelet Binding.	
341	Development of a new chemo-enzymatic catalytic route for synthesis of (S)-2-chlorophenylglycine. 2022 ,	
340	A Computational Study on the Interaction of NSP10 and NSP14: Unraveling the RNA Synthesis Proofreading Mechanism in SARS-CoV-2, SARS-CoV, and MERS-CoV.	1
339	Design of Peptides for Membrane Insertion: The Critical Role of Charge Separation.	0
338	Molecular Insights into the Effect of Nitrogen Bubbles on the Formation of Tetrahydrofuran Hydrates. 2022 , 27, 4945	1
337	A highly stretchable, UV resistant and underwater adhesive hydrogel based on xylan derivative for sensing. 2022 ,	0
336	Identification and Inhibition of the Druggable Allosteric Site of SARS-CoV-2 NSP10/NSP16 Methyltransferase through Computational Approaches. 2022 , 27, 5241	3
335	High-level expression and improved pepsin activity by enhancing the conserved domain stability based on a scissor-like model. 2022 , 167, 113877	
334	Antileishmanial activity, cytotoxicity and cellular response of amphotericin B in combination with crotamine derived from Crotalus durissus terrificus venom using in vitro and in silico approaches. 2022 , 217, 96-106	1
333	Exploring enzyme inhibition profiles of novel halogenated chalcone derivatives on some metabolic enzymes: Synthesis, characterization and molecular modeling studies. 2022 , 100, 107748	2
332	Water-Graphene non-bonded interaction parameters: Development and influence on molecular dynamics simulations. 2022 , 603, 154477	O
331	Molecular dynamics simulation study of covalently bound hybrid coagulants (CBHyC): Molecular structure and coagulation mechanisms. 2022 , 307, 135863	О
330	Investigation of membrane fouling phenomenon using molecular dynamics simulations: A review. 2022 , 661, 120874	O
329	Change in membrane fluidity induced by polyphenols is highly dependent on the position and number of galloyl groups. 2022 , 1864, 184015	1
328	Effects of thermostats/barostats on physical properties of liquids by molecular dynamics simulations. 2022 , 365, 120116	3
327	Molecular dynamics simulation on water/oil interface with model asphaltene subjected to electric field. 2022 , 628, 924-934	O
326	Large interfacial relocation in RBD-ACE2 complex may explain fast-spreading property of Omicron. 2022 , 1270, 133842	

325	Relative binding free energy calculations with transformato: A molecular dynamics engine-independent tool. 9,	0
324	Detecting the First Hydration Shell Structure around Biomolecules at Interfaces.	2
323	Effect of electric field intensity on electrophoretic migration and deformation of oil droplets in O/W emulsion under DC electric field: A molecular dynamics study. 2022 , 262, 118034	О
322	Slow water dynamics in polygalacturonate hydrogels revealed by NMR relaxometry and molecular dynamics simulation. 2022 , 298, 120093	O
321	Amphiphile regulated ionic-liquid-based aqueous biphasic systems with tunable LCST and extraction behavior. 2022 , 654, 130172	О
320	CO2-responsive surfactant for oil-in-water emulsification and demulsification from molecular perspectives. 2023 , 331, 125773	O
319	In-cell DNP NMR reveals multiple targeting effect of antimicrobial peptide. 2022, 6, 100074	0
318	Unveiling molecular details behind improved activity at neutral to alkaline pH of an engineered DyP-type peroxidase. 2022 , 20, 3899-3910	Ο
317	Current Perspective on Atomistic Force Fields of Polymers. 2022, 51-79	0
316	Tailoring the interaction between a gold nanocluster and a fluorescent dye by cluster size: creating a toolbox of range-adjustable pH sensors.	1
315	Interaction between two polyelectrolytes in monovalent aqueous salt solutions. 2022 , 24, 21112-21121	0
314	Molecular dynamics study of the interactions between a hydrophilic polymer brush on graphene and amino acid side chain analogues in water. 2022 , 24, 22877-22888	O
313	Mechanistic insights into the mitigation of A酶ggregation and protofibril destabilization by a d-enantiomeric decapeptide rk10. 2022 , 24, 21975-21994	2
312	The destructive mechanism of A¶¶2 protofibrils by norepinephrine revealed via molecular dynamics simulations. 2022 , 24, 19827-19836	2
311	Monitoring early-stage 軸myloid dimer aggregation by histidine site-specific two-dimensional infrared spectroscopy in a simulation study. 2022 , 24, 18691-18702	0
310	Does the inclusion of electronic polarisability lead to a better modelling of peptide aggregation?. 2022 , 12, 20829-20837	O
309	Deciphering the effect of mutations in MMAA protein causing methylmalonic acidemia (Accomputational approach. 2022 , 199-220	0
308	Mechanistic insight into the disruption of Tau R3 R 4 protofibrils by curcumin and epinephrine: an all-atom molecular dynamics study. 2022 , 24, 20454-20465	2

307	Molecular dynamic simulations of methane hydrate formation between solid surfaces: Implications for methane storage. 2023 , 262, 125511	1
306	Deciphering the importance of MD descriptors in designing Vitamin D Receptor agonists and antagonists using machine learning. 2023 , 118, 108346	O
305	Diffusion coefficient of ions through graphene nanopores. 2022 , 12, 085227	O
304	Structural basis for directional chitin biosynthesis.	4
303	Structures and membrane interactions of native serotonin transporter in complexes with psychostimulants.	О
302	The clinical drug candidate anle138b binds in a cavity of lipidic Bynuclein fibrils. 2022, 13,	1
301	Antimicrobial potential of a ponericin-like peptide isolated from Bombyx mori L. hemolymph in response to Pseudomonas aeruginosa infection. 2022 , 12,	О
300	Comprehensive evaluation of end-point free energy techniques in carboxylated-pillar[6]arene hostBuest binding: I. Standard procedure.	1
299	Skin permeability prediction with MD simulation sampling spatial and alchemical reaction coordinates. 2022 ,	2
298	Molecular Dynamics Simulations on the Elastic Properties of Polypropylene Bionanocomposite Reinforced with Cellulose Nanofibrils. 2022 , 12, 3379	1
297	Stitched peptides as potential cell permeable inhibitors of oncogenic DAXX protein.	О
296	Insights into Allosteric Mechanisms of the Lung-Enriched p53 Mutants V157F and R158L. 2022 , 23, 10100	O
295	Binding Thermodynamics and Dissociation Kinetics Analysis Uncover the Key Structural Motifs of Phenoxyphenol Derivatives as the Direct InhA Inhibitors and the Hotspot Residues of InhA. 2022 , 23, 10102	О
294	The Structures of Heterogeneous Membranes and Their Interactions with an Anticancer Peptide: A Molecular Dynamics Study. 2022 , 12, 1473	1
293	Identification of Potential New Aedes aegypti Juvenile Hormone Inhibitors from N-Acyl Piperidine Derivatives: A Bioinformatics Approach. 2022 , 23, 9927	2
292	Scalable Constant pH Molecular Dynamics in GROMACS.	2
291	Continuous millisecond conformational cycle of a DEAH box helicase reveals control of domain motions by atomic-scale transitions.	О
290	Computational modelling of diatom silicic acid transporters predicts a conserved fold with implications for their function and evolution. 2022 , 184056	O

289	Cyclic cystine knot and its strong implication on the structure and dynamics of cyclotides.	О
288	Function-Related Asymmetry of the Interactions between Matrix Loops and Conserved Sequence Motifs in the Mitochondrial ADP/ATP Carrier. 2022 , 23, 10877	1
287	Best Practices in Constant pH MD Simulations: Accuracy and Sampling.	1
286	Atomistic Insights into A315E Mutation-Enhanced Pathogenicity of TDP-43 Core Fibrils. 2022 , 13, 2743-2754	1
285	Comparison of allosteric signaling in DnaK and BiP using mutual information between simulated residue conformations.	0
284	Discovery and Structural and Functional Characterization of a Novel A-Superfamily Conotoxin Targeting 940 Nicotinic Acetylcholine Receptor. 2022 , 17, 2483-2494	1
283	Dissecting the Inhibitory Mechanism of the B -Crystallin Domain against A畢2 Aggregation and Its Effect on A畢2 Protofibrils: A Molecular Dynamics Simulation Study. 2022 , 13, 2842-2851	Ο
282	Interaction of Imidazo[4,5-a]Acridines with Acetylcholinesterase.	O
281	Ionic Strength and Solution Composition Dictate the Adsorption of Cell-Penetrating Peptides onto Phosphatidylcholine Membranes. 2022 , 38, 11284-11295	О
2 80	Reversible Unwrapping Algorithm for Constant-Pressure Molecular Dynamics Simulations.	1
279	Lignin Nanoparticle Morphology Depends on Polymer Properties and Solvent Composition: an Experimental and Computational Study.	0
278	The influence of antibody humanization on shark variable domain (VNAR) binding site ensembles.	O
277	In silico investigation of nonsynonymous single nucleotide polymorphisms in BCL2 apoptosis regulator gene to design novel protein-based drugs against cancer.	0
276	In silico drug repurposing and lipid bilayer molecular dynamics puzzled out potential breast cancer resistance protein (BCRP/ABCG2) inhibitors. 1-14	1
275	Assessing the Activation of Tyrosine Kinase KIT through Free Energy Calculations.	О
274	The Candida albicans virulence factor candidalysin polymerizes in solution to form membrane pores and damage epithelial cells. 11,	Ο
273	Spike protein-independent attenuation of SARS-CoV-2 Omicron variant in laboratory mice. 2022 , 40, 111359	1
272	Structure of the malaria vaccine candidate Pfs48/45 and its recognition by transmission blocking antibodies. 2022 , 13,	1

271	Investigation of bioactive compounds from Bacillus sp. against protein homologs CDC42 of Colletotrichum gloeosporioides causing anthracnose disease in cassava by using molecular docking and dynamics studies. 9,	О
270	In silico high throughput screening of ZINC database of natural compounds to identify novel histone deacetylase inhibitors.	O
269	Accurate and efficient constrained molecular dynamics of polymers through Newton method and special purpose code.	0
268	Development of pyrrolidine and isoindoline derivatives as new DPP8 inhibitors using a combination of 3D-QSAR technique, pharmacophore modeling, docking studies, and molecular dynamics simulations. 1-14	O
267	Differential Boric Acid and Water Transport in Type I and Type II Pores of Arabidopsis Nodulin 26-Intrinsic Protein.	O
266	Insights into the binding mode of AS1411 aptamer to nucleolin. 9,	O
265	Extending the Stochastic Titration CpHMD to CHARMM36m.	1
264	Microstructures of hydrophobic ionic liquids via tuning water networks: Theoretical and experimental investigations. 2022 , 367, 120483	O
263	Monovalent ion-mediated chargedharge interactions drive aggregation of surface-functionalized gold nanoparticles. 2022 , 14, 15181-15192	1
262	Amyloid fibrillation of the glaucoma associated myocilin protein is inhibited by epicatechin gallate (ECG). 2022 , 12, 29469-29481	O
261	The influence of saturation on the surface structure of mixed fatty acid-on-water aerosol: a molecular dynamics study.	O
260	Exploring the druggability of the binding site of aurovertin, an exogenous allosteric inhibitor of FOF1-ATP synthase. 13,	1
259	In Silico Characterization of African Swine Fever Virus Nucleoprotein p10 Interaction with DNA. 2022 , 14, 2348	O
258	Molecular modeling, molecular dynamics simulation, and essential dynamics analysis of grancalcin: An upregulated biomarker in experimental autoimmune encephalomyelitis mice. 2022 , 8, e11232	O
257	Structural basis for recognition of antihistamine drug by human histamine receptor. 2022, 13,	1
256	Small molecules targeting the disordered transactivation domain of the androgen receptor induce the formation of collapsed helical states. 2022 , 13,	3
255	The Spike Mutants Website: A Worldwide Used Resource against SARS-CoV-2. 2022 , 23, 13082	1
254	Hierarchical Virtual Screening and Binding Free Energy Prediction of Potential Modulators of Aedes Aegypti Odorant-Binding Protein 1. 2022 , 27, 6777	O

253	Increasing the Realism of in Silico pHLIP Peptide Models with a Novel pH Gradient CpHMD Method.	O
252	Biochemical and Structural Characterization of Chi-Class Glutathione Transferases: A Snapshot on the Glutathione Transferase Encoded by sll0067 Gene in the Cyanobacterium Synechocystis sp. Strain PCC 6803. 2022 , 12, 1466	O
251	DNA opening during transcription initiation by RNA polymerase II in atomic detail. 2022,	O
250	Aryl-Capped Lysine-Dehydroamino Acid Dipeptide Supergelators as Potential Drug Release Systems. 2022 , 23, 11811	O
249	Biological characterization of natural peptide BcI-1003 from Boana cordobae (anura): role in Alzheimer Disease and microbial infections	0
248	Resolving the microscopic hydrodynamics at the moving contact line. 2022 , 7,	2
247	Deciphering the Molecular Mechanism of Inhibition of 断ecretase (BACE1) Activity by a 2-Amino-imidazol-4-one Derivative. 2022 , 7,	1
246	Molecular simulation of lignin-related aromatic compound permeation through gram-negative bacterial outer membranes. 2022 , 102627	1
245	Cryo-EM structures of thermostabilized prestin provide mechanistic insights underlying outer hair cell electromotility. 2022 , 13,	0
244	A round-robin approach provides a detailed assessment of biomolecular small-angle scattering data reproducibility and yields consensus curves for benchmarking. 2022 , 78, 1315-1336	1
243	New hybrids based on benzimidazole and diazepine moieties: design, synthesis, characterization, molecular docking studies and their in vitro interactions with benzodiazepine receptors. 1-9	О
242	Structural impact of pathogenic SNPs on 胜ubulin using molecular dynamics study. 1-11	O
241	Kinetics of Acid-Catalyzed Dehydration of Alcohols in Mixed Solvent Modeled by Multiscale DFT/MD. 13193-13206	О
240	Pilus PilA of the naturally competent HACEK group pathogen Aggregatibacter actinomycetemcomitans stimulates human leukocytes and interacts with both DNA and proinflammatory cytokines. 2022 , 105843	O
239	In silicocharacterization of cysteine-stabilized 配efensins from neglected unicellular microeukaryotes.	O
238	Targeting Natural Plant Metabolites for Hunting SARS-CoV-2 Omicron BA.1 Variant Inhibitors: Extraction, Molecular Docking, Molecular Dynamics, and Physicochemical Properties Study. 2022 , 44, 5028-5047	O
237	Structural dynamics of the N-terminal SH2 domain of PI3K in its free and CD28 -bound states.	0
236	The impact of inhibitor size and flexibility on the binding pathways to c-Src kinase.	Ο

235	pH-dependent structural diversity of profilin allergens determines thermal stability. 3,	O
234	Exploring the Binding Process of Cognate Ligand to Add Adenine Riboswitch Aptamer by Using Explicit Solvent Molecular Dynamics (MD) Simulation. 2023 , 103-122	O
233	Helicene Structure between DNA and Cyanuric Acid: The Role of Noncovalent Interactions. 2022 , 126, 8508-8514	1
232	Identification of potential antifibrinolytic compounds against kringle-1 and serine protease domain of plasminogen and kringle-2 domain of tissue-type plasminogen activator using combined virtual screening, molecular docking, and molecular dynamics simulation approaches.	0
231	Synergistic Effects of IMX-104 Components in Membrane Absorption: A Computational Study.	0
230	Probing Methyl Group Dynamics in Proteins by NMR Cross-Correlated Dipolar Relaxation and Molecular Dynamics Simulations.	O
229	Comparative analyses and molecular videography of MD simulations on WT human SOD1. 2022 , 1217, 113929	0
228	Effect of inorganic salt concentration and types on electrophoretic migration of oil droplets in oil-in-water emulsion: A molecular dynamics study. 2022 , 367, 120549	O
227	Computational investigations of indanedione and indanone derivatives in drug discovery: Indanone derivatives inhibits cereblon, an E3 ubiquitin ligase component. 2022 , 101, 107776	0
226	Deciphering the electronic-level mechanism of Na+ transport in a graphdiyne desalination membrane with periodic nanopores. 2023 , 546, 116183	O
225	In silico assessment of missense point mutations on human cathelicidin LL-37. 2023 , 118, 108368	O
224	Structure and interaction between the novel graphene-like planar biphenylene network and DNA: Molecular dynamics simulations. 2023 , 146, 115547	O
223	Ion formation mechanism of cortisone molecules and clusters in charged nanodroplets.	0
222	Protein Unfolding with MoS2/SnS2 Heterostructure. 2022 ,	0
221	Dimethylmyricacene: An In Vitro and In Silico Study of a Semisynthetic Non-Camptothecin Derivative Compound, Targeting Human DNA Topoisomerase 1B. 2022 , 11, 3486	0
220	Thermal Stability Estimation of Single Domain Antibodies Using Molecular Dynamics Simulations. 2023 , 151-163	O
219	Quantifying the Effects of Lossy Compression on Energies Calculated from Molecular Dynamics Trajectories.	O
218	Insight into the Interaction of Furfural with Metallic Surfaces in the Electrochemical Hydrogenation Process, from in operando Raman Spectroscopy and Molecular Dynamics Simulations.	O

217	MOLECULAR DYNAMICS SIMULATION OF FOUR BIFLAVONOIDS WITH THE LEISHMANOLYSIN (gp63) PROTEIN OF Leishmania major.	O
216	The effect of intra-molecular bonds on the liquid-liquid critical point in modified-WAC models.	O
215	Lopinavir and Ritonavir have a high affinity to SARS-CoV-2 S-protein Receptor-Binding Domain sequenced in Brazil.	O
214	Simulated tempering-enhanced umbrella sampling improves convergence of free energy calculations of drug membrane permeation.	O
213	Structural properties of A順1個0) peptide in protonation stage of one, two, and three: New insights from the histidine protonation behaviors. 2022 ,	1
212	Comprehensive evaluation of end-point free energy techniques in carboxylated-pillar[6]arene hostguest binding: II. regression and dielectric constant.	2
211	Structural Effects of Spike Protein D614G Mutation in SARS-CoV-2. 2022 ,	О
210	Supercrystal engineering of atomically precise gold nanoparticles promoted by surface dynamics.	1
209	Activation and signaling mechanism revealed by GPR119-Gs complex structures. 2022, 13,	О
208	Structure determination of inactive-state GPCRs with a universal nanobody.	2
207	C3N Nanodots Impede A即eptides Aggregation Pathogenic Path in Alzheimer's Disease.	О
206	Bispecific antibodies affects of point mutations on CH3-CH3 interface stability. 2022, 35,	O
205	Evolutionary and structural aspects of Solanaceae RNases T2. 2023 , 46,	O
204	Study of potential inhibition of the estrogen receptor by cannabinoids using an in silico approach: Agonist vs antagonist mechanism. 2023 , 152, 106403	O
203	Hygroscopicity of ultrafine particles containing ammonium/alkylaminium sulfates: A Killer model investigation with correction of surface tension. 2023 , 294, 119500	O
202	Molecular dynamics study on water desalination performance and related mechanism of hydrophobic Al2O3 ceramic membrane. 2023 , 202, 123739	O
201	Role of supramolecular steric compression during photoinduced intramolecular hydrogen abstraction reactions of ketones and thioketones. 2023 , 437, 114442	O
200	A molecular dynamics investigation of Taq DNA polymerase and its complex with a DNA substrate using a solid-state nanopore biosensor. 2022 , 24, 29977-29987	O

199	Upstream of N-Ras C-terminal cold shock domains mediate poly(A) specificity in a novel RNA recognition mode and bind poly(A) binding protein during translation regulation.	0
198	Diffusion theory of molecular liquids in the energy representation and application to solvation dynamics.	O
197	How Accurate Is the Egg-Box Model in Describing the Binding of Calcium to Polygalacturonate? A Molecular Dynamics Simulation Study. 2022 , 126, 10206-10220	О
196	Inverse Design of Pore Wall Chemistry To Control Solute Transport and Selectivity.	O
195	Protein Structure Validation Derives a Smart Conformational Search in a Physically Relevant Configurational Subspace. 2022 , 62, 6217-6227	О
194	5-Methyl-cytosine stabilizes DNA but hinders DNA hybridization revealed by magnetic tweezers and simulations. 2022 , 50, 12344-12354	O
193	DeepPROTACs is a deep learning-based targeted degradation predictor for PROTACs. 2022, 13,	2
192	SARS-CoV-2 Delta Variant: Interplay between Individual Mutations and Their Allosteric Synergy. 2022 , 12, 1742	1
191	Duplex DNA Retains the Conformational Features of Single Strands: Perspectives from MD Simulations and Quantum Chemical Computations. 2022 , 23, 14452	О
190	Membrane Lipid Reshaping Underlies Oxidative Stress Sensing by the Mitochondrial Proteins UCP1 and ANT1. 2022 , 11, 2314	O
189	AMBER Drug Discovery Boost Tools: Automated Workflow for Production Free-Energy Simulation Setup and Analysis (ProFESSA). 2022 , 62, 6069-6083	О
188	Biological Characterization of Natural Peptide BcI-1003 from Boana cordobae (anura): Role in Alzheimer Disease and Microbial Infections. 2023 , 29,	O
187	Hydrophobicity of arginine leads to reentrant liquid-liquid phase separation behaviors of arginine-rich proteins. 2022 , 13,	1
186	Concentration Effect, Structural Properties, and Driving Force on A型8 Dimerization with and without Zn 2+ Cooperation: Learning from Replica Exchange Sampling**.	O
185	Use of multistate Bennett acceptance ratio method for free-energy calculations from enhanced sampling and free-energy perturbation.	1
184	Interactions of Apigenin and Safranal with the 5HT1A and 5HT2A Receptors and Behavioral Effects in Depression and Anxiety: A Molecular Docking, Lipid-Mediated Molecular Dynamics, and In Vivo Analysis. 2022 , 27, 8658	1
183	Lytic polysaccharide monooxygenase increases cellobiohydrolases activity by promoting decrystallization of cellulose surface. 2022 , 8,	1
182	Planar aggregation of the influenza viral fusion peptide alters membrane structure and hydration, promoting poration. 2022 , 13,	O

181	Multiple sub-state structures of SERCA2b reveal conformational overlap at transition steps during the catalytic cycle. 2022 , 41, 111760	1
180	How AberrantN-Glycosylation Can Alter Protein Functionality and Ligand Binding: an Atomistic View.	O
179	Initiation and Evolution of Pores Formed by Influenza Fusion Peptides Probed by Lysolipid Inclusion. 2022 ,	0
178	Structures of the Inhibitory Receptor Siglec-8 in Complex with a High-Affinity Sialoside Analogue and a Therapeutic Antibody.	O
177	Elucidating the Protonation State of the Esecretase Catalytic Dyad.	0
176	Fouling characteristics of microcrystalline cellulose during cross-flow microfiltration: Insights from fluid dynamic gauging and molecular dynamics simulations. 2022 , 121272	O
175	Bioactive compounds from Pandanous fascicularis as potential therapeutic candidate to tackle hepatitis a inhibition: Docking and molecular dynamics simulation study. 1-17	2
174	Conformation and energy investigation of microtubule longitudinal dynamic instability induced by natural products.	O
173	N -Substituted piperidine-3-carbohydrazide-hydrazones against Alzheimer's disease: Synthesis and evaluation of cholinesterase, beta-amyloid inhibitory activity, and antioxidant capacity.	0
172	Prediction of Water Diffusion in Wide Varieties of Polymers with All-Atom Molecular Dynamics Simulations and Deep Generative Models.	O
171	Phosphorylation of the Hsp90 co-chaperone Hop changes its conformational dynamics and biological function. 2022 , 167931	0
170	MoBioTools : A toolkit to setup quantum mechanics/molecular mechanics calculations.	O
169	Dynamic spatiotemporal determinants modulate GPCR:G protein coupling selectivity and promiscuity. 2022 , 13,	0
168	Building Quantitative Bridges between Dynamics and Sequences of SARS-CoV-2 Main Protease and a Diverse Set of Thirty-Two Proteins.	O
167	Impact of Polarization on the Ring Puckering Dynamics of Hexose Monosaccharides.	0
166	Investigation of the Interaction between Aloe´vera Anthraquinone Metabolites and c-Myc and C-Kit G-Quadruplex DNA Structures. 2022 , 23, 16018	Ο
165	Benchmark of force fields to characterize the intrinsically disordered R2-FUS-LC region.	0
164	How SARS-CoV-2 alters the regulation of gene expression in infected cells	O

163	AMBER Free Energy Tools: A New Framework for the Design of Optimized Alchemical Transformation Pathways.	1
162	MDexciteR: Enhanced Sampling Molecular Dynamics by Excited Normal Modes or Principal Components Obtained from Experiments.	Ο
161	Coenzyme corona formation on carbon nanotubes leads to disruption of the redox balance in metabolic reactions.	Ο
160	Unidirectional single-file transport of full-length proteins through a nanopore.	Ο
159	Atomistic Insights into the Inhibitory Mechanism of Tyrosine Phosphorylation against the Aggregation of Human Tau Fragment PHF6. 2023 , 127, 335-345	0
158	Theoretical Study on the Regulating Mechanism of the Transition Between the Open-closed State of hCtBP2: A Combined Molecular Dynamics and Quantum Mechanical Interaction Analysis.	O
157	Chetomin, a SARS-CoV-2 3C-like Protease (3CLpro) Inhibitor: In Silico Screening, Enzyme Docking, Molecular Dynamics and Pharmacokinetics Analysis. 2023 , 15, 250	0
156	Investigating the Solvent Effects on Binding Affinity of PAHsExBox4+ Complexes: An Alchemical Approach. 2023 , 127, 249-260	Ο
155	Capturing charge and size effects of ions at the graphenellectrolyte interface using polarizable force field simulations.	Ο
154	The pathogenic effect of SNPs on structure and function of human TLR4 using a computational approach. 1-14	Ο
153	Identification of small molecule inhibitors of CXCR4 han important drug target in renal fibrosis.	Ο
152	In Silico Mining of Natural Products Atlas (NPAtlas) Database for Identifying Effective Bcl-2 Inhibitors: Molecular Docking, Molecular Dynamics, and Pharmacokinetics Characteristics. 2023 , 28, 783	Ο
151	New Insights into the Structural and Binding Properties on AllMature Fibrils Due to Histidine Protonation Behaviors. 2023 , 14, 218-225	0
150	Fluorescent protein lifetimes report increased local densities and phases of nuclear condensates during embryonic stem cell differentiation.	O
149	Mapping DNA Conformations Using Single-Molecule Conductance Measurements. 2023, 13, 129	Ο
148	Discovery of inhibitors against SARS-CoV-2 main protease using fragment-based drug design. 2023 , 371, 110352	Ο
147	Insights into Lewis/Brfisted acidity of metal chlorides and solvent effect of alcohols for synthesis of Evalerolactone by combining molecular dynamics simulations and experiments. 2023 , 335, 126749	0
146	EGCG attenuates	Ο

145	Free energy landscape of wrapping of lipid nanocluster by polysaccharides. 2023, 294, 106956	O
144	Electrophoretic coalescence behavior of oil droplets in oil-in-water emulsions containing SDS under DC electric field: A molecular dynamics study. 2023 , 338, 127258	O
143	Molecular interactions of resveratrol with A斛2 peptide and fibril during in-vitro A斛2 aggregation. 2023 , 7, 100060	O
142	Hyper-mobile Water and Raman 2900 cml Peak Band of Water Observed around Backbone Phosphates of Double Stranded DNA by High-Resolution Spectroscopies and MD Structural Feature Analysis of Water. 2023 , 127, 285-299	O
141	On the Permeation of Polychlorinated Dibenzodioxins and Dibenzofurans through Lipid Membranes: Classical MD and Hybrid QM/MM-EDA Analysis. 2023 , 13, 28	O
140	Mechanism of ∰hairpin formation in AzoChignolin and Chignolin.	O
139	Development of hidden Markov modeling method for molecular orientations and structure estimation from high-speed atomic force microscopy time-series images. 2022 , 18, e1010384	O
138	Polyelectrolyte Influence on Beta-Hairpin Peptide Stability: A Simulation Study. 2023 , 127, 359-370	O
137	Interfacial dynamics and growth modes of -microglobulin dimers.	O
136	Increasing the O2 Resistance of the [FeFe]-Hydrogenase CbA5H through Enhanced Protein Flexibility. 2023 , 13, 856-865	O
135	Free-Energy Profiles for Membrane Permeation of Compounds Calculated Using Rare-Event Sampling Methods. 2023 , 63, 259-269	O
134	Different pKa Shifts of Internal GLU8 in Human	O
133	Resistance to a tyrosine kinase inhibitor mediated by changes to the conformation space of the kinase.	O
132	Probing the bioactive compounds of Kigelia africana as novel inhibitors of TNF-社onverting enzyme using HPLC/GCMS analysis, FTIR and molecular modelling. 1-25	O
131	Assessment of Different Parameters on the Accuracy of Computational Alanine Scanning of Protein Protein Complexes with the Molecular Mechanics/Generalized Born Surface Area Method. 2023 , 127, 944-954	O
130	The membrane activity of the antimicrobial peptide caerin 1.1 is pH dependent. 2023,	O
129	Revealing the Molecular Interactions between Human ACE2 and the Receptor Binding Domain of the SARS-CoV-2 Wild-Type, Alpha and Delta Variants. 2023 , 24, 2517	1
128	Upstream of N-Ras C-terminal cold shock domains mediate poly(A) specificity in a novel RNA recognition mode and bind poly(A) binding protein.	O

127	Solvation Structure and Dynamics of Aqueous Solutions of Au+ Ions: A Molecular Dynamics Simulation Study.	О
126	A physicochemical cause of betaine lipid evolutionary loss in seed plants?.	O
125	Plant Terpenoid Permeability through Biological Membranes Explored via Molecular Simulations. 2023 , 127, 1144-1157	0
124	Effect of Charge State on the Equilibrium and Kinetic Properties of Mechanically Interlocked [5]Rotaxane: A Molecular Dynamics Study. 2023 , 127, 1254-1263	O
123	Effect of the QM Size, Basis Set, and Polarization on QM/MM Interaction Energy Decomposition Analysis.	1
122	Enhanced Grand Canonical Sampling of Occluded Water Sites Using Nonequilibrium Candidate Monte Carlo.	O
121	Sigmoid Accelerated Molecular Dynamics: An Efficient Enhanced Sampling Method for Biosystems. 2023 , 14, 1103-1112	0
120	Druggable sites identification in Streptococcus mutans VicRK system evaluated by catechols. 1-16	Ο
119	Human Amylin in the Presence of SARS-COV-2 Protein Fragments.	O
118	Structural Insights into Plasticity and Discovery of Flavonoid Allosteric Inhibitors of Flavivirus NS2BNS3 Protease. 2023 , 3, 71-92	O
117	High-density liquid (HDL) adsorption at the supercooled water/vapor interface and its possible relation to the second surface tension inflection point. 2023 , 158, 054503	2
116	Antiviral activity and molecular modeling studies on 1H-indole-2,3-diones carrying a naphthalene moiety. 2023 , 1281, 135100	O
115	Computational assessment of hexadecane freezing by equilibrium atomistic molecular dynamics simulations. 2023 , 638, 743-757	1
114	Molecular recognition of SARS-CoV-2 spike protein with three essential partners: exploring possible immune escape mechanisms of viral mutants. 2023 , 29,	O
113	The Impact of Pathogenic and Artificial Mutations on Claudin-5 Selectivity from Molecular Dynamics Simulations. 2023 ,	0
112	Oxidation of Dueling Cysteine Promotes Subunit Exchange in SOD1.	O
111	Molecular Dynamics Simulation of Hexagonal Boron Nitride Slit Membranes for Wastewater Treatment. 2023 , 121842	O
110	Inhibition effect of novel amphiphilic poly(amino acid)s on methane hydrate. 2023, 113, 204971	Ο

109	Novel NQO1 substrates bearing two nitrogen redox centers: Design, synthesis, molecular dynamics simulations, and antitumor evaluation. 2023 , 134, 106480	О
108	Whether carbon nanotubes are suitable for delivering small drugs with aromatic rings through non-covalent adsorption?. 2023 , 378, 121595	O
107	Mechanistic insight into a graphene-like stimulus-responsive desalination membrane from molecular dynamics and first principles. 2023 , 136, 109910	O
106	Molecular dynamics simulation study of DNA conformation changes caused by the dinuclear platinum(II) complexes with the bisphosphonate group. 2023 , 243, 112179	O
105	GAP positions catalytic H-Ras residue Q61 for GTP hydrolysis in molecular dynamics simulations, complicating chemical rescue of Ras deactivation. 2023 , 104, 107835	O
104	Molecular insights into the inhibition mechanism of harringtonine against essential proteins associated with SARS-CoV-2 entry. 2023 , 240, 124352	O
103	Interaction of neutral and protonated Tamoxifen with the DPPC lipid bilayer using molecular dynamics simulation. 2023 , 194, 109225	O
102	Diffusion in intact secondary cell wall models of plants at different equilibrium moisture content. 2023 , 9, 100105	O
101	Miscibility of Phosphatidylcholines in Bilayers: Effect of Acyl Chain Unsaturation. 2023, 13, 411	O
100	Accurate and efficient constrained molecular dynamics of polymers using Newton's method and special purpose code. 2023 , 288, 108742	O
99	Exposure to the electric field: A potential way to block the aggregation of histidine tautomeric isomers of hmyloid. 2023 , 232, 123385	O
98	Evaluating the active site-substrate interplay between x-ray crystal structure and molecular dynamics in chorismate mutase. 2023 , 158, 065101	O
97	Unexpected Behavior of Chloride and Sulfate Ions upon Surface Solvation of Martian Salt Analogue. 2023 , 7, 350-359	O
96	The Impact of Pathogenic and Artificial Mutations on Claudin-5 Selectivity from Molecular Dynamics Simulations.	O
95	Long-time-step molecular dynamics can retard simulation of protein-ligand recognition process. 2023 , 122, 802-816	O
94	Phosphate aggregation, diffusion, and adsorption on kaolinite in saline solutions by molecular dynamics simulation. 2023 , 233, 106844	O
93	Fast, Accurate, and System-Specific Variable-Resolution Modeling of Proteins. 2023, 63, 1260-1275	0
92	In silico identification of a promising inhibitor of Fusarium oxysporum f. sp. Lycopersici, Secreted in Xylem 1 protein.	O

91	Structure of Geobacter cytochrome OmcZ identifies mechanism of nanowire assembly and conductivity. 2023 , 8, 284-298	О
90	Entropically-Driven Co-assembly of l-Histidine and l-Phenylalanine to Form Supramolecular Materials. 2023 , 17, 3506-3517	О
89	Molecular Mechanism in the Disruption of Chronic Traumatic Encephalopathy-Related R3 R 4 Tau Protofibril by Quercetin and Gallic Acid: Similarities and Differences. 2023 , 14, 897-908	O
88	Thermodynamics and kinetics of an A-U RNA base pair under force studied by molecular dynamics simulations. 2023 , 107,	O
87	Understanding the self-assembly dynamics of A/T absent f our-way DNA junctions with sticky ends at altered physiological conditions through molecular dynamics simulations. 2023 , 18, e0278755	0
86	Molecular Dynamics Refinement of Open State Serotonin 5-HT3A Receptor Structures. 2023 , 63, 1196-1207	O
85	Benchmarking Molecular Dynamics Force Fields for All-Atom Simulations of Biological Condensates.	0
84	Design, synthesis, and biological evaluation of some novel naphthoquinone-glycine /	O
83	Caffeic Acid Has Antiviral Activity against Ilhūs Virus In Vitro. 2023 , 15, 494	0
82	Molecular dynamics simulations reveal the effect of mutations in the RING domains of BRCA1-BARD1 complex and its relevance to the prognosis of breast cancer. 1-19	O
81	Correlation between protein conformations and water structure and thermodynamics at high pressure: A molecular dynamics study of the Bovine Pancreatic Trypsin Inhibitor (BPTI) protein. 2023 , 158, 095102	0
80	Structure-modified polymeric carbon-dots with lowered retention and enhanced colloidal stability in porous media for tracer application at extreme reservoir condition. 2023 , 32, 101014	O
79	Stability of the A#2 Peptide in Mixed Solutions of Denaturants and Proline. 2023, 127, 1572-1585	0
78	Self-inhibited State of Venezuelan Equine Encephalitis Virus (VEEV) nsP2 Cysteine Protease: A Crystallographic and Molecular Dynamics Analysis. 2023 , 435, 168012	O
77	Engineered Glycosidase for Significantly Improved Production of Naturally Rare Vina-Ginsenoside R7. 2023 , 71, 3852-3861	0
76	Molecular dynamics simulations reveal the importance of amyloid-beta oligomer	O
75	Discovery of potent inhibitors targeting Glutathione S-transferase of Wuchereria bancrofti: a step toward the development of effective anti-filariasis drugs.	O
74	Conformational changes in the human Cx43/GJA1 gap junction channel visualized using cryo-EM. 2023 , 14,	О

73	Structural Characterization of Nanobodies during Germline Maturation. 2023, 13, 380	O
7 ²	Allosteric regulation of 骨eaction stage I in tryptophan synthase upon the 且igand binding. 2023 , 158, 115101	O
71	Venetoclax analogs as promising anticancer therapeutics via targeting Bcl-2 protein: in-silico drug discovery study. 1-17	O
70	Energy Coupling and Stoichiometry of Zn2+/H+Antiport by the Cation Diffusion Facilitator YiiP.	O
69	Static Binding and Dynamic Transporting-Based Design of Specific Ring-Chain-Ring Acetylcholinesterase Inhibitor: From Galantamine to Natural Product.	0
68	Influence of ALS -linked M337V mutation on the conformational ensembles of TDP-43 321B40 peptide monomer and dimer.	1
67	Million-atom molecular dynamics simulations reveal the interfacial interactions and assembly of plant PSII-LHCII supercomplex. 2023 , 13, 6699-6712	0
66	Design-Rules for Stapled Alpha-Helical Peptides with On-Target In Vivo Activity: Application to Mdm2/X dual antagonists.	O
65	Water∄ motions in x-y and z directions of 2D nanochannels: Entirely different but tightly coupled.	0
64	Simulated Tempering-Enhanced Umbrella Sampling Improves Convergence of Free Energy Calculations of Drug Membrane Permeation. 2023 , 19, 1898-1907	O
63	In-silico natural product database mining for novel neuropilin-1 inhibitors: molecular docking, molecular dynamics and binding energy computations. 2023 , 17,	0
62	Computational design of a cyclic peptide that inhibits the CTLA4 immune checkpoint.	O
61	Structural basis for DARC binding in reticulocyte invasion byPlasmodium vivax.	O
60	Designing antimicrobial peptides using deep learning and molecular dynamic simulations. 2023 , 24,	O
59	Molecular recognition of bio-active triterpenoids from Swertia chirayita towards hepatitis Delta antigen: a mechanism through docking, dynamics simulation, Gibbs free energy landscape. 1-14	2
58	Long-range communication between transmembrane- and nucleotide-binding domains does not depend on drug binding to mutant P-glycoprotein. 1-10	O
57	Mechanistic Insight into the Amyloid Fibrillation Inhibition of Hen Egg White Lysozyme by Three Different Bile Acids. 2023 , 127, 2198-2213	0
56	Atomistic origins of biomass recalcitrance in organosolv pretreatment. 2023 , 272, 118587	O

55	Solvation free energy arithmetic for small organic molecules. 2023, 44, 1263-1277	0
54	ALS-Linked A315T and A315E Mutations Enhance	O
53	In Silico-Based Structural Evaluation to Categorize the Pathogenicity of Mutations Identified in the RAD Class of Proteins. 2023 , 8, 10266-10277	0
52	Antimicrobial cellulose paper tuned with chitosan fibers for high-flux oil/water separation. 2023 , 312, 120794	O
51	Intermediate-state-trapped mutants pinpoint G protein-coupled receptor conformational allostery. 2023 , 14,	0
50	Cryo-EM structures of human Cx36/GJD2 neuronal gap junction channel. 2023 , 14,	Ο
49	Identification of host genomic biomarkers from multiple transcriptomics datasets for diagnosis and therapies of SARS-CoV-2 infections. 2023 , 18, e0281981	0
48	Do specific ion effects influence the physical chemistry of aqueous graphene-based supercapacitors? Perspectives from multiscale QMMD simulations. 2023 , 207, 292-304	1
47	Insights into substrate transport and water permeation in the mycobacterial transporter MmpL3. 2023 ,	0
46	Conformational Behavior of SARS-Cov-2 Spike Protein Variants: Evolutionary Jumps in Sequence Reverberate in Structural Dynamic Differences. 2023 , 19, 2120-2134	O
45	Molecular analyses of the C-terminal CRAF variants associated with cardiomyopathy reveal their opposing impacts on the active conformation of the kinase domain. 1-11	0
44	Discovery of a Novel 3site State as the Multi-Substrate Bound State of P450cam.	O
43	Comprehensive Evaluation of End-Point Free Energy Techniques in Carboxylated-Pillar[6]arene Host [uest Binding: III. Force-Field Comparison, Three-Trajectory Realization and Further Dielectric Augmentation. 2023 , 28, 2767	0
42	Methane Gas Bubbles Affecting the Formation and Distribution of Hydrates in Kaolinite Slit Pores: A Molecular Dynamics Study. 2023 , 37, 5102-5113	O
41	Uncovering the folding mechanism of pertactin: A comparative study of isolated and vectorial folding. 2023 ,	O
40	Unraveling the Aquaporin-3 Inhibitory Effect of Rottlerin by Experimental and Computational Approaches. 2023 , 24, 6004	O
39	Structure of interpolymer complex between poly(acrylic acid) and poly(ethylene oxide) in aqueous salt solution: a molecular dynamics simulation study. 2023 , 49, 743-757	0
38	Human Amylin in the Presence of SARS-COV-2 Protein Fragments. 2023 , 8, 12501-12511	Ο

37	Electric-field induced entropic effects in liquid water.	O
36	In silico characterization of cysteine-stabilized H efensins from neglected unicellular microeukaryotes. 2023 , 23,	O
35	Structural mechanism of Fab domain dissociation as a measure of interface stability. 2023 , 37, 201-215	O
34	Identification of new oxospiro chromane quinoline-carboxylate antimalarials that arrest parasite growth at ring stage. 1-22	O
33	Mechanism of antibody-specific deglycosylation and immune evasion by Streptococcal IgG-specific endoglycosidases. 2023 , 14,	0
32	How SARS-CoV-2 Alters the Regulation of Gene Expression in Infected Cells. 2023 , 14, 3199-3207	O
31	Converging PMF calculations of antibiotic permeation across an outer membrane porin with sub-kilocalorie per mole accuracy.	0
30	Energetics and kinetics of membrane permeation of photoresists for bioprinting.	O
29	Conserved Conformational Dynamics Reveal a Key Dynamic Residue in the Gatekeeper Loop of Human Cyclophilins. 2023 , 127, 3139-3150	0
28	Effect of temperature on hepatitis a virus and exploration of binding mode mechanism of phytochemicals from tinospora cordifolia: an insight into molecular docking, MM/GBSA, and molecular dynamics simulation study. 1-17	0
27	Connecting Diffraction Experiments and Network Analysis Tools for the Study of Hydrogen-Bonded Networks. 2023 , 127, 3109-3118	0
26	Mechanistic Insights into the Binding of Different Positron Emission Tomography Tracers to Chronic Traumatic Encephalopathy Tau Protofibrils.	O
25	Efficient seawater desalination in lamellar nanochannel-based boridene filtration membrane.	O
24	Mutual induced-fit mechanism drives binding between intrinsically disordered Bim and cryptic binding site of Bcl-xL. 2023 , 6,	O
23	The targeted next-generation sequence revealed SMAD4, AKT1, and TP53 mutations from circulating cell-free DNA of breast cancer and its effect on protein structure IA computational approach. 1-14	0
22	WrappingII rapping versus Extraction Mechanism of Bactericidal Activity of MoS2 Nanosheets against Staphylococcus aureus Bacterial Membrane. 2023 , 39, 5440-5453	0
21	Single-molecule fingerprinting of protein-drug interaction using a funneled biological nanopore. 2023 , 14,	0
20	A Computational Biology Study on the Structure and Dynamics Determinants of Thermal Stability of the Chitosanase from Aspergillus fumigatus. 2023 , 24, 6671	O

19	Constant chemical potentialquantum mechanicalholecular dynamics simulations of the graphenellectrolyte double layer. 2023 , 158, 134714	O
18	Deep Eutectic Solvents for the Enzymatic Synthesis of Sugar Esters: A Generalizable Strategy?. 2023 , 11, 5926-5936	Ο
17	Molecular Dynamics Simulations Reveal the Conformational Transition of GH33 Sialidases. 2023 , 24, 6830	0
16	Continuous millisecond conformational cycle of a DEAH box helicase reveals control of domain motions by atomic-scale transitions. 2023 , 6,	Ο
15	Enhancement of neutrophil chemotaxis by trans-anethole-treated Staphylococcus aureus strains. 2023 , 18, e0284042	О
14	Molecular Recognition of Methacryllysine and Crotonyllysine by the AF9 YEATS Domain. 2023 , 24, 7002	O
13	Computational simulation of self-cleaning carbon-based membranes with zeolite porous structure for desalination. 2023 , 136, 109925	0
12	Activation loop plasticity and active site coupling in the MAP kinase, ERK2.	O
11	The Bynuclein Monomer May Have Different Misfolding Mechanisms in the Induction of Bynuclein Fibrils with Different Polymorphs. 2023 , 13, 682	0
10	Experimental and Simulation Studies on Hematite Interaction with Na-Metasilicate Pentahydrate. 2023 , 28, 3629	O
9	Uncovering allostery and regulation in SORCIN through molecular dynamics simulations. 1-14	O
8	Non-equilibrium virus particle dynamics: Microsecond MD simulations of the complete Flock House virus capsid under different conditions. 2023 , 215, 107964	O
7	Structural basis of BAM-mediated outer membrane Harrel protein assembly. 2023, 617, 185-193	O
6	Measuring pico-Newton Forces with Lipid Anchors as Force Sensors in Molecular Dynamics Simulations. 2023 , 127, 4081-4089	Ο
5	Paradoxical effect of Albn protein levels of ABCA1 in astrocytes, microglia, and neurons isolated from C57BL/6 mice: an in vitro and in silico study to elucidate the effect of Albn ABCA1 in the brain cells. 1-14	О
4	Interaction between microplastics and humic acid and its effect on their properties as revealed by molecular dynamics simulations. 2023 , 455, 131636	O
3	Kinetic and structural studies of Mycobacterium tuberculosis dihydroorotate dehydrogenase reveal new insights into class 2 DHODH inhibition. 2023 , 1867, 130378	О
2	Markov State Models Reconcile Conformational Plasticity of GTPase with Its Substrate Binding Event.	O

Design and Identification of Inhibitors for the Spike-ACE2 Target of SARS-CoV-2. **2023**, 24, 8814

О